
Electronic Thesis and Dissertation Repository

9-28-2018 11:30 AM

A Targeted Investigation of the Upper Contact Unit of the Sudbury Igneous Complex in the North Range, Sudbury Impact Structure, Canada

Lindsay E. Debono
The University of Western Ontario

Supervisor
Osinski, Gordon R.
The University of Western Ontario

Graduate Program in Geology

A thesis submitted in partial fulfillment of the requirements for the degree in Master of Science

© Lindsay E. Debono 2018

Follow this and additional works at: <https://ir.lib.uwo.ca/etd>



Part of the [Geochemistry Commons](#), and the [Geology Commons](#)

Recommended Citation

Debono, Lindsay E., "A Targeted Investigation of the Upper Contact Unit of the Sudbury Igneous Complex in the North Range, Sudbury Impact Structure, Canada" (2018). *Electronic Thesis and Dissertation Repository*. 5944.

<https://ir.lib.uwo.ca/etd/5944>

This Dissertation/Thesis is brought to you for free and open access by Scholarship@Western. It has been accepted for inclusion in Electronic Thesis and Dissertation Repository by an authorized administrator of Scholarship@Western. For more information, please contact wlsadmin@uwo.ca.

Abstract

The Sudbury Igneous Complex (SIC) represents the remnant of a crystalline impact melt sheet of the Sudbury impact structure; and is historically and presently a strategic exploration target sustaining the region's prolific mining camp. In order to better understand the SIC, it is critical to investigate the chilled upper contact of the SIC, which has historically received little recognition. Through field observations, whole rock geochemistry, petrography, and electron microprobe analysis, this study concludes that the SIC upper contact is in fact extensive across the North Range of the SIC. Additionally, the geochemistry of the SIC units, offset dykes, and upper contact unit (UCU) of the SIC presented here lead to the conclusion that the UCU roof rocks represent a more accurate proxy than the offset dykes for the initial composition of the SIC. Finally, this study indicates that the UCU lithology is no longer considered an intrusive melt of the basal Onaping Formation breccias.

Keywords

Sudbury Igneous Complex, impact melt sheets, geochemistry, mineralogy, impact cratering

Co-Authorship Statement

The collaborative nature of this project entailed co-authorship on the integrated article comprising Chapter 2 of this document. Geochemistry data produced in this study was combined with data for the Sudbury Igneous Complex and offset dykes from the North Range, specifically from publications and theses by Denise Anders, Eric Pilles, Adam Coulter, and Anne Therriault. Glencore supported the field component of this study by providing access to field sampling locations in Levack Township. Dr. Gordon Osinski supervised the project and contributed to the editing and writing of this thesis, with support from Dr. Richard Grieve.

Acknowledgments

I would like to acknowledge and thank my supervisors Dr. Gordon “Oz” Osinski and Dr. Richard Grieve for their patience, support, and guidance throughout this project. I thank Oz for the great time outdoors during field work and field courses -hiking, climbing, bush whacking, canoeing, doing battle with Sudbury’s summer insects, and discussing geology at campfires had in Sudbury and the southwest US. Thanks is extended to Peter Lightfoot for visiting the “Sudbury Group” and providing us with his expertise and knowledge in support of our graduate studies projects.

Thank you to the staff at Glencore’s Fraser mine for being so supportive and providing access to sampling areas. Thanks to Marc Beauchamp for providing guidance with the field-emission electron microprobe and associated software used for this project. I am very grateful for the financial support I received from the SEG Canada Foundation which has allowed me to conduct the analyses for this project. I am also grateful for UWO’s Dept. of Earth Sciences Robert Hodder travel bursaries, and UWO’s Global Opportunities awards which provided me with the amazing opportunity to travel and study the geology of the beautiful southwest US and Colombia.

Thank you to the SEG London Student Chapter for the great times while exploring the geology of northern Ontario, the southwest US, and Colombia. The professors and staff in the Dept. of Earth Sciences are thanked for their support and companionship that gives the department the comraderie it has. Big thanks to Arya for sharing his amazing figure editing talents, and Patrick for putting up with my geochemical calculation questions. I owe the following folks a huge thank you for the geo chatting, idea-bouncing, campfires, rock climbs, canoe trips, pub times, and keeping my feet on the ground: JonO, Jess, Steph, Luke, Diana, Dyl, Andrea, Yaozhu, Danielle, Neera, Karen, Mailyng, Kienan, and Peter to name but a few.

Finally, thank you Mum and Dad - who immigrated from their home country of Malta - for providing the best for me and constantly supporting me while I break the ice undertaking academia in Canada, through thick and thin. Thank you to my sister, Meg, for being a strong example and constantly encouraging me during my time in graduate school. Inħobbok ħafna.

Id-dinja tgħallmek aktar minn imgħallmek.

– *Maltese Proverb*

Table of Contents

Abstract.....	i
Co-Authorship Statement.....	ii
Acknowledgments.....	iii
Table of Contents.....	v
List of Tables.....	vii
List of Figures.....	viii
List of Appendices.....	xii
List of Abbreviations.....	xiii
Chapter 1	1
1 Introduction.....	1
1.1 Impact Cratering.....	2
1.1.1 Shock Effects.....	6
1.2 Sudbury Geology.....	6
1.2.1 Target Rocks.....	8
1.3 The Sudbury Igneous Complex (SIC).....	10
1.3.1 Sudbury Igneous Complex Ni-Cu-PGE Sulfide Ores.....	13
1.3.2 The Onaping Formation and Onaping Intrusion.....	14
1.4 References.....	17
Chapter 2	26
2 The Upper Contact Unit (roof rocks) of the Sudbury Igneous Complex, North Range, Sudbury impact structure, Canada.....	26
2.1 Introduction.....	26
2.1.1 Geological Setting.....	27
2.2 Methodology.....	36

2.3 Observations and Results	38
2.3.1 Field Observations	38
2.3.2 Petrographic and Microscopic Observations	45
2.3.3 X-Ray Fluorescence Geochemistry	54
2.4 Discussion	56
2.4.1 The UCU as “Roof Rocks” for the SIC	56
2.4.2 The UCU in the SIC Single-Melt System.....	58
2.4.3 The Effects of MFCI Activity on the UCU	61
2.5 Summary and Concluding Remarks	63
2.6 References.....	65
Chapter 3	76
3 Conclusions and Suggestions for Future Work.....	76
3.1 Conclusions.....	76
3.2 Suggestions for Future Work	78
3.3 References.....	80
Appendices.....	81
Curriculum Vitae	819

List of Tables

Table 2.1. A history of the previous nomenclature of the “Onaping Intrusion”. Modified from Anders et al. (2015).....	35
Table 2.2. Previously mapped units in comparison to ground truthing results from this study.	444
Table 2.3. Modal percentages of the UCU by point counting.	49
Table 2.4. Frequency occurrence of clast and coroneae compositions observed via clast analysis.....	52

List of Figures

- Figure 1.1. Cross sections illustrating the three stages of impact cratering. The left column shows the processes and geomorphology associated with the formation of simple craters (<2 – 4 km), and the right showing that of complex crater. Note the differences in processes associated with the movement of ejecta material, impact melt, and target rocks that take place between simple and complex craters. From Osinski and Pierazzo (2013). 4
- Figure 1.2. (A) Photomicrograph under XPL of PDFs in quartz hosted in Levack Gneiss from Wisner Township, Sudbury. PDFs are “decorated” with fluid inclusions along the deformation planes. (B) Photograph of shattercones hosted in Mississauga Formation photographed from Coniston Hydro Road, Sudbury... 6
- Figure 1.3. Simplified geological map of the Sudbury impact structure. Modified from Coulter (2016)... 8
- Figure 1.4. A stratigraphic section of the Huronian Supergroup, illustrating the depositional successions and igneous intrusions with the corresponding depositional environment over time from Long (2009)... 10
- Figure 1.5. (A) Stratigraphic column of the South and North Ranges of the SIC with conventional nomenclature. (B) Proposed, new, nomenclature of SIC units. “Plag”: plagioclase; “Grano”: granophyre; “Qz”: quartz; “Fm”: formation; “S.R.”: South Range. Modified from Therriault et al. (2002). 11
- Figure 2.1. A simplified map of the Sudbury Basin and the "bullseye" pattern representing the SIC, Onaping Formation, and Whitewater Group. Red dashed boxes represent the field sites in this study. Drill core analyzed in Anders et al (2015) are shown by “X”. Modified from Ames et al. (2005), and Coulter and Osinski. (2015)... 29
- Figure 2.2. A simplified cross section displaying the stratigraphic arrangement between the Superior and Southern Provinces pre- and post-impact. (A) Pre-impact: The Southern Province overlies the rocks of the Superior Province, with thickening towards the southwest. (B) Post-immediate impact: The rocks of the Southern Province are excavated, uplifted

upwards and outwards to form the crater rim. The SIC melt sheet occurs between the uplifted target rocks. Modified from Brocoum and Dalziel (1974). 31

Figure 2.3. (1) Sample Preparation: Field samples were cut and made into polished, carbon coated thin sections. (2) BSE Scans and Stitching: entire thin sections were scanned in a series of tiles, combined via stitching using the Guide-Net mapping program. (3) Image Processing: The BSE thin section images were imported into ImageJ™ software and processed to enhance the brightness and contrast between the potassium feldspar grains from the remaining mineral phases. A threshold was applied yielding a binary basemap where grains of interest (K-spar) are selected (in black) from other mineral phases (white). (4) Particle Analysis: The Particle Analysis tool in ImageJ™ was selected to measure the long axis of each individual K-spar grain. (5) Particle Analysis Results: The data results containing the long axis measurements were used to calculate average grain size for the particular sample being analyzed..... 37

Figure 2.4. Field areas are organized into "clusters" numbered from one to three for simplicity. Field images coupled with photomicrographs from respective clusters show characteristics of the UCU throughout the North Range investigation. Cluster 1 shows an example of a clast in UCU matrix at the outcrop scale, and a photomicrograph showing typical UCU matrix. Cluster 2 shows a highly weathered UCU outcrop with a photomicrograph of a quartzite clast with a reaction corona, surrounded by UCU matrix. Cluster 3 shows a sheared UCU outcrop, where the matrix appears to have undergone deformation and the clasts appear to not have been affected or affected to a lesser degree. The photomicrograph shows the shear textures of the UCU matrix juxtaposed against a quartzite clast. 39

Figure 2.5. (A) Photo of a well-exposed, typical outcrop of the UCU, previously mapped as Onaping Intrusion by Ames et al. (2005). Note the granitoid and quartzite clasts, and sulfide “blebs” suspended in the grey matrix. (B, C) Outcrops of the Upper Contact Unit of the SIC located at the North Range-East Range junction, previously mapped as Onaping Intrusion by Ames et al. (2005). Note the sheared texture of the dark grey matrix of the Garson Member and the UCU. Subrounded to rounded granitoid and quartzite clasts are hosted in the matrix of both units. 40

Figure 2.6. (A) Typical outcrop of fine-grained clast-rich granophyre. Note clast compositions are the same as the UCU. (B) Hand sample of fine-grained clast-rich granophyre. Red dashed line indicates clast boundary where a granitic clast is to the right of the line. (C) Example of a well-exposed outcrop at area mapped at “melt bodies”, west of Highway 144, Red dashed line outlines boundary of quartzite clasts.. 45

Figure 2.7. PPL (A) and XPL (B) photomicrographs of a sample of UCU. Hydrothermal alteration manifested as saussuritization of plagioclase laths. (C) Typical UCU texture exhibiting intergrowth of feldspar and quartz. (D) Photomicrograph of a sample of “melt body”. Note the likeness in texture and mineralogy between the UCU and “melt bodies”.. . 46

Figure 2.8. UCU matrix grain size data. (A) K-spar grain sizes from this study. (B) Feldspar grain sizes from Anders et al. (2015). (C) Amphibole and feldspar grain sizes from Brillinger (2011). (D) All grain sizes from plots A – C combined for comparison. Note the finer grain sizes in data from this study, due to semi-automatic particle analysis in ImageJ™ capable of detecting sub-mm scale grains. An overall negative relationship occurs between UCU matrix grain size and distance from the granophyre contact, for K-spar, feldspar (plagioclase and albite), and amphibole..... 48

Figure 2.9. (A) A bar graph showing the percent frequency of quartzite, granitoid, saussurite, and mafic clast compositions across 236 clasts analyzed across 15 thin sections of UCU. (B) Data from this study combined with data from Anders et al. (2015) illustrating an increase in clast content in the UCU with increasing distance from the granophyre contact. Note x-axis breaks. (C) Data from this study representing a slight trend of increasing clast size in the UCU with increasing distance from the granophyre contact. Note the two outliers circled by dashed line, resulting from each thin section containing one large clast..... 51

Figure 2.10. (A, B) Optical photomicrographs (PPL) showing decorated (inclusions) PDFs in quartz in the UCU. Up to three PDF orientations (labelled) are observed. Note the micrographic texture on the margins of the quartz grains. (C, D, E, F) Photomicrographs in XPL (left) and PPL (right) of the sulfide “blebs” observed in the UCU, comprised of chalcopyrite, pyrrhotite and pentlandite. Note the intergrowth nature of the sulfide bleb and igneous matrix..... 53

Figure 2.11. (A) Major elements plotted as mole % averages for units of the SIC, offset dykes, and UCU, specific to the North Range. (B) Average REEs plotted for the SIC, SIC units (Naldrett et al., 1984; Therriault et al., 2002), and offset dykes Hess, Foy, Parkin, Trill, and Pele (Anders, 2016; Coulter, 2016; Pilles, 2016; Pilles et al., 2017, 2018) of the North Range. The UCU* (n = 7) trend is representative of samples ~270 m from the granophyre contact, and the UCU**(n = 6) is representative of those from ~1400m from the granophyre contact. (C) The average REE composition of the SIC in the North Range (from norite to granophyre) compared to individual UCU samples, inclusive of “Onaping Intrusion” and “melt bodies” samples. Note the overall depletion of REE in the UCU due to primitive nature of the UCU melt compared to the SIC melt..... 55

Figure 2.12. A simplified stratigraphic column (not to scale) representing a transect performed west of Highway 144, from the granophyre, fine-grained quartz-rich granophyre, UCU (as discontinuous sheets), and the Onaping Formation. Note the transitional contact relationships of a single-melt system (the SIC) between the granophyre (clast-rich) and UCU (clast-rich). A sharp contact is indicated between the UCU and Sandcherry Member. Clasts of UCU are seen hosted within the Sandcherry Member, emplaced via MFCI activity.....59

List of Appendices

Appendix A. Geochemical data used for this study.....	53
---	----

List of Abbreviations

Ab: Albite

BSE: Backscattered electron

CPX: Clinopyroxene

EDS: Energy dispersive spectroscopy

EPMA: Earth and Planetary Materials Analysis

Ga: giga-annum or one billion years in geological time

HREE: Heavy rare earth element

ICP-MS: Inductively coupled plasma mass spectrometry

K-spar: Potassium feldspar

LREE: Light rare earth element

MFCI: Melt-fuel-coolant interaction

Mol: Moles

OI: Onaping Intrusion

Opx: Orthopyroxene

PDF: Planar deformation feature

PGE: Platinum group elements

Plag: Plagioclase

PPL: Plane polarized light microscopy

REE: Rare earth element

SIC: Sudbury Igneous Complex

UCU: Upper Contact Unit

XPL: Cross polarized light microscopy

XRF: X-Ray fluorescence spectroscopy

Chapter 1

1 Introduction

The 1.85 Ga Sudbury impact structure is recognized as one of the world's largest impact structures that is also host to world-class ore deposits that have been exploited over the past 130 years. The evolution and formation of the Sudbury Igneous Complex (SIC) is known to have played a critical role in the formation of ore deposits and the geological processes that have shaped the overall impact structure (Lightfoot, 2017). However, the evolution of the SIC and its present-day structure are not fully understood. Historically, the upper contact of the SIC has received little recognition, despite such a unit expected to occur as is inherent with coherent impact melt sheets including the SIC (Grieve et al., 2010). Until a recent study by Anders et al. (2015), an upper contact for the SIC has received little recognition. The purpose of the thesis is to build upon the preliminary study by Anders et al. (2015) and conduct a targeted investigation of the upper contact of the SIC across the North Range of the Sudbury Basin. Chapter 1 introduces the processes involved with impact cratering to provide context for the formation of the Sudbury impact structure and SIC, followed by a discussion on the geology specific to the Sudbury impact structure. Chapter 2 discusses the methodologies used in the investigation of the upper contact of the SIC throughout the North Range. Results from field sampling, ground truthing, petrographic, microscopic, and geochemical analyses of the "Onaping Intrusion", "melt bodies", granophyre, and Sandcherry Member conducted for the project are also presented. Chapter 2 then includes a discussion and interpretation of the results, ending with concluding remarks. Chapter 3 is comprised of the summary of results for the study and suggestions for future work.

1.1 Impact Cratering

Geological processes such as plate tectonics and volcanism are unique to only some of the solid planetary bodies within the Solar System; however, impact cratering is a common geological process that all solid bodies in the Solar System share (Osinski and Pierazzo, 2013). A hypervelocity impact by a comet or asteroid and subsequent crater modification, depending on the scale of the impact, takes seconds to minutes to occur, making impact cratering an exceptionally unique and complex geological process (Melosh, 1989). On Earth, impact craters are not as commonly observed and preserved as on other solid bodies in the Solar System due to the rock record being constantly erased by the ongoing processes of plate tectonics and erosion. Three main stages illustrate the sequence of processes involved in a hypervelocity impact: (1) contact and compression, (2) excavation, and (3) modification (Fig. 1.1) (Gault et al., 1968; Osinski and Pierazzo, 2013). Post-impact hydrothermal activity is increasingly included as a final stage depending on the impact structure being considered; in the case of the Sudbury impact structure, hydrothermal activity is recognized as an intrinsic stage in its evolution (Kieffer and Simonds, 1980; Ames et al., 2008; Grieve et al., 1991).

The contact and compression stage begins with the contact of the projectile and the target surface. Based on impact crater modelling, the penetration depth of the projectile in the target rock is one to two times the diameter of the projectile (Kieffer and Simonds, 1980). Pressures at the point of impact between the projectile and target rock can reach several thousand times greater than that of the Earth's ambient atmospheric pressure (Osinski and Pierazzo, 2013). The kinetic energy that is transferred from the projectile to the target rock travels through the target rock as shockwaves faster than the speed of sound and occur at the interface between compressed and uncompressed rock (Ahrens and O'Keefe, 1972; Osinski and Pierazzo, 2013). Shocked target

material is compressed via pressure-volume work and is decompressed by a rarefaction wave and subsequent adiabatic release (Melosh, 1985; Osinski et al., 2018). Upon adiabatic release, some pressure-volume work applied to the target material is recovered; remaining unrecovered pressure-volume work in the target material manifests as waste heat, which causes impact melting and vapourization of the target material (Gault et al., 1968; Osinski et al., 2018). As shockwaves in the target rock are reflected, they approach the free upper surface of the projectile as a rarefaction wave, resulting in complete vapourization or melting of the projectile (Melosh, 1989; Osinski and Pierazzo, 2013).

Excavation of the crater occurs as a result of concentric shock waves radiating through the target rock from the point of impact by the projectile, and causes mobilization of the target material, initiating the excavation flow of target material to form the transient crater (Melosh, 1989). An excavated zone and displaced zone within the transient crater form as a result of the excavation flow field; material in the upper excavated zone is ejected outside of the crater rim as an ejecta blanket, and material in the lower displaced zone is locally displaced and remains within the transient cavity (Kenkmann et al., 2014). However, evidence from Earth and various Solar System objects indicate that some material from the displaced zone is also transported out of the transient crater to form a second layer of melt-rich ejecta (Osinski et al., 2011). In the case of complex craters, central uplift of the crater floor commences during the excavation stage; however, this process continues in the subsequent modification stage (Osinski et al., 2011).

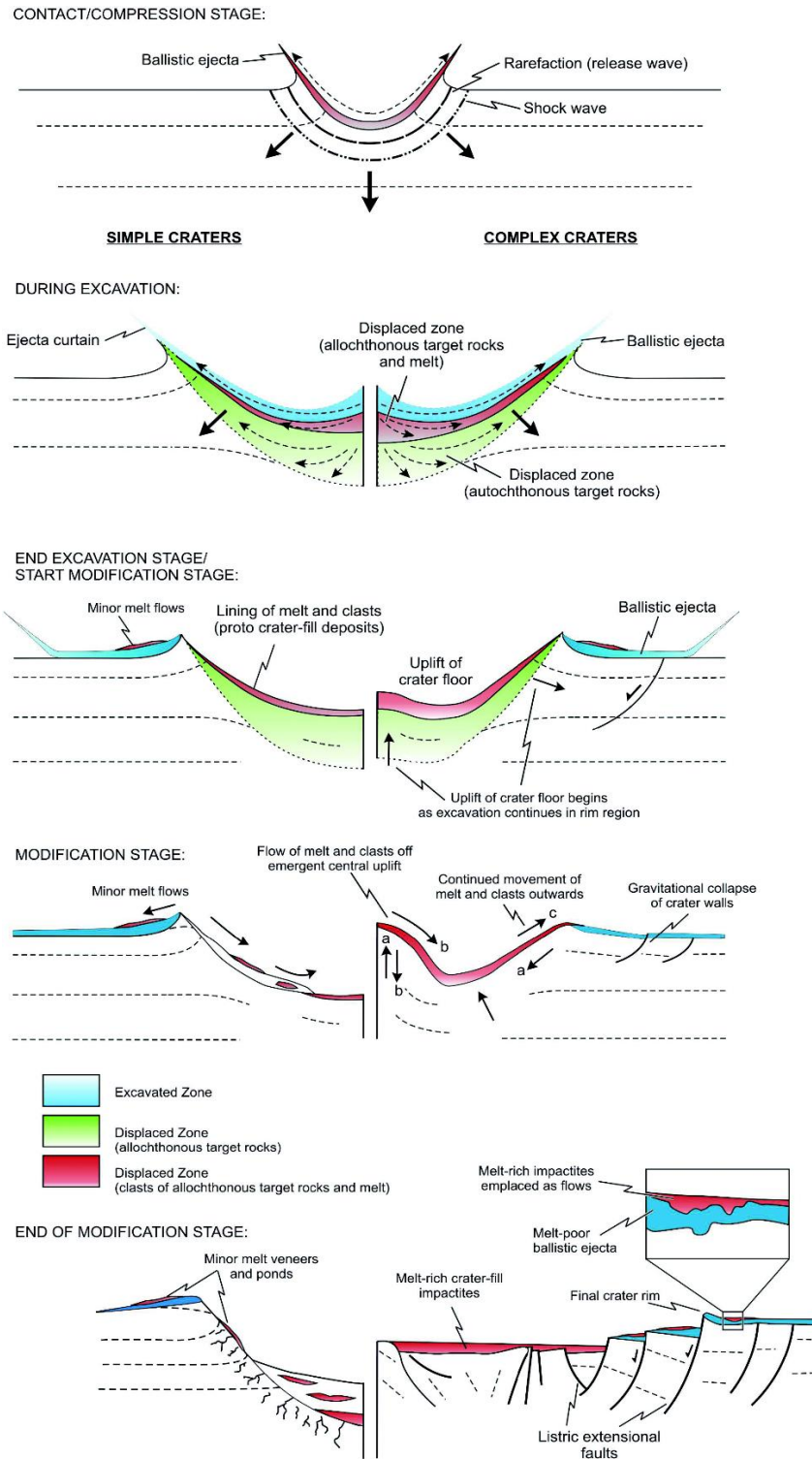


Figure 1.1. Cross sections illustrating the three stages of impact cratering. The left column shows the processes and geomorphology associated with the formation of simple craters (<2 – 4 km), and the right showing that of complex crater. Note the differences in processes associated with the movement of ejecta material, impact melt, and target rocks that take place between simple and complex craters. From Osinski and Pierazzo (2013).

The crater modification stage is dependent on the physical properties of the target rock and how it behaves under the effects of gravity (Osinski and Pierazzo, 2013; Melosh and Ivanov, 1999). Complex craters are greater than 2 – 4 km in diameter on Earth and, therefore, structurally unstable under the effects of gravity and undergo slumping at the crater walls during collapse (Melosh and Ivanov, 1999). The gravitational collapse of the crater yields three types of complex crater morphologies: (1) central uplift, (2) peak-ring, and (3) multi-ring basin (Osinski and Pierazzo, 2013). The gravity-driven slumping that takes place at the crater walls results in an inward and upward movement of material in the centre of the crater, resulting in a central uplift (Osinski and Pierazzo, 2013). With increasing crater diameter, the central uplift can grow higher than the surrounding crater rim height; gravitational forces render the central uplift unstable and cause it to collapse in a downward and outward motion (Kenkmann et al., 2014). As the material at the outer margins of the central uplift collapses downward and outward, it becomes emplaced above collapsed transient cavity material as a peak ring (Kenkmann et al., 2014; Morgan et al., 2016). Some complex craters transform into multi-ring basins after modification and exhibit multiple ring structures parallel to the crater rim (Kenkmann et al., 2014); a peak-ring or multi-ring basin classification for the Sudbury impact structure is currently uncertain. Traditionally, the processes involved in the formation of multi-ring basins have not been fully understood. However, recent studies on the Orientale Basin on the Moon have shown that multiple ring structures observed at impact structures form as a result of multiple steep (~50° to 80° dip) normal faults occurring parallel and between the crater rim and peak-ring, as a result of the collapse of the transient cavity (Nahm et al., 2013; Potter et al., 2013). In contrast, simple craters lack central uplifts, and thus, peak rings due to their smaller diameter and lesser susceptibility to gravity-induced collapsing (Osinski and Pierazzo, 2013).

1.1.1 Shock Effects

Impactites are rocks that have been created and/or modified by hypervelocity impact cratering processes (Stöffler and Grieve, 2007). Impactites such as impact melt rocks do not appear unique from ordinary geological products. However, shock effects such as shattercones, planar deformation features (PDFs), high pressure polymorphs, and isotopic anomalies are indicators of hypervelocity impacts and are required to formally identify impact structures (Ferrière and Osinski, 2013) (Fig.1.2).

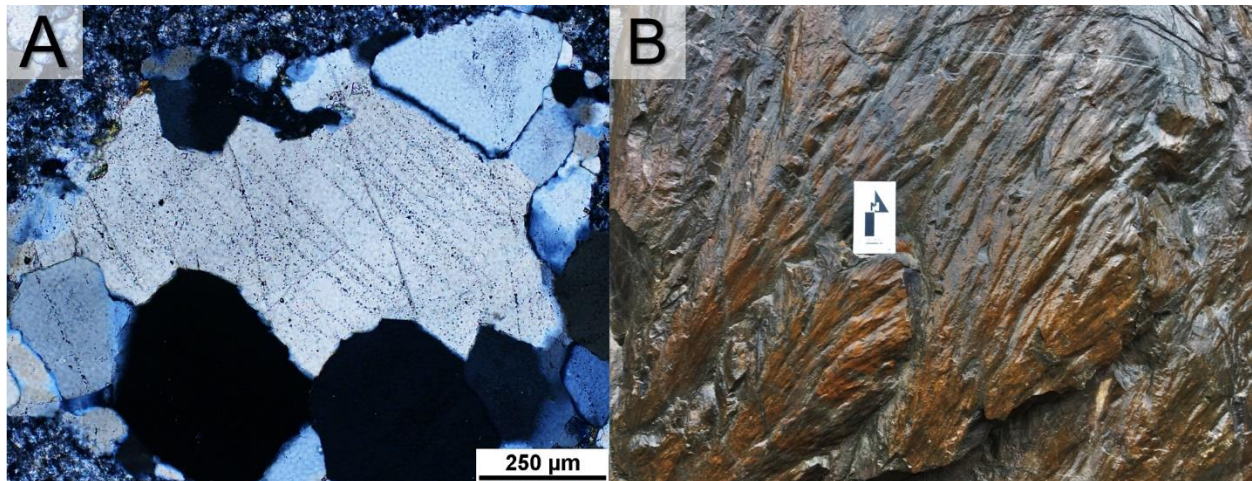


Figure 1.2. (A) Photomicrograph under XPL of PDFs in quartz hosted in Levack Gneiss from Wisner Township, Sudbury. PDFs are “decorated” with fluid inclusions along the deformation planes. (B) Photograph of shattercones hosted in Mississauga Formation photographed from Coniston Hydro Road, Sudbury.

1.2 Sudbury Geology

The 1.85 Sudbury impact structure is a remnant of a tectonically deformed complex crater, with an original diameter of ~200 – 250 km (Krogh et al., 1984; Dietz, 1964; Deutsch et al., 1995; Peredery and Morrison, 1984; Rousell, 1975). Syn- to post-impact tectonism associated with the 1.9 – 1.8 Ga Penokean orogeny, 1.77 – 1.60 Ga Yavapai-Mazatzal orogeny, ~1.45 Ga Chieflakian event, and ~1.0 Ga Grenville orogeny, contributed to the structural deformation of

the crater into an elliptical basin ~60 km by 27 km, comprising the North, South, and East Ranges (Giblin, 1984; Grieve et al., 1991; Spray and Scott, 2000; Péntek et al., 2013). Hydrothermal activity as a result of the impact and also the post-impact Yavapai-Mazatzal orogeny resulted in hydrothermal alteration and metasomatic overprinting throughout the Sudbury impact structure (Ames et al., 2008). The North Range footwall-SIC contact dips ~35° south, the East Range ~70° west, and the South Range ~55° north, expressing the varying degrees of post-impact tectonism that shaped the Sudbury impact structure (Lenauer and Riller, 2017; Pattison, 2009; Péntek et al., 2013). The present exposure exhibits a general “bullseye” pattern of the stratigraphy, with exposure of the units situated higher up in the stratigraphy are located towards the centre and vice versa. (Fig. 1.3).

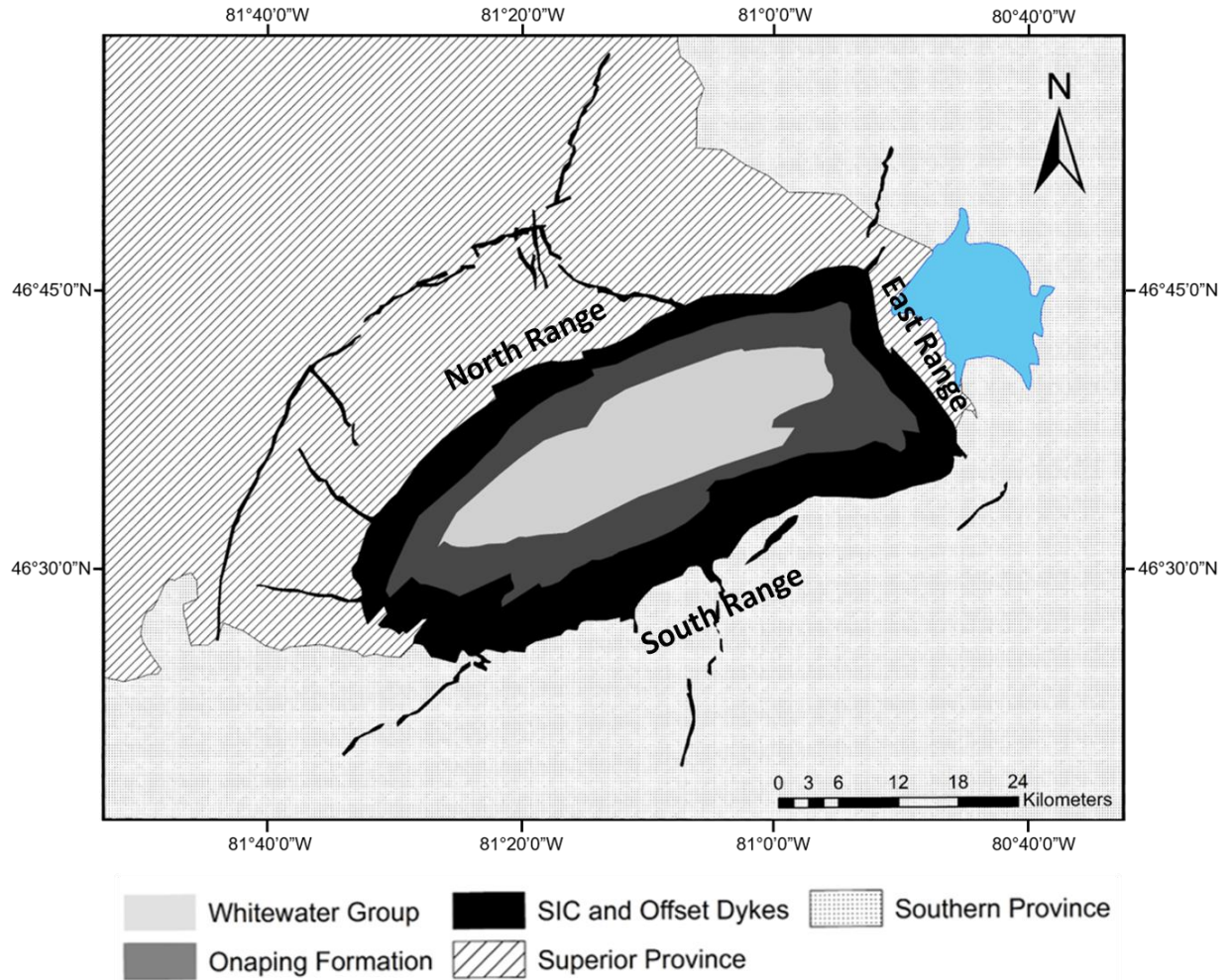


Figure 1.3. Simplified geological map of the Sudbury impact structure. Modified from Coulter (2016).

1.2.1 Target Rocks

The target lithologies and footwall of the Sudbury impact structure consist of rocks of the Archean Superior Province and the Paleoproterozoic Southern Province, located north and south of the impact structure, respectively. The Superior Province is composed of greenstone granites, gneisses, metasedimentary rocks, and granitic intrusions. The Superior Province lithologies including the Levack Gneiss, Benny Greenstone Belt, and Cartier Batholith are spatially relevant to the Sudbury impact structure and are, collectively, 2.61 – 2.65 Ga in age (Krogh et al., 1984;

Meldrum et al., 1997). The Kenoran orogeny took place during 2.72 – 2.68 Ga and resulted in the deformation of the Benny Greenstone Belt and Levack Gneiss, and subsequent igneous activity, the Cartier Batholith (Krogh et al., 1984).

Metavolcanic and metasedimentary rocks comprise the Paleoproterozoic Southern Province are representative of a ~2.48 – 2.2 Ga long Wilson Cycle including a rifting and passive margin phase during the break-up of Kenorland, and a collisional phase associated with the 1.9 – 1.8 Ga Penokean orogeny (Corfu and Easton, 2001; Brocoum and Dalziel, 1974; Long, 2009). The Huronian Supergroup comprises the majority of the Southern Province and is predominantly represented by sandstones, mudstones, carbonates, and conglomerates, with minor occurrences of volcanics (Long, 2009). Regional greenschist facies metamorphism of the Huronian Supergroup is attributed to the Penokean orogeny, with amphibolite facies occurring locally (Long, 2009; Spray and Scott, 2000). Figure 1.4 illustrates the stratigraphy of the Huronian Supergroup in temporal reference to the associated rifting and passive margin stages (Long, 2009). prior to the 1.85 Ga impact event, the Southern Province had overlain the Superior Province (Brocoum and Dalziel, 1974; Corfu and Easton, 2001). The impact event took place in a foreland marine basin of the Penokean orogeny (Grieve et al., 2010), and resulted in the removal of the supracrustal rocks of the Southern Province and caused the underlying Superior Province rocks to be exposed at the surface (Brocoum and Dalziel, 1974; Dressler et al., 1996).

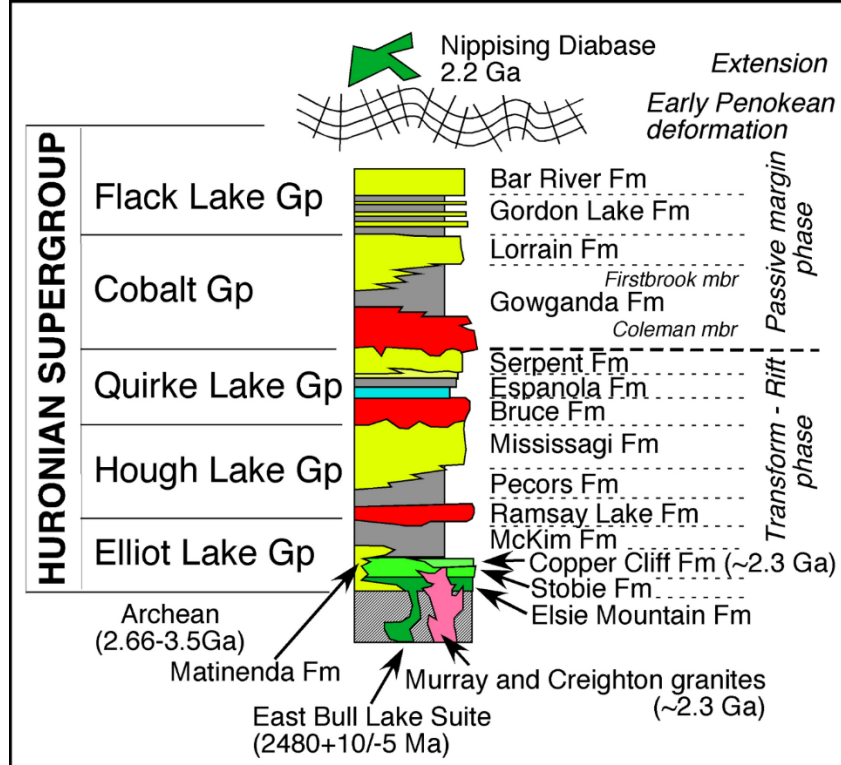


Figure 1.4. A stratigraphic section of the Huronian Supergroup, illustrating the depositional successions and igneous intrusions with the corresponding depositional environment over time from Long (2009).

1.3 The Sudbury Igneous Complex (SIC)

Historically, the SIC was termed the Sudbury Nickel Irruptive and was proposed to be an intrusive magmatic mass (Barlow, 1904, 1906). Based on a correct prediction of a footwall location for impact-induced shatter cones, Deitz (1964) was the first to suggest that the “irruptive” is, rather, the remains of an “astrobleme”. The SIC is now recognized as the eroded remnant of the coherent differentiated impact melt sheet of the Sudbury impact structure, with an estimated original volume of ~8,000–14,000 km³ (Deutsch et al., 1995; Grieve, 1994; Grieve et al., 2010; Therriault et al., 2002). An age of 1.85 Ga was determined by Krogh et al. (1984) based on U-Pb isotopes measured in zircon grains found throughout the SIC. The SIC is

comprised of three main units which overly a footwall sublayer (from bottom to top): norite, quartz gabbro, and granophyre (Gibbins and McNutt, 1975; Grieve et al., 2010; Dietz, 1964; Deutsch et al., 1995; Card, 1978; Anders et al., 2015). It is important to note that the nomenclature is not petrographically accurate, but is based on past field observations (Dietz, 1964). Based on geochemical results, Therriault et al. (2002) suggests the following nomenclature to better represent the units of the SIC: Lower Unit (previously norite), Middle Unit (previously quartz gabbro), Upper Unit (previously granophyre) (Fig. 1.5).

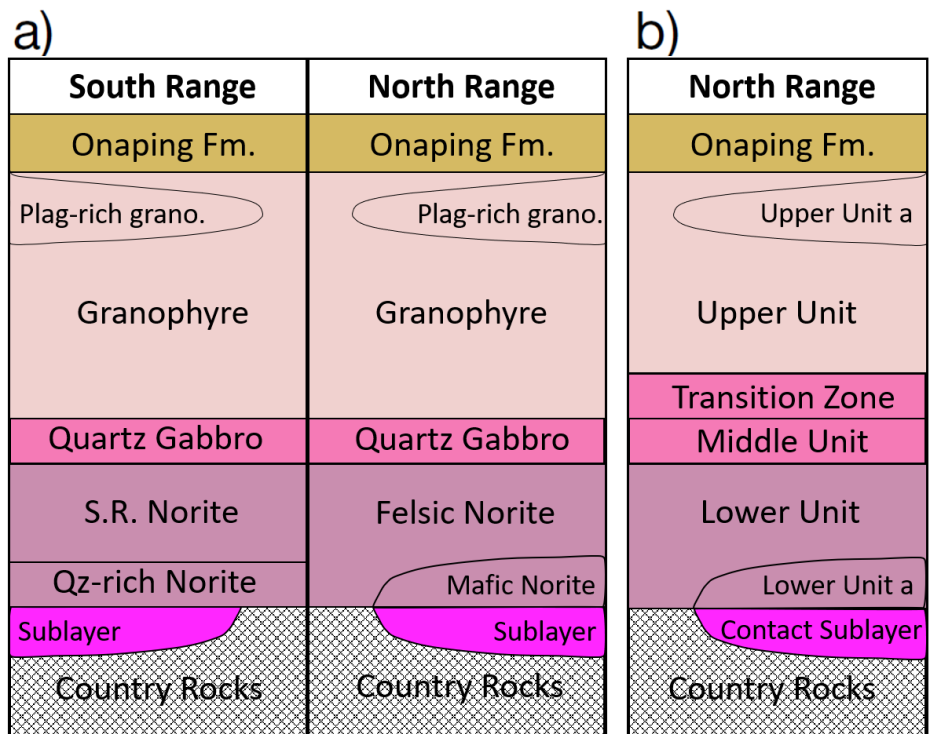


Figure 1.5. (A) Stratigraphic column of the South and North Ranges of the SIC with conventional nomenclature. (B) Proposed, new, nomenclature of SIC units. “Plag”: plagioclase; “Grano”: granophyre; “Qz”: quartz; “Fm”: formation; “S.R.”: South Range. Modified from Therriault et al. (2002).

The average thickness of the SIC is 2.5 km (Naldrett and Hewins, 1984); however, considerable thickness variations occur throughout the North Range (~800 m to 2750 m) and the South Range

(~3970 m to 6380 m) of the SIC (Dreuse et al., 2010; Lenauer and Riller, 2017). Thickness variations are attributed to crater floor topography and variations in the degree of syn- and post-impact tectonism resulting in folding and overturning, predominantly in the South Range (Dreuse et al., 2010; Lenauer and Riller, 2017). It is possible that thickness variations in the SIC are also the result of the presence or absence of an overlying insulator such as the rocks of the Onaping Formation that overly the SIC (Grieve et al., 2010).

Due to the superheated nature of the impact melt sheet, a resulting thermal aureole, up to 2 km wide, into the surrounding country rock yielded three main facies zones of thermal metamorphism: albite-epidote hornfels (1000 m wide), hornblende hornfels (900 m wide), and pyroxene hornfels (200 m) (Péntek et al., 2013; Boast and Spray, 2006). Hydrothermal activity associated with the SIC and post-impact orogenies coupled with contact metamorphism, resulted in hydrothermal alteration and metasomatic overprinting throughout the Sudbury impact structure (Boast and Spray, 2006; Molnár et al., 2001). Heat from the superheated melt sheet initiated thermal erosion and assimilation of the surrounding footwall, thereby forming footwall troughs and embayments that served as structural traps for magmatic ores (Péntek et al., 2008, 2013; Dreuse et al., 2010; O’Callaghan et al., 2016). Partial melting and mixing at the footwall-melt sheet interface further characterizes the effects of the thermal aureole (Péntek et al., 2013, 2008).

Radial offset dykes are observed originating from the SIC, specifically at footwall embayment structures, and radiate away from the SIC into the country rock (Card, 1978). Concentric offset dykes are observed occurring parallel to the elliptical SIC boundary, and on occasion, intersect radial offset dykes (Wood and Spray, 1998). The Sudbury offset dykes have traditionally been referred to as quartz diorite or “QD”, however, they are more accurately granodioritic in

composition (Pilles et al., 2017; Lightfoot and Keays, 2001). Currently, the offset dykes are considered to be geochemically indicative of the composition of the undifferentiated impact melt sheet (Lightfoot et al., 1997).

1.3.1 Sudbury Igneous Complex Ni-Cu-PGE Sulfide Ores

The earliest recognized presence of ore mineralization was made by a government land surveyor, A. P. Salter, in 1856 (Giblin, 1984; Lightfoot, 2017). At a location nearby Creighton Mine in Sudbury, Salter observed an attraction anomaly with a compass needle and noted the occurrence of iron in the rocks. An investigation of the rocks in the area revealed concentrations of copper and nickel (Giblin, 1984). The discovery of nickel that initiated the development of the Sudbury mining camp occurred during the construction of the Canadian Pacific Railway in 1883, whereby Thomas Flanagan noticed copper (nickel) sulfides in the rock being excavated to accommodate the railway (Lightfoot, 2017). Further investigation led to the establishment of Murray Mine in Sudbury (Lightfoot, 2017).

At present, the SIC is recognized as a significant influential component in the formation of Ni-Cu-PGE sulfide ore deposits at Sudbury, largely due to the superheated nature of the impact melt sheet (Grieve et al., 1991). According to Keays and Lightfoot (2004), the melt sheet was superheated with a temperature of 1700 °C, which allowed the SIC melt to have a sulfur capacity ~5 times greater than that of the SIC liquidus temperature of ~1200 °C. Three main styles characterize the ore deposits associated with the impact structure, including: (1) contact style, (2) footwall style, and (3) offset dyke-hosted. The contact style deposits are found between the SIC-footwall contact, specifically in troughs and embayments that serve as structural traps and host disseminated to semi-massive Fe-Ni-Cu-PGE sulfides (Morrison, 1984; McNamara et al., 2017).

Footwall deposits are situated within the target rocks below the SIC and are located up to 1 km away from the SIC (Morrison et al., 1994). Relative to contact deposits, they are more enriched in Ni-Cu-PGEs and contain higher Cu/Ni ratios with increasing distance from the SIC (McNamara et al., 2017; Péntek et al., 2008; Morrison et al., 1994). The Sudbury offset dykes originate from SIC embayment structures, and host semi-massive and disseminated pyrrhotite, pentlandite, and chalcopyrite mineralization (Morrison, 1984). Lightfoot and Farrow (2002) suggest that the sulfides found in the offset dykes originally formed within the melt sheet and were later injected into the offset dykes.

1.3.2 The Onaping Formation and the Onaping Intrusion

The Onaping Formation stratigraphically overlies the SIC and is the lowermost formation of the Whitewater Group (Muir and Peredery, 1984). The Onaping Formation is recognized as a hydrothermally altered ~1.5 km-thick suite of post-impact breccias (Ames et al., 2002). The Onaping Formation is conventionally divided into the Garson, Sandcherry, and Dowling (Lower, Middle, Upper) members. Unlike the Sandcherry and Dowling members, the Garson Member only occurs in the South Range (Coulter and Osinski, 2015). The Sandcherry member is ~500 m in maximum thickness and is comprised of massive to crudely bedded equant shard and fluidal units of vitric fragments suspended in microcrystalline matrix (Ames et al., 2002; Grieve et al., 2010). Granitoid and quartz lithic clasts deriving from the country rock are also suspended in the microcrystalline matrix (Grieve et al., 2010). The Dowling Member is characterized by a greater matrix component than the Sandcherry Member, and has lenticular, cusped, and amygdaloidal shards suspended within the matrix (Ames et al., 1998). Further up in the stratigraphy, the Dowling Member exhibits laminar bedding which has been interpreted as a sub-aqueous

depositional environment involving re-working and re-deposition of mass flow deposits (Ames et al., 2002; Grieve et al., 2010).

The Onaping Formation has historically been considered as a series of fallback breccias (Beales and Lozej, 1975; Ames et al., 1998); however, Grieve et al. (2010) suggest there was another major contributing factor in the deposition of the Onaping Formation. The Sudbury impact structure was formed in a foreland basin environment and, thus, inundation of the structure by sea water was a significant component in post-impact processes and intrinsic to the evolution of the Onaping Formation (Grieve et al., 2010). Thus, it was proposed that melt-fuel-coolant interaction (MFCI) explosions were a subsequent phreatomagmatic process after the impact melt sheet was infiltrated by and mixing with sea water (Grieve et al., 2010; Ames, 1999; Gibbins, 1994). As sea water reaches the superheated impact melt sheet, steam bubbles would expand and collapse (Grieve et al., 2010). Subsequent implosion of the bubbles would send seismic waves causing brittle fracturing of the melt sheet and explosive ejection of melt fragments (Grieve et al., 2010). The successions of deposited fragmented material would build up a series analogous to the Onaping Formation (Grieve et al., 2010; Ames, 1999; Gibbins, 1994). MFCI explosions provide an explanation for the sorted nature of the lower parts of the Onaping Formation, the laterally discontinuous igneous bodies at the base of the Onaping Formation, and for igneous bodies suspended higher up in the Onaping Formation (Anders et al., 2015; Grieve et al., 2010).

The Onaping Formation reportedly hosts laterally discontinuous, semi-conformable clast-rich igneous bodies along the base of the formation, and igneous pods higher up in the formation (Ames et al., 2002). These igneous bodies are up to 300 m in thickness and occur as discontinuous sheets between the granophyre and Sandcherry Member (Grieve et al., 2010). Such igneous bodies have been termed “melt bodies” by Muir and Peredery (1984), and the “Onaping

Intrusion” by Ames et al. (1998). Little work has been done to analyze the “melt bodies” of the Onaping Formation; however, early observations by Muir and Peredery (1984) suggested that the melt bodies have an igneous matrix and host granitoid and quartzite clasts. Field observations and geochemistry of the Onaping Intrusion are similar to those of the “melt bodies”; both lithologies are dioritic in composition (Anders et al., 2015; Brillinger, 2011; Gibbins, 1994; Dressler et al., 1996; Muir and Peredery, 1984). Comparative trace element work by Anders et al. (2015) indicates that the Onaping Intrusion is nearly identical to the average norite from drill core 70011 from the North Range (Therriault et al., 2002). Trace element compositions between the average granophyre from drill core 70011 from the North Range and Onaping Intrusion indicate that the Onaping Intrusion is genetically related to the granophyre, evidenced by similar relative trace element abundances (Anders et al., 2015). Evidence of shock metamorphism is exhibited as PDFs in quartz clasts throughout the Onaping Intrusion (Anders et al., 2015). These results indicate an impact melt origin for the so-called Onaping Intrusion and, therefore, it has been suggested that the Onaping Intrusion be referred to as the Upper Contact Unit of the SIC (Anders et al., 2015). The work of Anders et al., (2015) was restricted to two drill cores and one surface location (Joe Lake) in the northwest region of the North Range. Although the Garson Member is currently considered a constituent of the Onaping Formation, geochemical and stratigraphic similarities exist between the Onaping Intrusion and Garson Member, which indicates that both share the same origin as impact melt rocks (Coulter and Osinski, 2015).

1.4 References

- Ames, D.E., 1999, Geology and regional hydrothermal alteration of the crater-fill, Onaping Formation: Association with Zn-Pb-Cu mineralization, Sudbury structure, Canada. PhD. Thesis #406, Dept. of Earth Sciences, Carleton University, Ottawa, Ontario, Canada.
- Ames, D.E., Davidson, A., and Wodicka, N., 2008, Geology of the Giant Sudbury Polymetallic Mining Camp, Ontario, Canada: *Economic Geology*, v. 103, p. 1057–1077.
- Ames, D.E., Golightly, J.P., Lightfoot, P.C., and Gibson, H.L., 2002, Vitric compositions in the Onaping Formation and their relationship to the Sudbury Igneous Complex, Sudbury structure: *Economic Geology*, v. 97, p. 1541–1562.
- Ames, D.E., Watkinson, D.H., and Parrish, R.R., 1998, Dating of a regional hydrothermal system induced by the 1850 Ma Sudbury impact event: *Geology*, v. 26, p. 447–450.
- Anders, D., Osinski, G.R., Grieve, R.A.F., and Brillinger, D.T.M., 2015, The Basal Onaping Intrusion in the North Range: Roof rocks of the Sudbury Igneous Complex: *Meteoritics & Planetary Science*, v. 50, p. 1577–1594.
- Barlow, A.E., 1904, Report on the Origin, Geological Relations and Composition of the Nickel and Copper Deposits in the Sudbury Mining District, Ontario, Canada: Geological Survey of Canada Annual Report, Canada, p. 873.
- Barlow, A.E., 1906, On the origin and relations of the nickel and copper deposits of Sudbury, Ontario, Canada: *Economic Geology*, v. I, p. 454–466.

- Beales, F.W., and Lozej, G.P., 1975, Sudbury Basin Sediments and the Meteoritic Impact Theory of Origin for the Sudbury Structure: *Canadian Journal of Earth Sciences*, v. 12, p. 629–635.
- Boast, M., and Spray, J.G., 2006, Superimposition of a thrust-transfer fault system on a large impact structure: Implications for Ni-Cu-PGE exploration at Sudbury: *Economic Geology*, v. 101, p. 1583–1594.
- Brillinger, D.T.M., 2011, Possible evolution of the Onaping Intrusion as an impact melt rock at the Joe Lake Area, Sudbury, Ontario: University of Western Ontario, 44 p.
- Brocoum, S.J., and Dalziel, I.W.D., 1974, The Sudbury Basin, the Southern Province, the Grenville Front, and the Penokean Orogeny: *Bulletin of the Geological Society of America*, v. 85, p. 1571–1580.
- Card, K.D., 1978, Geology of the Sudbury-Manitoulin Area: Districts of Sudbury and Manitoulin: Ontario Ministry of Natural Resources, v. 166.
- Corfu, F., and Easton, R.M., 2001, U-Pb evidence for polymetamorphic history of Huronian rocks within the Grenville front tectonic zone east of Sudbury, Ontario, Canada: *Chemical Geology*, v. 172, p. 149–171.
- Coulter, A.B., 2016, Recent discoveries in the Ni-Cu-PGE bearing Trill and Parkin offset dykes, Sudbury impact structure, Canada: MSc. Thesis #3473, University of Western Ontario, Ontario, Canada, 137 p.

- Coulter, A.B., and Osinski, G.R., 2015, The nature and origin of the Garson Member of the Onaping Formation, Sudbury impact structure, Canada: Geological Society of America, v. Special Paper, p. 165–176.
- Deutsch, A., Grieve, R.A.F., Avermann, M., Bischoff, L., Brockmeyer, P., Buhl, D., Lakomy, R., Müller-Mohr, V., Ostermann, M., and Stöffler, D., 1995, The Sudbury Structure (Ontario, Canada): a tectonically deformed multi-ring impact basin: *Geologische Rundschau*, v. 84, p. 697–709.
- Dietz, R.S., 1964, Sudbury Structure as an Astrobleme: *The Journal of Geology*, v. 72, p. 412–434.
- Dressler, B.O., Weiser, T., and Brockmeyer, P., 1996, Recrystallized impact glasses of the Onaping Formation and the Sudbury Igneous Complex, Sudbury Structure, Ontario, Canada: *Geochimica et Cosmochimica Acta*, v. 60, p. 2019–2036.
- Dreuse, R., Doman, D., Santimano, T., and Riller, U., 2010, Crater floor topography and impact melt sheet geometry of the Sudbury impact structure, Canada: *Terra Nova*, v. 22, p. 463–469.
- Ferrière, L., and Osinski, G.R., 2013, Shock Metamorphism. In Osinski, G.R., and Pierazzo, E., eds., *Impact Cratering: Processes and Products*, Wiley-Blackwell, p. 106–124.
- Gault, D. E., Quaide, W. L., and Oberbeck, V. R., 1968, Impact cratering mechanics and structures: *Shock Metamorphism of Natural Materials*, p. 87–99.

- Gibbins, S.F.M., 1994, Geology, geochemistry, stratigraphy and mechanisms of emplacement of the Onaping Formation, Dowling area, Sudbury Structure, Ontario, Canada: MSc. Thesis, Laurentian University, Ontario, Canada, 304 p.
- Gibbins, W., and McNutt, R., 1975, Rubidium-Strontium mineral ages and polymetamorphism at Sudbury, Ontario: *Canadian Journal of Earth Sciences*, v. 12, p. 1990–2003.
- Giblin, P.E., 1984, History of Exploration and Development, of Geological Studies and Development of Geological Concepts, in Pye, E.G., Naldrett, A.J., and Giblin, P.E. eds., *Geology and Ore Deposits of the Sudbury Structure*, Ontario Geological Survey Special Volume 1, p. 3–23.
- Grieve, R.A.F., Ames, D.E., Morgan, J. V., and Artemevia, N., 2010, The evolution of the Onaping Formation at the Sudbury impact structure: *Meteoritics & Planetary Science*, v. 45, p. 759–782.
- Grieve, R.A.F., Stöffler, D., and Deutsch, A., 1991, The Sudbury Structure - controversial or misunderstood? *Journal of Geophysical Research-Planets*, v. 96, p. 22753–22764.
- Keays, R.R., and Lighfoot, P.C., 2004, Formation of Ni-Cu-PGE sulphide mineralisation in the Sudbury Impact Melt Sheet: *Mineralogy and Petrology*, v. 82, no. 3. p. 217-258.
- Kenkmann, T., Poelchau, M.H., and Wulf, G., 2014, Structural geology of impact craters: *Journal of Structural Geology*, v. 62, p. 156–182.
- Kieffer, S.W., and Simonds, C.H., 1980, The role of volatiles and lithology in the impact cratering process: *Reviews of Geophysics*, v. 18, p. 143–181.

- Krogh, T.E., Davis, D.W., and Corfu, F., 1984, Precise U-Pb zircon and baddeleyite ages for the Sudbury area: The geology and ore deposits of the Sudbury structure, v. 1, p. 431–446.
- Lenauer, I., and Riller, U., 2017, A trishear model for the deformation of the Sudbury Igneous Complex, Canada: *Journal of Structural Geology*, v. 97, p. 212–224.
- Lightfoot, P.C., 2017, Nickel Sulfide Ores and Impact Melts: Origin of the Sudbury Igneous Complex: Elsevier.
- Lightfoot, P.C., and Farrow, C.E.G., 2002, Geology, Geochemistry, and Mineralogy of the Worthington Offset Dike: A Genetic Model for Offset Dike Mineralization in the Sudbury Igneous Complex: *Economic Geology*, v. 97, p. 1419–1446.
- Lightfoot, P.C., and Keays, R.R., 2001, Sulfide saturation history and ore genesis in the Sudbury Igneous Complex: constraints from Main Mass, Sublayer, and Offset geology and geochemistry: v. 3238, p. 1.
- Lightfoot, P.C., Morrison, G.G., Bite, A., and Farrell, P., 1997, Geochemical Relationships in the Sudbury Igneous Complex: Origin of the Main Mass and Offset Dikes: *Economic Geology*, v. 92, p. 289–307.
- Long, D.G.F., 2009, The Huronian Supergroup, in Rousell, D., and Brown, G., eds., *A Field Guide to the Geology of Sudbury, Ontario*, Ontario Geological Survey Open File Report 6243, p. 14–30.
- McNamara, G.S., Leshner, C.M., and Kamber, B.S., 2017, New feldspar lead isotope and trace element evidence from the Sudbury igneous complex indicate a complex origin of associated

Ni-Cu-PGE mineralization involving underlying country rocks: *Economic Geology*, v. 112, p. 569–590.

Meldrum, A., Abdel-Rahman, A.F.- M., Martin, R.F., and Wodicka, N., 1997, The nature, age and petrogenesis of the Cartier Batholith, northern flank of the Sudbury Structure, Ontario, Canada: *Precambrian Research*, v. 82, p. 265–285.

Molnár, F., Watkinson, D.H., and Jones, P.C., 2001, Multiple hydrothermal processes in footwall units of the North Range, Sudbury Igneous Complex, Canada, and implications for the genesis of vein-type Cu-Ni-PGE deposits: *Economic Geology*, v. 96, p. 1645–1670.

Melosh, H.J., 1985, Impact cratering mechanics: Relationship between the shock wave and excavation flow: *Icarus*, v. 62, p. 339–343.

Melosh, H.J., 1989, *Impact cratering—A geologic process*: New York, Oxford University Press, 245 p
Melosh, H., 1979, Acoustic fluidization: A new geologic process?: *Journal of Geophysical Research*, v. 84, p.7513 – 7520.

Melosh, H.J., and Ivanov, B.A., 1999, Impact Crater Collapse: *Annual Review of Earth and Planetary Sciences*, v. 27, p. 385–415.

Morgan, J. V., Gulick, S.P.S., Bralower, T., Chenot, E., Christeson, G., Claeys, P., Cockell, C., Collins, G.S., Coolen, M.J.L., Ferrière, L., Gebhardt, C., and Goto, K., 2016, The formation of peak rings in large impact craters: v. 354, p. 878–882.

Morrison, G.G., 1984, Morphological features of the Sudbury structure in relation to an impact origin. In Pye, E.G., Naldrett, A.J., and Giblin, P.E., eds., *The Geology and Ore Deposits of the Sudbury Structure: Ontario Geological Survey, Special Volume 1*, p. 513–520.

Morrison, G.G., Jago, B.C., White T.L., 1994, Footwall mineralization of the Sudbury Igneous Complex. In Lightfoot P.C. and Naldrett A.J., eds., *Proceedings of the Sudbury-Noril'sk Symposium: Ontario Geological Survey, Special Volume 5*, p. 57-64.

Muir, T.L., and Peredery, W. V., 1984, The Onaping Formation. In Pye, E.G., Naldrett, A.J., and Giblin, P.E., eds., *The geology and ore deposits of the Sudbury Structure: Ontario Geological Survey Special Volume 1*, p. 235-251.

Nahm, A.L., Öhman, T., and Kring, D.A., 2013, Normal faulting origin for the cordillera and outer rock rings of Orientale basin, the Moon: *Journal of Geophysical Research E: Planets*, v. 118, p. 190–205.

Naldrett, A.J., and Hewins, R.G., 1984, The main mass of the Sudbury Igneous Complex. In Pye, E.G., Naldrett A.J., and Giblin P.E., eds., *The geology and ore deposits of the Sudbury Structure: Ontario Geological Survey Special Volume 1*, p. 235-251.

O'Callaghan, J.W., Osinski, G.R., Lightfoot, P.C., Linnen, R.L., and Weirich, J.R., 2016, Reconstructing the geochemical signature of Sudbury Breccia, Ontario, Canada: Implications for its formation and trace metal content: *Economic Geology*, v. 111, p. 1705–1729.

- Osinski, G.R., Grieve, R.A.F., Bleacher, J.E., Neish, C.D., Pilles, E.A., and Tornabene, L.L., 2018, Igneous rocks formed by hypervelocity impact: *Journal of Volcanology and Geothermal Research*, v. 353, p. 25–54.
- Osinski, G.R., and Pierazzo, E., 2013, Impact cratering: processes and products. In Osinski, G.R. and Pierazzo, E. eds., *Impact Cratering: Processes and Products*, Wiley-Blackwell, p. 1–20.
- Osinski, G.R., Tornabene, L.L., and Grieve, R.A.F., 2011, Impact ejecta emplacement on terrestrial planets: *Earth and Planetary Science Letters*, v. 310, p. 167–181.
- Pattison, E.F., 2009, Sudbury Igneous Complex. In Rousell, D., and Brown, G., eds., *A Field Guide to the Geology of Sudbury, Ontario*: Ontario Geological Survey, p. 56–74.
- Péntek, A., Molnár, F., Tuba, G., Watkinson, D.H., and Jones, P.C., 2013, The significance of partial melting processes in hydrothermal low sulfide Cu-Ni-PGE mineralization within the footwall of the Sudbury Igneous Complex, Ontario, Canada: *Economic Geology*, v. 108, p. 59–78.
- Péntek, A., Molnár, F., Watkinson, D.H., and Jones, P.C., 2008, Footwall-type Cu-Ni-PGE mineralization in the Broken Hammer area, Wisner township, North Range, Sudbury structure: *Economic Geology*, v. 103, p. 1005–1028.
- Pilles, E.A., Osinski, G.R., Grieve, R.A.F., Smith, D.A., and Bailey, J.M., 2017, Chemical variations and genetic relationships between the Hess and Foy offset dikes at the Sudbury impact structure: *Meteoritics and Planetary Science*, v. 52, p. 2647–2671.

- Potter, R.W.K., Kring, D.A., Collins, G.S., Kiefer, W.S., and McGovern, P.J., 2013, Numerical modeling of the formation and structure of the Orientale impact basin: *Journal of Geophysical Research: Planets*, v. 118, p. 963–979.
- Rousell, D.H., 1975, The origin of foliation and lineation in the Onaping formation and the deformation of the Sudbury Basin: *Canadian Journal of Earth Sciences*, v. 12, p. 1379–1395.
- Spray, J.G., and Scott, R.G., 2000, The South Range Breccia Belt of the Sudbury Impact Structure: A possible terrace collapse feature: *Meteoritics and Planetary Science*, v. 35, p. 505–520.
- Stöffler, D., and Grieve, R.A.F., 2007, Impactites: *Metamorphic Rocks: A Classification and Glossary of Terms, Recommendations of the International Union of Geological Sciences*, p. 82–92, 111-125-242.
- Therriault, A.M., Fowler, A.D., and Grieve, R.A.F., 2002, The Sudbury Igneous Complex - an impact melt sheet?: *Economic Geology*, v. 97, p. 1521–1540.
- Wood, C.R., and Spray, J.G., 1998, Origin and Emplacement of Offset Dykes in the Sudbury impact structure: Constraints from Hess: *Meteoritics and Planetary Science*, v. 33, p. 337–347.

Chapter 2

2 The Upper Contact Unit (roof rocks) of the Sudbury Igneous Complex, North Range, Sudbury impact structure, Canada

2.1 Introduction

The melting of large rock volumes of target material is a characteristic of hypervelocity impact (see recent review by Osinski et al., 2018). Like any large igneous body, a chilled upper phase or “roof rocks” is predicted to occur at the top of impact melt sheets on Earth and other planetary bodies. These rocks, by definition, would be classified as impact melt rocks (Grieve et al., 2010), specifically, an igneous rock which hosts clasts of assimilated fallback material (Grieve et al., 2010; Onorato et al., 1978). The Sudbury Basin hosts the largest exposed impact melt sheet on Earth, known as the Sudbury Igneous Complex (SIC) (Grieve et al., 2010). Initially, the SIC was considered as an endogenic intrusive magmatic mass and was termed the Sudbury Nickel Irruptive, being, compared to layered mafic intrusions (Barlow, 1904, 1906; Barnes et al., 2015; Naldrett, 1989). As with layered mafic intrusions, the roof and floor rocks of impact melt sheets should exhibit a finer grain size than the main mass and represent the initial composition of the magmatic body due to relatively rapid cooling and crystallization rates (Grieve et al., 2010).

Until recently, there has been very little to no recognition of an upper chilled phase or roof rocks occurring in the upper reaches of the SIC (Therriault et al., 2002; Grieve et al., 2010; Anders et al., 2015). However, a study of two drill cores from the North Range (core 70011 from 46.725272N 81.059688W, core 52847 from 46.682925N, 81.194327W) by Anders et al. (2015) suggested that parts of a unit previously termed the “Onaping Intrusion” (Ames et al., 1998, 2002, 2005, 2008) exhibits geochemical and petrographical evidence with characteristics consistent with being the roof rocks of the SIC. This calls into question the conventional

characterization of the Onaping Intrusion as being a post-impact igneous body that intruded into the base of the Onaping Formation. Indeed, the Onaping Intrusion has traditionally been categorized as a component of the complex series of breccias of the Onaping Formation that overlie the SIC (Ames et al., 1998, 2002). Furthermore, the Onaping Intrusion has also been mapped as occurring in higher stratigraphic levels of the Onaping Formation and the origin of these rocks remains enigmatic.

This study builds on the preliminary, geographically limited study of Anders et al. (2015), and carries out a targeted investigation of the Onaping Intrusion throughout the entire North Range of the SIC. In addition to the Onaping Intrusion, we also investigated other igneous bodies within the Onaping Formation, including quartz diorite (Ames, 2005), and the so-called “melt bodies” which have been described as hypabyssal igneous intrusions due to their texture, structure, and stratigraphic position (Muir and Peredery, 1984; Ames, 2005).

The SIC has been the strategic exploration target behind the production of world-class Ni-Cu-PGE deposits at Sudbury due to the profound influence on ore deposit evolution and formation (Lightfoot, 2017). It is critical to investigate the roof rocks of the SIC to improve our understanding of the ore-hosting complex and the processes involved in its geological evolution and formation. Additionally, investigating the roof rocks of the SIC can provide further insight on impact melting and impact cratering processes on Earth and throughout the Solar System.

2.1.1 Geological Setting

The Sudbury Basin observed today is the tectonized, eroded remnant of a ~1.85 Ga impact structure that formed due to an asteroid or comet impact that occurred within a foreland marine basin setting during the Penokean orogeny (Dietz, 1964; Krogh et al., 1984; Ames et al., 2008;

Grieve et al., 2010). Syn- and post-impact tectonism associated with the 1.9 – 1.8 Ga Penokean orogeny, 1.77 – 1.60 Ga Yavapai-Mazatzal orogeny, ~1.45 Chieflakian event, and ~1.0 Ga Grenville orogeny, deformed the structure from a ~200 km diameter impact structure into a subsequently eroded ~60 km by 27 km elliptical basin yielding the North, South, and East Ranges (Giblin, 1984; Grieve et al., 1991; Spray and Scott, 2000; Péntek et al., 2013). The most prominent feature remaining of the impact structure is the differentiated 2.5 – 3.0 km thick impact melt sheet, or SIC, which is divided into the following units that overlay a footwall sublayer (from bottom to top): norite, quartz gabbro, and granophyre (Gibbins and McNutt, 1975; Grieve et al., 2010; Dietz, 1964; Deutsch et al., 1995; Card, 1978; Anders et al., 2015). Post-impact tectonism and erosion has resulted in a “bullseye” pattern exposure of the SIC units, whereby stratigraphically higher SIC units are exposed as the inner “rings” of the bullseye, and lower units are exposed towards the outer ring (Fig. 2.1).

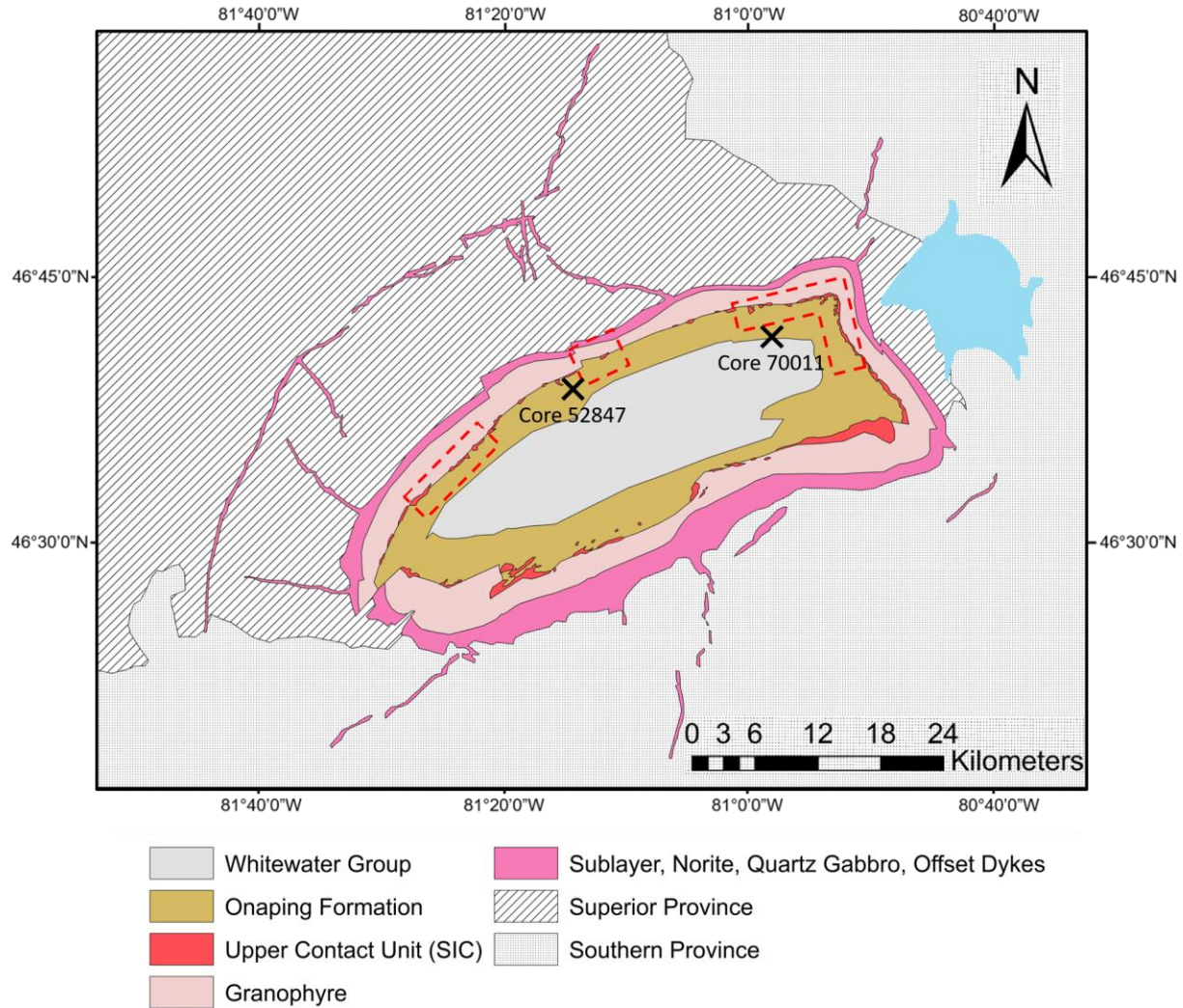


Figure 2.1. A simplified map of the Sudbury Basin and the "bullseye" pattern representing the SIC, Onaping Formation, and Whitewater Group. Red dashed boxes represent the field sites in this study. Drill core analyzed in Anders et al (2015) are shown by "X". Modified from Ames et al. (2005), and Coulter and Osinski. (2015).

Radial and concentric offset dykes of granodioritic composition originate from the melt sheet and occur throughout the surrounding country rock (Lightfoot et al., 1997). The SIC hosts the three main styles of ore deposits at the Sudbury mining camp: (1) contact style, (2) footwall style, and (3) offset dyke-hosted. The effects of thermal erosion from the superheated melt sheet resulted in the formation of troughs and embayments at the SIC-footwall contact that function has structural

traps hosting disseminated to massive Fe-Ni-Cu-PGE sulfides (Morrison, 1984; McNamara et al., 2017). Footwall style deposits occur within the footwall and are more enriched in Ni-Cu-PGEs as well as contain higher Cu/Ni ratios with increasing distance from the SIC (Morrison, 1984; Péntek et al., 2008; McNamara et al., 2017). The offset dykes originate from embayment structures in the footwall, and predominantly host semi-massive and disseminated pyrrhotite, pentlandite, and chalcopyrite mineralization (Morrison, 1984). The footwall of the SIC is comprised of rocks of the Archean Superior Province and the Paleoproterozoic Southern Province, located north and south of the impact structure, respectively (Brocoum and Dalziel, 1974). Prior to the ~1.85 Ga impact event, the metavolcanic and metasedimentary rocks of the Southern Province had stratigraphically overlain the greenstone rocks of the Superior Province (Brocoum and Dalziel, 1974). The excavation stage of the impact event resulted in the removal of material including that of the Southern Province, thereby exposing the underlying rocks of the Superior Province (Fig. 2.2) (Brocoum and Dalziel, 1974).

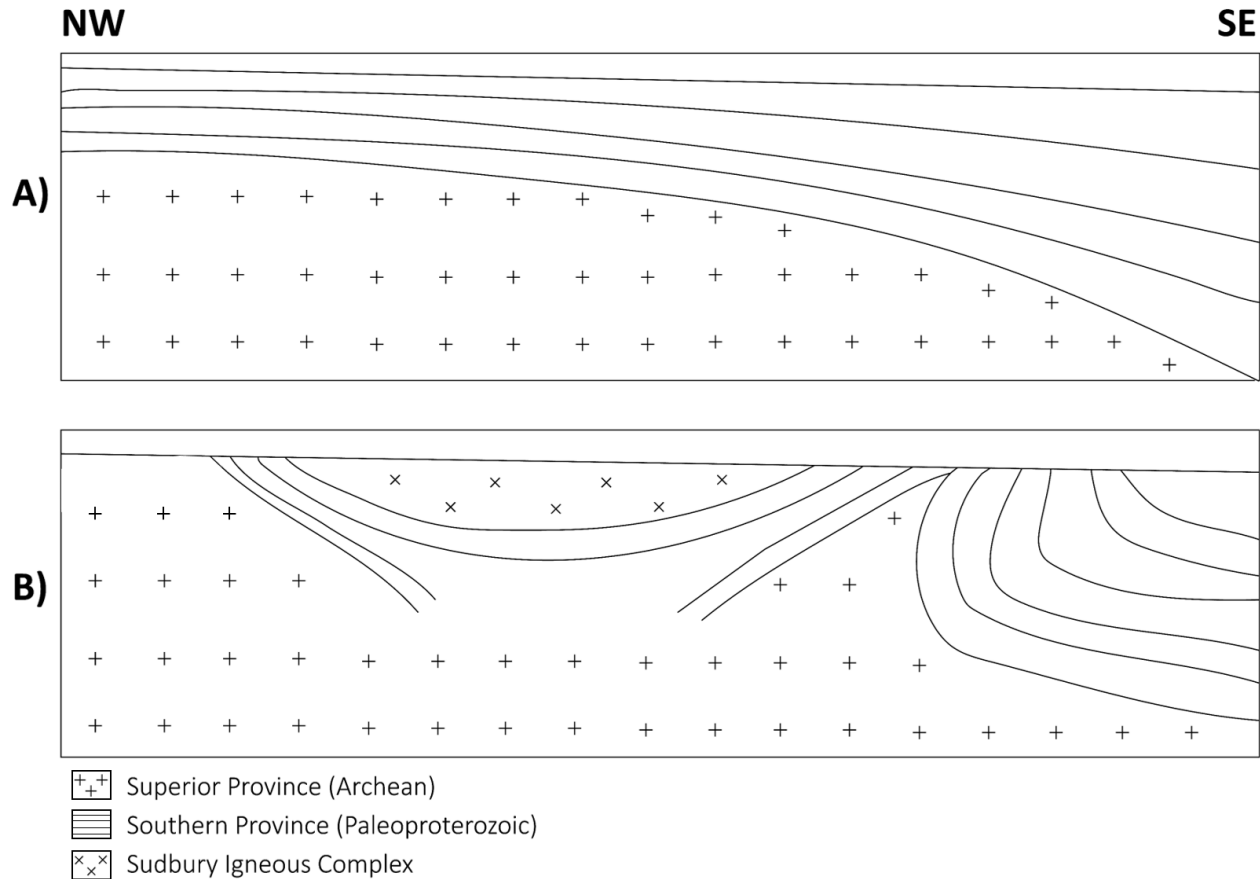


Figure 2.2. A simplified cross section displaying the stratigraphic arrangement between the Superior and Southern Provinces pre- and post-impact. (A) Pre-impact: The Southern Province overlies the rocks of the Superior Province, with thickening towards the southwest. (B) Post-immediate impact: The rocks of the Southern Province are excavated, uplifted upwards and outwards to form the crater rim. The SIC melt sheet occurs between the uplifted target rocks. Modified from Brocoum and Dalziel (1974).

The SIC is overlain by a ~2.9 km thick series of post-impact units known as the Whitewater Group, which is divided into the following units (from bottom to top): the Onaping, Vermilion, Onwatin, and Chelmsford Formations (Fig. 2.1) (Dietz, 1964; Beales and Lozej, 1975; Muir and Peredery, 1984; Gibbins, 1994). The Vermilion Formation hosts Zn-Pb-Cu VMS deposits within carbonate and turbidite units, which is overlain by the carbonaceous shale of the Onwatin Formation, followed by greywacke turbidites of the Chelmsford Formation (Gibbins, 1994). The

Onaping Formation is a ~1.4 – 1.5 km thick complex series of breccias divided into the (from bottom to top) Garson, Sandcherry, and Dowling members (Ames et al., 2002; Grieve et al., 2010). The Garson Member only occurs in the South Range, whereas the Sandcherry and Dowling members occur throughout the North, South, and East Ranges (Fig. 2.1) (Brocoum and Dalziel, 1974; Avermann and Brockmeyer, 1992; Ames et al., 2002; Lafrance et al., 2008; Coulter and Osinski, 2015). The typical range of relative thickness ratios between “fallback” breccia to coherent impact melt sheet is from ~1.6 to 1:16 (Grieve et al., 2010); in the case of the Sudbury Basin, the thickness ratio of the Onaping Formation breccia to that of the SIC melt sheet is significantly large (~1:2), whereby the SIC is 2.5 – 30 km thick (Therriault et al. 2002) and the Onaping Formation is 1.4 – 1.6 km thick (Ames et al., 1998, 2002). The excess volume of fallback material warrants speculation as to its evolution and suggests that the present Onaping Formation was shaped by other complex processes. A hypothesis presented by Grieve et al. (2010) proposes that the breccias of the Onaping Formation formed as a result of phreatomagmatic activity or melt-fuel-coolant interaction (MFCI) activity between the hot impact melt sheet and cooler inundating sea water. The hypothesis demonstrates that as sea water comes in contact with the superheated impact melt sheet, steam bubbles expand and collapse (Grieve et al., 2010). Subsequent implosion of the bubbles sends seismic waves causing brittle fracturing of the melt sheet and explosive ejection of melt fragments (Grieve et al., 2010). Explosive brecciation of impact melt, roof rocks, and fallback material results in mixing of equant breccias and vitric clasts between the lithologies, ultimately forming the complex series of breccias of the Sandcherry member (Grieve et al., 2010; O’Sullivan et al., 2016). The overlying Dowling member exhibits clasts which are lenticular in shape and are finer grained than those of the Sandcherry member, alluding to a change in nature of MFCI activity, namely the water:melt

mass ratio, throughout the duration of the evolution of the Onaping Formation (Grieve et al., 2010; Ames et al., 2002). In addition to MFCI activity, wash-in of fallback debris from outside the crater rim is considered a possible contribution of material in the Onaping Formation (Peredery, 1972b; Gibbins, 1994).

2.1.1.1 The “Onaping Intrusion”, Upper Contact Unit of the SIC

Along approximately 50% of the granophyre-Onaping Formation contact an igneous unit previously termed the “Onaping Intrusion” occurs as discontinuous semi-conformable sheets up to 300 m thick (Fig. 2.1) (Muir and Peredery, 1984; Avermann and Brockmeyer, 1992; Gibbins, 1994; Ames et al., 1998; Ames, 1999; Grieve et al., 2010; Brillinger, 2011; Anders et al., 2015). The so-called Onaping Intrusion is generally described as having a fine- to medium-grained grey to dark-grey matrix which is predominantly comprised of interlocking intergrowth of feldspar and quartz (Avermann and Brockmeyer, 1992; Gibbins, 1994; Grieve et al., 2010; Anders et al., 2015). Feldspar abundance in the Onaping Intrusion is dominated by plagioclase in the upper reaches, whereas the lower reaches are more dominated by potassium feldspar and an increase in patches of micrographic intergrowth (Ames, 1999; Anders et al., 2015). Lesser amounts of pyroxene, hornblende, and biotite also occur within the matrix, and occasionally yield secondary alteration minerals such as chlorite, epidote, and calcite (Ames, 1999; Anders et al., 2015). Rounded to subrounded clasts suspended in the matrix are typically quartzite or granitic in composition followed by lesser amounts of mafic clasts, consistent with the target lithologies (Stevenson, 1963; Gibbins, 1994; Ames, 1999; Grieve et al., 2010; Anders et al., 2015). Reaction coronae commonly occur around clasts and indicate past thermal and chemical reactions at the clast-matrix interface (Gibbins, 1994; Grieve et al., 2010; Anders et al., 2015). Grains within assimilated quartzite clasts exhibit planar deformation features (PDFs) as a result of impact-

induced shock metamorphism, with common orientation angles of $\sim 21 - 25^\circ$ (Therriault et al., 2002; Anders et al., 2015). Matrix grain size and clast abundance trends in the Onaping Intrusion relative to distance from the SIC have previously been reported, whereby matrix grain size decreases with increasing distance (moving upward in the stratigraphy, herein) from the granophyre and clast abundance increases with increasing distance from the granophyre (Stevenson, 1963; Gibbins, 1994; Anders et al., 2015). Both trends are attributed to a combination of factors: (1) A thermal gradient whereby higher temperatures occur in the lower parts of the Onaping Intrusion due to approaching the upper surface of the hot SIC. Mineral phases in the lower Onaping Intrusion undergo a longer cooling period and therefore exhibit larger grain sizes relative to the mineral phases in the cooler upper reaches of Onaping Intrusion (Grieve et al., 2010; Anders et al., 2015). In addition to the temperature gradient, thermal equilibrium taking place between assimilated cooler clasts as fallback material in the upper Onaping Intrusion would have further promoted a relatively rapid crystallization period in the upper Onaping Intrusion (Grieve et al., 2010; Anders et al., 2015). (2) Complete assimilation of clasts in the lower reaches of the Onaping Intrusion would be the result of approaching higher temperatures as the SIC contact is approached (Grieve et al., 2010; Anders et al., 2015). Conversely, the upper cooler reaches of the Onaping Intrusion exhibits a greater abundance and size of clasts due to partial melting and an overall lesser degree of assimilation of clasts (Grieve et al., 2010; Anders et al., 2015). The Onaping Intrusion-granophyre contact has been reported to be gradational, whereas the contact between the Onaping Intrusion and the breccias of the Onaping Formation is sharp (Gibbins, 1994; Ames, 1999; Grieve et al., 2010; Anders et al., 2015).

Historically, the Onaping Intrusion is an enigmatic unit of the Sudbury impact structure, evidenced by the multiple different theories and suggestions made as an attempt to explain the geological processes involved in its evolution and emplacement (Table 2.1).

Table 2.1. A history of the previous nomenclature of the “Onaping Intrusion”. Modified from Anders et al. (2015).

Nomenclature	Author/s
Upper Contact Unit (UCU) of the SIC	Anders et al. (2015)
Basal Onaping Intrusion	Ames et al. (2005, 2008); Grieve et al. (2010)
Basal intrusion	Ames et al. (1998); Gibbins et al. (2004)
Basal intrusion (basal member + melt bodies inclusive)	Gibbins (1994)
Melt bodies	Muir and Peredery (1984)
Basal member	Muir (1981, 1983); Peredery (1972a, b)
Tectonic quartzite breccia	Stevenson (1961, 1963, 1972)
Rhyolite breccia, rhyolite	Thomson (1957); Williams (1957)
Rhyolite, agglomerate	Burrows and Rickaby (1930)
Trout Lake conglomerate	Coleman (1905)
Quartzite conglomerate	Bell (1983)

However, a recent study conducted in the Joe Lake area by Anders et al. (2015) indicated that the Onaping Intrusion is not related to nor a component of the complex series of breccias of the Onaping Formation, but rather a unit genetically related to the SIC, specifically, as the roof rocks of the complex. As such, it was suggested that the “Onaping Intrusion” term be discontinued and the term “Upper Contact Unit” of the SIC be used (Anders et al., 2015). The findings and conclusions by Anders et al. (2015) are further supported by suggestions previously made by Stevenson (1963), Peredery (1972a), Brockmeyer and Deutsch (1989), Stöffler et al. (1989), Avermann and Brockmeyer (1992), Deutsch et al. (1990, 1995), and Grieve et al. (2010).

Although there has been little literature specifically on the Onaping Intrusion in the South Range of the Sudbury Basin, Muir and Peredery (1984) describes the Garson member of the Onaping Formation as the “Basal Member (Onaping Intrusion) of the South Range”. While the Garson Member is traditionally considered a constituent of the Onaping Formation confined to the South Range, its stratigraphic position, geochemistry, and outcrop characteristics are analogous with that of the Onaping Intrusion in the North Range. Therefore, it was suggested that both units are in actuality the same unit, namely, the UCU, and share the same impact melt origin (Coulter and Osinski, 2015).

2.2 Methodology

A total of 114 hand samples were collected from the North Range of the Sudbury Basin along and proximal to the granophyre-Onaping Formation contact (Fig. 2.1). Hand samples were collected in dispersed and transect fashion based on outcrop availability, and ground truthing was conducted with reference to the most recent geological maps in 1:50 000 scale of the Sudbury region (Ames et al. (2005) and 1:10 000 scale of the Onaping Formation (Gibbins et al., 2004). An Olympus BX51 microscope at the University of Western Ontario was used to carry out transmitted and reflected light optical microscopy on 80 thin sections from the 114 collected samples. Mineral modal analysis via point counting was conducted on 14 selected thin sections which were chosen based on best representability of the UCU. Clast content, size, and composition of 236 clasts from 15 thin sections of UCU were analyzed using a Nikon Eclipse LV100 POL microscope with built-in Nikon NIS Elements software. The clast data set produced from this study was combined and compared with those of Anders et al. (2015).

A JEOL JXA-8530F field emission electron microprobe at the Earth and Planetary Materials Analysis (EPMA) Laboratory at the University of Western Ontario was used to conduct energy

dispersive spectroscopy (EDS) and backscattered electron (BSE) imagery on 21 and 17 samples, respectively. Semi-quantitative analysis was used to confirm mineral phases using EDS. Beam conditions were 15kV accelerating voltage at 20 – 200nA current, with a 10 second counting time. Grain sizes of potassium feldspar (K-spar) grains within the UCU were chosen as a representative proxy, measured using BSE imagery, and processed using ImageJ™ software in order to collect measurement data (Fig. 2.3).

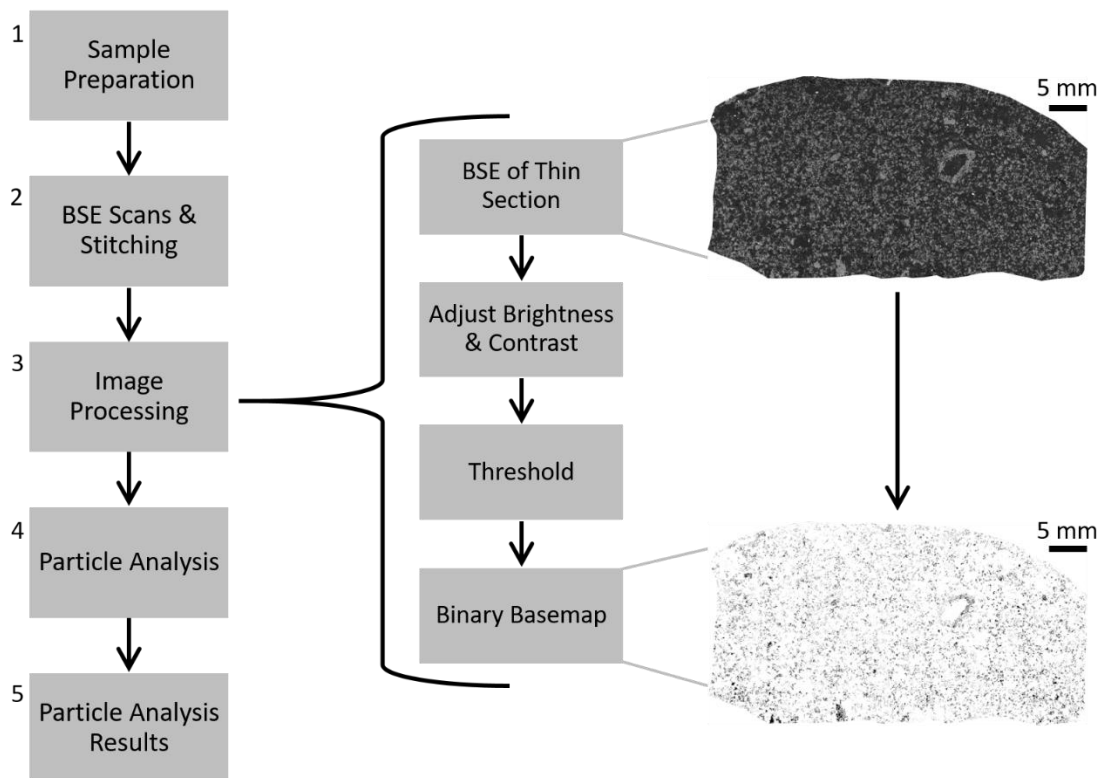


Figure 2.3. (1) Sample Preparation: Field samples were cut and made into polished, carbon coated thin sections. (2) BSE Scans and Stitching: entire thin sections were scanned in a series of tiles, combined via stitching using the Guide-Net mapping program. (3) Image Processing: The BSE thin section images were imported into ImageJ™ software and processed to enhance the brightness and contrast between the potassium feldspar grains from the remaining mineral phases. A threshold was applied yielding a binary basemap where grains of interest (K-spar) are selected (in black) from other mineral phases (white). (4) Particle Analysis: The Particle Analysis tool in ImageJ™ was selected to measure the long axis of each individual K-spar grain. (5) Particle Analysis Results: The data results containing the long axis measurements were used to calculate average grain size for the particular sample being analyzed.

Inductively coupled plasma mass spectrometry (ICP-MS) and XRF (X-ray fluorescence spectroscopy) whole rock geochemistry was carried out to obtain major, trace, and rare earth element (REE) data on 38 samples. The 38 samples were selected based on little to no visible clast content throughout the matrix at the hand sample scale, and, at the University of Western Ontario, were milled into pulps and sent for XRF and ICP-MS analysis to the Department of Earth Sciences' XRF laboratory (University of Western Ontario) and ALS Ltd. in Sudbury, Ontario, respectively. Geochemical data produced from this study was combined with geochemical data from SIC units in the North Range (Naldrett et al. 1984; Therriault et al., 2002), and from the North Range offset dykes (Anders, 2016; Coulter, 2016; Pilles, 2016; Pilles et al., 2017, 2018). REE data was normalized to C1 Chondrite data (Sun and McDonough, 1995).

2.3 Observations

2.3.1 Field Observations

Outcrops of the UCU and host units were investigated and sampled across the North Range of the Sudbury Basin (Fig. 2.4). The fresh surface of the UCU is grey to dark-grey, and weathers light-grey to dark-grey. In cases where the matrix is medium grained, an igneous texture is observed, comprised of quartz, feldspar phases, and amphibole. Very fine grains of the matrix exhibit a sugary texture. Towards the east end of the North Range and the North Range-East Range junction, an increase in shear deformation occurs in the matrix at the outcrop scale and appears similar to the Garson Member in the South Range (Fig. 2.4, Cluster 3; Fig. 2.5 B, C).

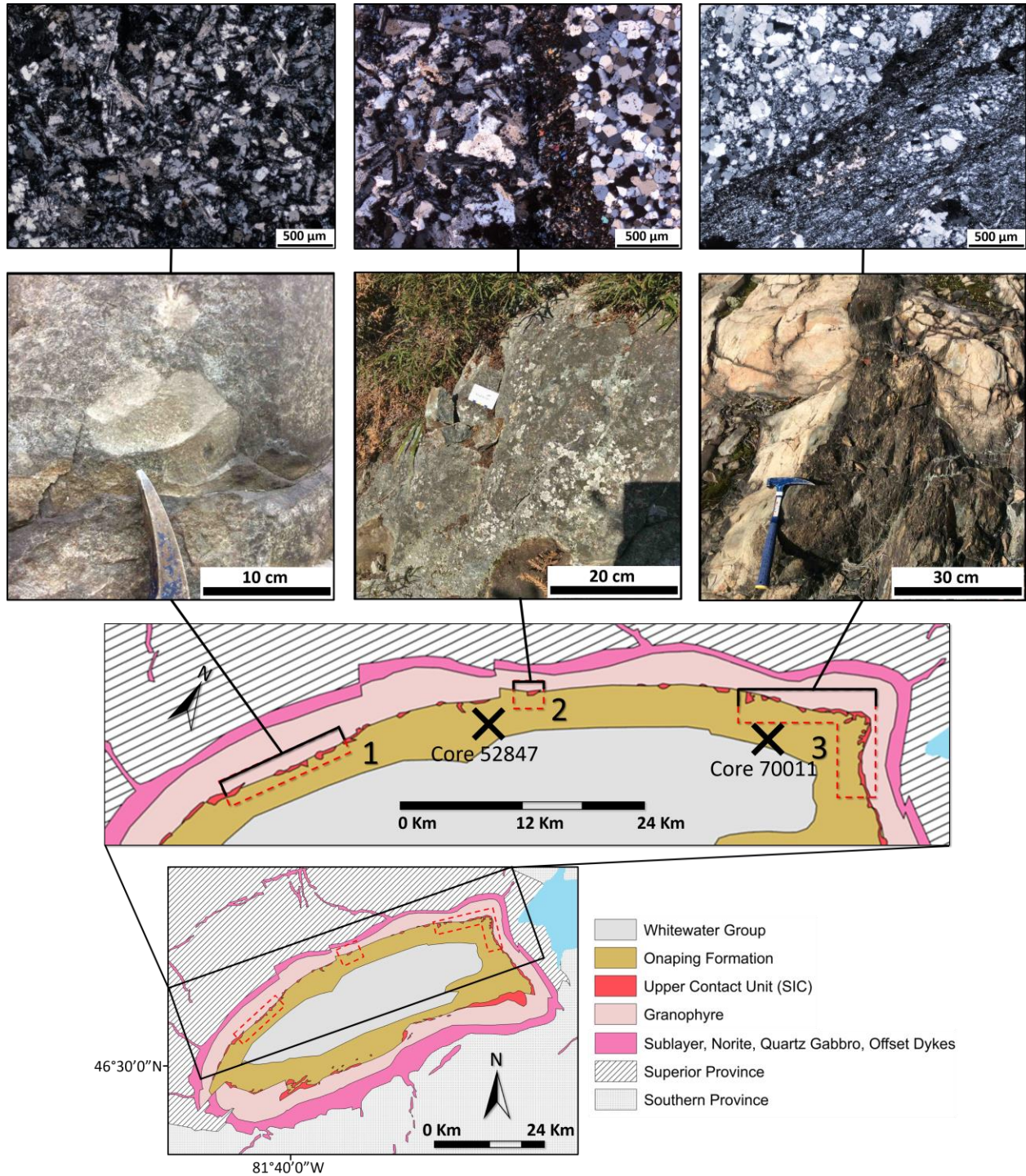


Figure 2.4. Field areas are organized into "clusters" numbered from one to three for simplicity. Field images coupled with photomicrographs from respective clusters show characteristics of the UCU throughout the North Range investigation. Cluster 1 shows an example of a clast in UCU matrix at the outcrop scale, and a photomicrograph showing typical UCU matrix. Cluster 2 shows a highly weathered UCU outcrop with a photomicrograph of a quartzite clast with a reaction corona, surrounded by UCU matrix. Cluster 3 shows a sheared UCU outcrop, where the matrix appears to have undergone deformation and the clasts appear to not have been affected or

affected to a lesser degree. The photomicrograph shows the shear textures of the UCU matrix juxtaposed against a quartzite clast.

Typically, the UCU matrix contains ~40% subrounded to rounded clasts, however, clast content overall ranges between 5 – 75%. Such clasts are ~72% quartzite, 25% granitoid, and <3% mafic clasts which have either sharp boundaries with the matrix or exhibit finer grained reaction rims, consistent with chemical and/or thermal reactions at the clast-matrix interface. Clast size ranges from mm-scale to ~5 m, whereby mafic clasts occur as mm-scale and felsic clasts dominate the entire clast size range. Subrounded oxidized sulfide metal “blebs” are also observed with sharp contacts with the matrix, are <5 cm in diameter, and comprise 1 – 5% of the total “clast” abundance (Fig. 2.5 A). As observed in the field, pyrrhotite is the dominant sulfide comprising the sulfide blebs.



Figure 2.5. (A) Photo of a well-exposed, typical outcrop of the UCU, previously mapped as Onaping Intrusion by Ames et al. (2005). Note the granitoid and quartzite clasts, and sulfide “blebs” suspended in the grey matrix. (B, C) Outcrops of the Upper Contact Unit of the SIC located at the North Range-East Range junction, previously mapped as Onaping Intrusion by Ames et al. (2005). Note the sheared texture of the dark grey matrix of the Garson Member and the UCU. Subrounded to rounded granitoid and quartzite clasts are hosted in the matrix of both units.

With reference to distance from the granophyre contact, clast size and abundance as well as grain size trends in the UCU was observed in the field. The UCU located distally from the granophyre contact exhibits a fine-grained igneous matrix, containing 20 – 75% clasts that range in size from mm-scale to ~5 m. Proximal to the granophyre contact, the matrix is coarser grained and contains <5% clasts ranging in size from mm-scale to 10 cm. Locally clast-free patches ~10 m in diameter occur sporadically throughout the UCU where the matrix in such patches is aphanitic in texture.

Outcrops of granophyre appear identical across the North Range, exhibiting greyish-pink weathered surfaces and characteristic “blocky” fractures. Fresh surfaces reveal a phaneritic texture of coarse grained alkali feldspar, quartz, plagioclase, and hornblende laths arranged in interlocking fashion. Outcrops of the upper reaches of the granophyre, within 10 m of the UCU, exhibit a finer grained texture with up to 80% clast content, with clast size ranging from 5 cm to 0.5 m. Clasts are predominantly quartzite and granitic in composition.

The Sandcherry Member of the Onaping Formation is easily identified in the field where the outcrop surfaces are weathered, contributing to greater contrast between the beige coloured equant shards and fluidal fragments (~75% of total volume) with the dark brown to grey Sandcherry matrix (~25% of total volume). Fresh surfaces of the Sandcherry have lower contrast, which can cause the Sandcherry to be confused with very fine grained UCU.

The contact between the UCU and granophyre is transitional over ~5 m and is demonstrated by an increase in grain size, greater abundance of hornblende laths and feldspars, and a gradational change in colour from grey to greyish pink as the granophyre is approached. No direct observation of the contact between conformable UCU and Sandcherry Member could be made due to heavy overburden and vegetation coverage; however, the contact could be discerned

within ~40 cm. “Pods” of UCU are observed in the lower stratigraphy of the Onaping Formation, specifically, the Sandcherry Member. An example of such a pod is an outcrop located ~350 m east-south-east of Gravel Lake, where the contact between the UCU pod and surrounding Sandcherry Member of the Onaping Formation did not appear distinct or sharp; instead, the contact can be discerned within a range of <1 m. Clast content and grain sizes across UCU pods are inconsistent. However, of those observed, ~85% contained >60% clast content. In outcrops where the UCU is absent and the Sandcherry Member is adjacent to the granophyre, the contact is sharp. At such contacts the granophyre appears medium to coarse grained and is weathered to a greyish pink colour.

With reference to the most recent 1:50 000 scale geological map of the Sudbury region (Ames et al., 2005), and the 1:10 000 scale geological map of the Dowling, Morgan, Levack, and Balfour Townships (Gibbins et al., 2004), a number of inconsistencies (Table 2.2) were noted upon ground truthing and further investigated using optical microscopy and EDS for confirmation. Inconsistencies discovered by ground truthing were initially noted based field observations including textures, the presence or absence of clasts, and mineralogy. Additionally, we were not able to identify the “pipe-like” bodies of Onaping Intrusion reported in the literature (Gibbins, 1994; Ames, 1999, 2005). The so-called “transitional zone” (Ames, 2005) that is proposed to occur between the granophyre and the Onaping Intrusion is rather the occurrence of clast-rich fine-grained granophyre observed in the field (Figs. 2.6 A, B). Well-exposed examples of “melt bodies” (Muir and Peredery, 1984) occur in the Onaping Falls area, west of Highway 144, and exhibit identical characteristics to the UCU (Fig. 2.6 C). Specifically, outcrops of melt bodies weather to grey to dark-grey in colour, host rounded to subrounded clasts, and has a dark grey

fresh surface exhibited by the very fine-grained groundmass. Clast compositions are consistent with that of the UCU and are also rounded to subrounded (Fig. 2.6 C).

Table 2.2. Previously mapped units in comparison to ground truthing results from this study.

Sample	Sample coordinates	Mapped as	Author/s	This study
SUD-LED-1132	*	OI-granophyre transitional zone	Gibbins et al. (2004)	Fine-grained, clast-rich granophyre
SUD-LED-1167	46.625202, -81.332569	Sandcherry Member	Gibbins et al. (2004); Ames et al. (2005)	Upper Contact Unit
SUD-LED-1168	46.603681, -81.368162	Sandcherry Member	Gibbins et al. (2004); Ames et al. (2005)	Upper Contact Unit
SUD-LED-1172	46.603857, -81.369830	Quartz diorite	Gibbins et al. (2004); Ames et al. (2005)	Sandcherry Member
SUD-LED-1184	46.603257, -81.370208	Quartz diorite	Gibbins et al. (2004); Ames et al. (2005)	Sandcherry Member
SUD-LED-1195	*	OI-granophyre transitional zone	Gibbins et al. (2004);	Fine-grained, clast-rich granophyre
SUD-LED-1223	46.631148, -81.330199	Onaping Intrusion	Gibbins et al. (2004); Ames et al. (2005)	Sandcherry Member
SUD-LED-1231	46.624363, -81.334764	Onaping Intrusion	Gibbins et al. (2004); Ames et al. (2005)	Sandcherry Member
SUD-LED-1234	46.631274, -81.330218	Onaping Intrusion	Gibbins et al. (2004); Ames et al. (2005)	Sandcherry Member
SUD-LED-1235	46.627214, -81.339385	Quartz diorite	Gibbins et al. (2004)	Upper Contact Unit
SUD-LED-1244	46.624308, -81.334748	Onaping Intrusion	Gibbins et al. (2004); Ames et al. (2005)	Sandcherry Member
SUD-LED-1247	46.624363, -81.334708	Onaping Intrusion	Gibbins et al. (2004); Ames et al. (2005)	Sandcherry Member
SUD-LED-1248	46.627310, -81.336684	Sandcherry Member	Gibbins et al. (2004)	Upper Contact Unit
SUD-LED-1249	46.627211, -81.339266	Quartz diorite	Gibbins et al. (2004)	Upper Contact Unit

*All encountered Onaping Intrusion (OI)-granophyre contacts, North Range.

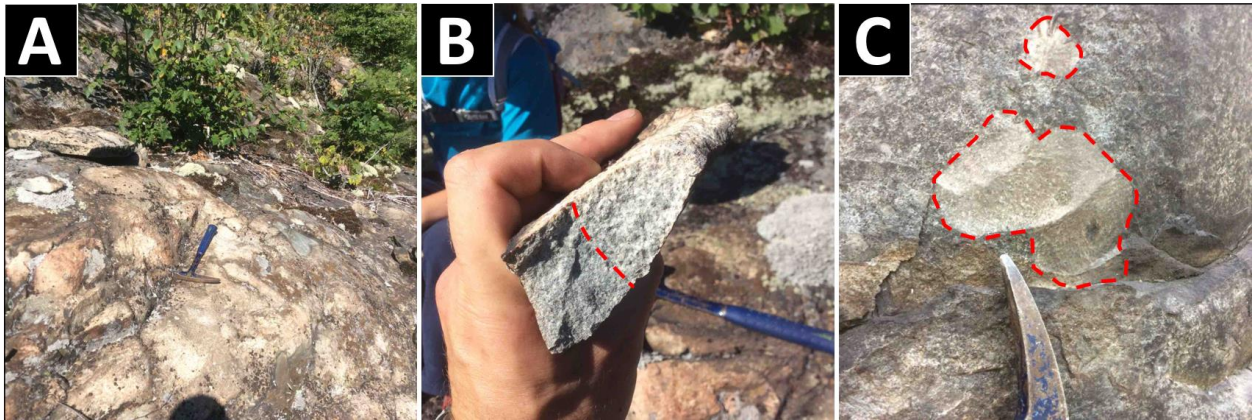


Figure 2.6. (A) Typical outcrop of fine-grained clast-rich granophyre. Note clast compositions are the same as the UCU. (B) Hand sample of fine-grained clast-rich granophyre. Red dashed line indicates clast boundary where a granitic clast is to the right of the line. (C) Example of a well-exposed outcrop at area mapped at “melt bodies”, west of Highway 144, Red dashed line outlines boundary of quartzite clasts.

2.3.2 Petrographic and Microscopic Observations

2.3.2.1 Matrix of the UCU

The matrix of the UCU is clast-bearing, and predominantly comprised of an interlocking intergrowth of sub- to euhedral feldspar and quartz, followed by lesser amounts of K-spar, amphiboles (hornblende, actinolite, tremolite, and cummingtonite), pyroxene, biotite, and sulfides (Fig. 2.7; Table 2.3). A secondary micrographic quartz-feldspar texture reminiscent of the granophyre, is also observed in matrix samples sourced relatively proximal to the granophyre contact. Some quartz grains exhibit micrographic textures along the clast boundary, however, upon detection of PDFs within the quartz it is determined that the shocked quartz is derived from shocked country rock and are therefore assimilated clasts and/or xenocrysts.

Evidence of hydrothermal alteration manifests as chloritization of hornblende, pyroxene, and biotite. Saussuritization of plagioclase is also common evidence of hydrothermal alteration in the UCU (Fig. 2.7 B). Saussuritization of plagioclase yields saussurite group minerals, including: epidote, sericite, and albite. Such mineral phases occur as small grains within larger plagioclase grains. This texture is not to be confused with the entirely igneous poikilitic texture.

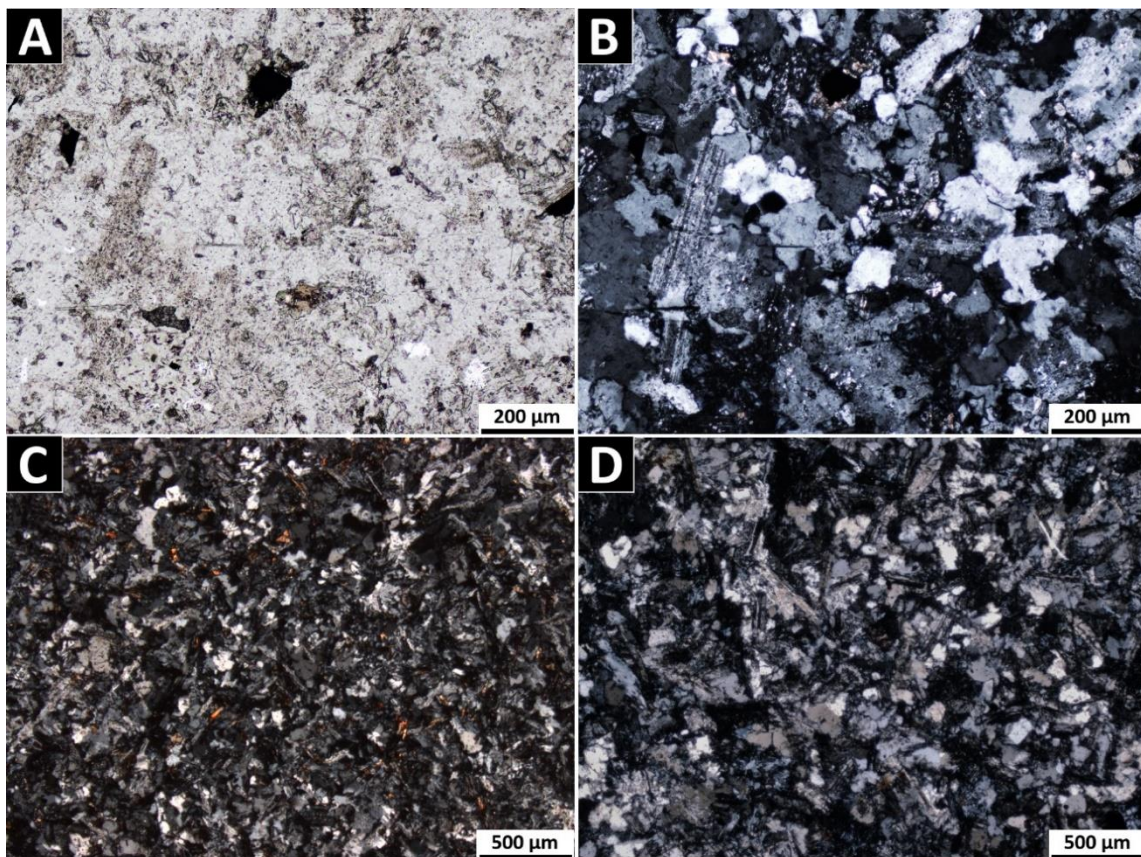


Figure 2.7. PPL (A) and XPL (B) photomicrographs of a sample of UCU. Hydrothermal alteration manifested as saussuritization of plagioclase laths. (C) Typical UCU texture exhibiting intergrowth of feldspar and quartz. (D) Photomicrograph of a sample of “melt body”. Note the likeness in texture and mineralogy between the UCU and “melt bodies”.

Petrographic analysis revealed that matrix grain size is not consistent throughout the UCU. K-spar grain size analysis via BSE imagery and image analysis using ImageJ™ (Fig. 2.3) yield a matrix grain size trend, whereby K-spar grain sizes in the UCU increases as the distance to the granophyre contact decreases (Fig. 2.8 A). These results are further supported by those from Anders et al. (2015) and Brillinger (2011) (Fig. 2.8 B – D). Samples taken from outcrops of “melt bodies” (Muir and Peredery, 1984) located west of Onaping Falls and Highway 144, exhibit identical microscopic characteristics to that of the UCU such as matrix mineral phases, texture, and the presence of clasts (Fig 2.7 D). Therefore, the term “UCU” will also be applied to the “melt bodies”.

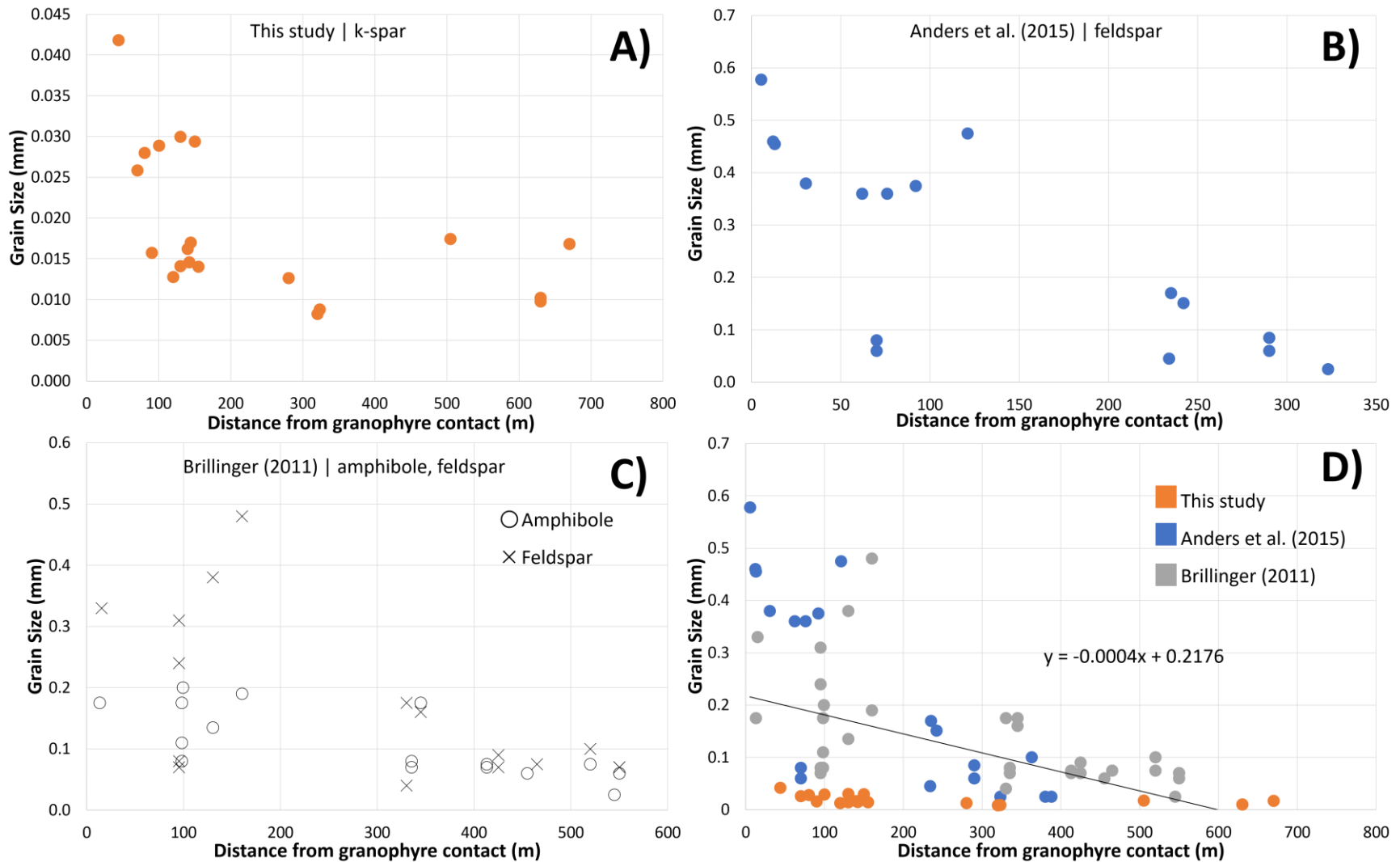


Figure 2.8. UCU matrix grain size data. (A) K-spar grain sizes from this study. (B) Feldspar grain sizes from Anders et al. (2015). (C) Amphibole and feldspar grain sizes from Brillinger (2011). (D) All grain sizes from plots A – C combined for comparison. Note the finer grain sizes in data from this study, due to semi-automatic particle analysis in ImageJ™ capable of detecting sub-mm scale grains. An overall negative relationship occurs between UCU matrix grain size and distance from the granophyre contact, for K-spar, feldspar (plagioclase and albite), and amphibole.

Table 2.3. Modal percentages of the UCU by point counting.

Sample	1100	1110	1113	1120	1138	1168	1194	1197	1219	1120	1235	1239	1311	1201
Matrix	96.3	89.7	97.9	100	100	95.8	97.1	78.3	85.3	94.8	98.8	100	93.9	97.4
Clasts	3.7	10.3	2.1	0	0	4.2	2.9	21.7	14.7	5.2	1.2	0	6.1	2.6
K-spar	n.d.	4.7	0	9.3	5.4	3.5	6.5	3.6	n.d.	4.4	3.7	12.1	3.4	6.1
Plag & Ab	19.3	38.2	49.4	26.2	27.2	33.8	32.5	31.1	28.2	39.7	31.9	31.3	28.4	12.7
Quartz	37.3	37.1	35.3	35.5	34.1	44.1	27.2	22.3	21.3	24.9	24.4	35.1	35.1	18.9
Chlorite	n.d.	9.7	7.4	13.9	10.2	7.2	5.6	11.1	6.2	13.5	14.1	n.d.	n.d.	10.1
Biotite	5.5	n.d.	n.d.	n.d.	n.d.	0.3	n.d.	0.1	2.4	2.1	n.d.	1.7	2.8	n.d.
Amphibole	11.5	n.d.	2.1	n.d.	1.7	1.4	4.1	6.2	n.d.	0.9	6.1	4.5	3.9	4.7
Epidote	17.7	n.d.	1.5	6.2	0.2	3.6	6.8	2.2	4.8	3.9	6.2	5.3	4.9	10.9
Opx	1.1	n.d.	0.7	0.6	n.d.	0.4	2.1	0.6	0.5	0.3	0.1	2.4	0.8	0.2
Cpx	0.8	n.d.	0.5	1.2	n.d.	0.7	2.8	1.1	4.7	0.8	0.2	3.7	0.7	0.1
Opagues	3.1	n.d.	1	4.4	3.1	0.8	3.2	n.d.	6.1	4.3	3.4	3.9	5.3	n.d.
Saussurite	n.d.	n.d.	n.d.	2.7	18.1	n.d.	6.3	n.d.	11.1	n.d.	8.7	n.d.	8.6	33.7
Points	1861	1918	1915	1926	1936	1874	1887	1919	1865	1945	1905	1850	1915	1877

Note: All samples catalogued as "SUD-LED-####".
n.d.: not detected.

2.3.2.2 Clasts and Sulfide “Blebs” of the UCU

Clasts are suspended throughout the matrix and comprise 20 – 75% of the UCU. In this study, a total of 236 clasts from 15 thin sections of UCU were analyzed for composition, size, and abundance. Results from this data set show the clasts are subrounded to rounded and are quartzite (80%), granitoid (7%), or mafic (5%) in composition (Fig. 2.9 A), consistent with field observations. Approximately 8% of the clast content analyzed consists of granitic clasts that have subsequently become heavily saussuritized as a result of hydrothermal alteration in the UCU (Fig. 2.9 A). A clast abundance trend relative to the granophyre contact is revealed in the data from this study and that of Anders et al. (2015), whereby clast abundance (%) in the UCU decreases with increasing distance from the granophyre contact (Fig 2.9 B). The average clast size of the 236 clasts measured is 3.8 mm along the long axes. Although a very slight trend is observed where clast size increases in the UCU with increasing distance from the granophyre contact (Fig. 2.9 C), a much stronger trend is observed in the field at the outcrop scale. This is not reflected in the petrographic analysis due to thin sections prepared based on the presence of small sized clasts in order to prevent data bias by including large, dominating clasts with boundaries that exceed thin section dimensions.

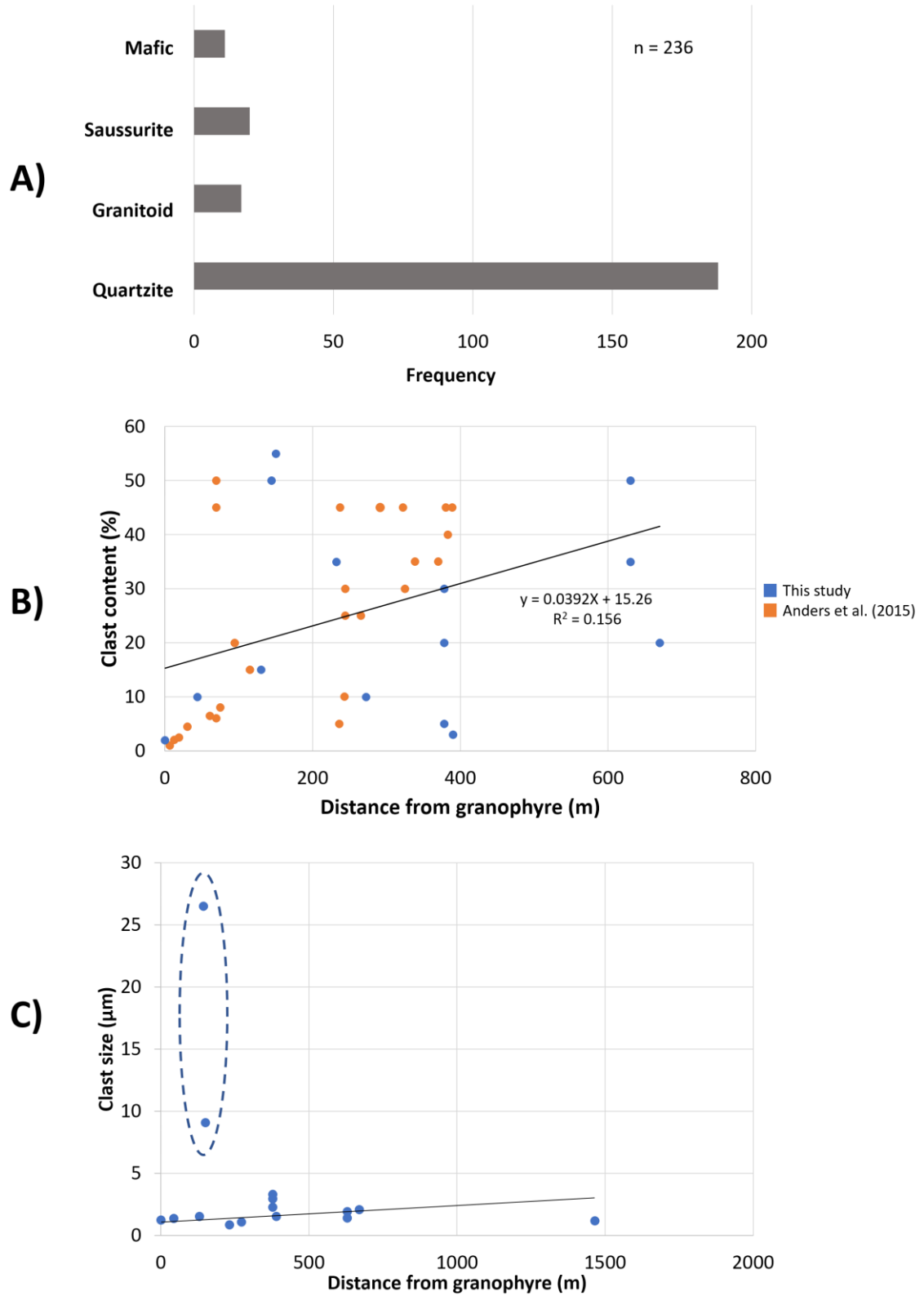


Figure 2.9. (A) A bar graph showing the percent frequency of quartzite, granitoid, saussurite, and mafic clast compositions across 236 clasts analyzed across 15 thin sections of UCU. (B) Data from this study combined with data from Anders et al. (2015)

illustrating an increase in clast content in the UCU with increasing distance from the granophyre contact. Note x-axis breaks. (C) Data from this study representing a slight trend of increasing clast size in the UCU with increasing distance from the granophyre contact. Note the two outliers circled by dashed line, resulting from each thin section containing one large clast.

Mafic, and felsic reaction coronae commonly occur around clasts of quartzite, granitoid, and mafic composition (Fig. 2.4, Cluster 2); however, not all clasts exhibit reaction coronae. Coronae occur as felsic (equigranular quartz and feldspar laths) or mafic (equigranular clinopyroxene, orthopyroxene, and amphibole) compositions (Table 2.4).

Table 2.4. Frequency occurrence of clast and coronae compositions observed via clast analysis.

	Clast composition	Coronae composition
Most frequent	Felsic	Mafic
↑	Felsic	None
↕	Mafic	None
↓	Mafic	Felsic
Less frequent	Felsic	Felsic

Quartz grains in clasts and as xenocrysts commonly exhibit annealed, decorated PDFs as a result of impact-induced shock metamorphism. Fluid inclusions along the PDFs vary in size between 0.5 μm to 1 μm , with an average distance of $\sim 1500 \mu\text{m}$ between sets. On the flat stage, one and two orientations of PDFs are frequently observed, whereas three orientations are less frequent (Figs. 2.10 A, B).

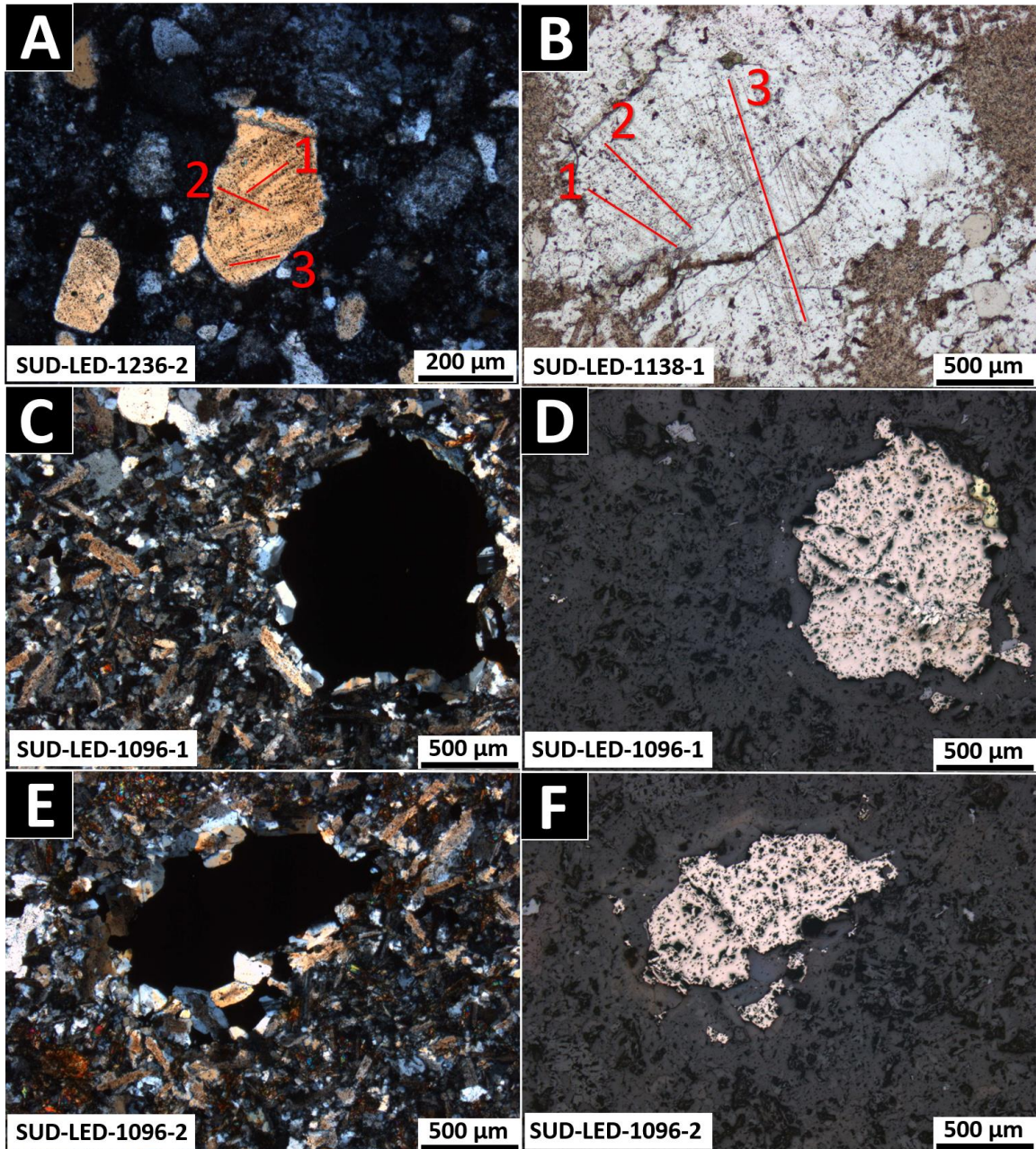


Figure 2.10. (A, B) Optical photomicrographs (PPL) showing decorated (inclusions) PDFs in quartz in the UCU. Up to three PDF orientations (labelled) are observed. Note the micrographic texture on the margins of the quartz grains. (C, D, E, F) Photomicrographs in XPL (left) and PPL (right) of the sulfide “blebs” observed in the UCU, comprised of chalcopyrite, pyrrhotite and pentlandite. Note the intergrowth nature of the sulfide bleb and igneous matrix.

As observed in the field, sulfide “blebs” account for <5% of the total “clast” abundance of the UCU. Observed via optical microscopy, such sulfides predominantly occur as disseminated blebs in the UCU as intergrowths with the igneous matrix (Fig. 2.10 C – F). Sulfide phases include ~40% chalcopyrite, 23% pentlandite, 30% pyrrhotite, 5% pyrite, and <2% arsenopyrite. EDS and BSE imagery were utilized to analyze crystal habit at the micrometer scale, revealing sub- to anhedral grains of tetragonal or octahedral chalcopyrite, and cubic pyrite. Lesser amounts of galena, cobaltite (Co-Ni solid solution), ilmenite, sphalerite, and argentopentlandite were observed in the UCU using EDS. More rarely, silver is also observed as silver telluride and is also found in association with uranium, caesium, and neodymium. EDS analysis revealed the following sulfide textures, from most common to least common: pentlandite exsolution flames in pyrrhotite in preferred orientations; pyrrhotite-hosted blebs and stringers, and euhedral inclusions of Fe-cobaltite; and finally, pentlandite exsolution lamellae in chalcopyrite.

2.3.3 ICP-MS and X-Ray Fluorescence Geochemistry

Major element ICP-MS and XRF analysis data (Fig. 2.11 A) indicates compositional variation in the UCU across the North Range; however, the variations coincide with the composition of components of the SIC. The average UCU is a compositionally more primitive, mafic melt in comparison to the average SIC, and is most comparable to the norite and offset dykes (Fig. 2.11 A).

Figures 2.11 B – C represents rare-earth element data of the UCU analyzed in this study and Anders et al. (2015), the North Range SIC (Naldrett et al., 1984; Therriault et al., 2002), and offset dykes (Anders, 2016; Coulter, 2016; Pilles, 2016; Pilles et al., 2017,

2018) and normalized to C1 chondrite data (Sun and McDonough, 1995). Similarities across the relative elemental composition ratios occur throughout the UCU and SIC units. Additionally, a negative europium anomaly in the UCU is consistent in the average SIC in the North Range (Figs. 2.11 B – D) due to plagioclase crystallization in the SIC, particularly in the granophyre and quartz gabbro. With respect to the offset dykes in the North Range, the UCU also shares similar relative elemental compositions (Figs 2.11 B – D). All units are enriched in light rare earth elements (LREE) and depleted in heavy rare earth elements (HREE). Relative to the SIC units, the UCU has overall depletion of REEs that is greater with increased distance from the granophyre contact (Figs. 2.11 B, D).

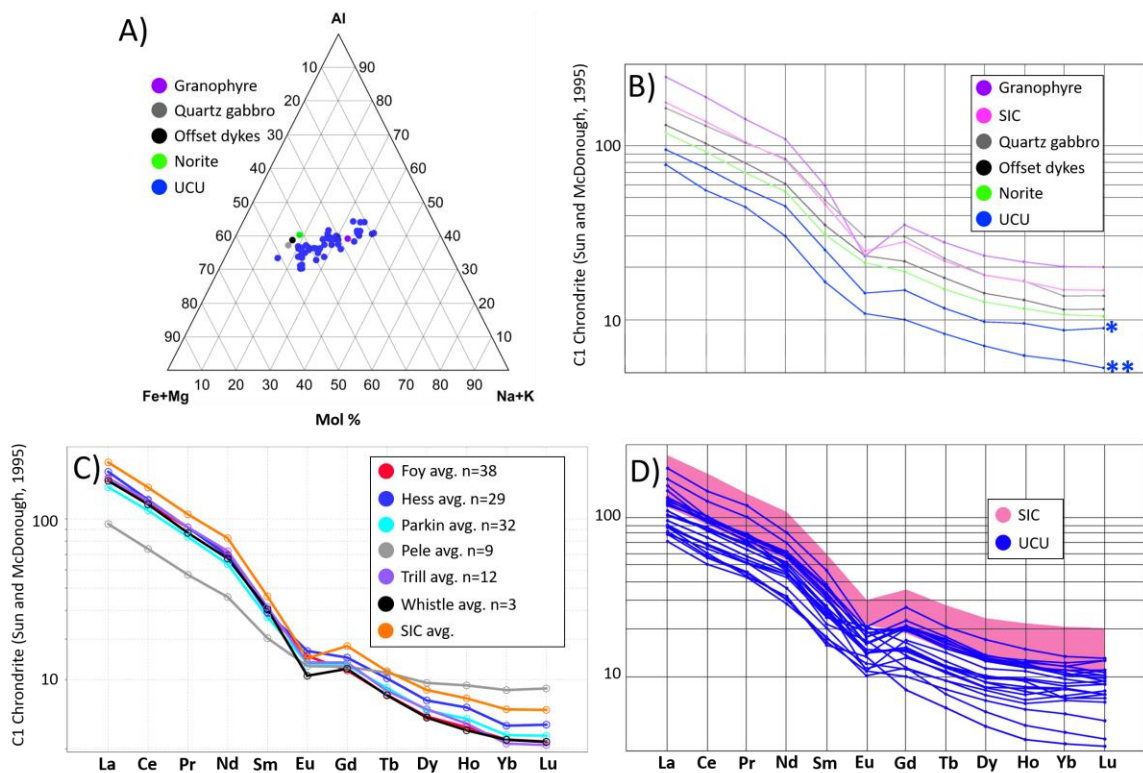


Figure 2.11. (A) Major elements plotted as mole % averages for units of the SIC, offset dykes, and UCU, specific to the North Range. (B) Average REEs plotted for the SIC, SIC units (Naldrett et al., 1984; Therriault et al., 2002), and offset dykes Hess, Foy, Parkin, Trill, and Pele (Anders, 2016; Coulter, 2016; Pilles, 2016; Pilles et al., 2017, 2018) of the North Range. The UCU* (n = 7) trend is representative of samples ~270 m from the granophyre contact, and the UCU** (n = 6) is representative of those from ~1400m from the granophyre contact. (C) The average REE composition of the SIC in the North Range

(from norite to granophyre) compared to individual UCU samples, inclusive of “Onaping Intrusion” and “melt bodies” samples. Note the overall depletion of REE in the UCU due to primitive nature of the UCU melt compared to the SIC melt.

2.4 Discussion

A recent study by Anders et al. (2015) based on two drill cores in the North Range proposed that the previously termed “Onaping Intrusion” represents the roof rocks of the SIC and should be termed “Upper Contact Unit” (UCU) of the SIC, rather than being intrusive unit in the Onaping Formation. This study builds upon on the concept of the UCU and its implied occurrence along the entire granophyre-Onaping Formation contact and consisted of a targeted investigation of the UCU across the North Range.

2.4.1 The UCU as “Roof Rocks” for the SIC

The UCU of the SIC is proposed to be analogous to roof rocks of layered mafic intrusions, thus, it is subjected to relatively rapid cooling rather than the underlying superheated proto-SIC melt sheet or “main mass”. Here, the UCU that is conformable and directly overlying the granophyre is discussed; nonconformable pods of UCU are discussed in the following section. Rapidly cooled roof rocks occupying the upper reaches of the melt sheet act as an insulating layer, contributing to heat retention in the underlying material (Therriault et al., 2002; Prevec and Cawthorn, 2002). Therefore, it is logical to presume that the presence and/or thickness of the melt sheet roof rocks is directly influenced by the thickness of the underlying melt sheet. Compared to the melt sheet at depth, the upper reaches are subjected to relatively rapid cooling and crystallization via radiative heat losses and thermal equilibration with assimilated cooler clasts from fallback debris. The combined effects result in relatively finer grained clast-

rich melt rocks in the upper portions of the impact melt sheet, as we observed in the field and in thin section. Importantly, the UCU exhibits coarsening in grain size in regions proximal to the underlying impact melt sheet, which can be ascribed to the increase in temperature.

Clasts in the UCU originate from the country rocks of the Superior and Southern provinces. This is reflected in the clast composition as determined in this study: quartzite (80%), granitoid (7%), and mafic (5%), with the remaining 8% of the clast content being previously granitic and subsequently subjected to saussuritization via impact-induced hydrothermal activity. It is visibly notable that the clast content decreases as the granophyre contact is approached, due to increasing temperatures and, thus, greater degree of melting of clasts. As a result, it is likely that very little to no clasts gravitationally migrated to the most lower reaches of the UCU due to complete melting of clasts. This is evident in the REE data, which reveals a depletion of REE in samples of the UCU sourced proximal to the granophyre or lowest in the UCU, where clasts are less abundant. In samples sourced distally from the granophyre or higher up in the UCU exhibit an enrichment of REE, where clast abundance is relatively greater (Figs. 2.11 B, D). The less contaminated, clast-free, lower reaches of the UCU are geochemically primitive relative to the upper regions where clast assimilation and melting have altered the geochemical composition the greatest.

Quartz grains in clasts, and xenocrysts exhibit highly decorated PDFs, testament to the widespread impact-generated hydrothermal activity (Ames et al., 1998; Ames, 1999). The occurrence of PDFs in the UCU further supports an impact melt origin for the unit. In addition to clasts, blebs of sulfides occur throughout the matrix and are predominantly

comprised of chalcopyrite, pentlandite, pyrrhotite, pyrite, and arsenopyrite (Figs. 2.10 C – F). Pentlandite is predominantly observed occurring as exsolution flames from a high-temperature, pyrrhotite solid solution (Naldrett and Kullerud, 1967; Craig and Kullerud, 1969; Francis et al., 1976). The occurrence of sulfides as blebs in the UCU is consistent with the nature of the proto-SIC, whereby immiscible sulfide blebs occurred dispersed throughout the impact melt sheet prior to sulfide fractionation (Ebel and Naldrett, 1996; Lightfoot, 2017).

2.4.2 The UCU in the SIC Single-Melt System

The transitional nature of the granophyre-UCU contact observed in the field and thin section is an indication that both units are genetically related having previously been part of a single impact melt system, the proto-SIC. Evidence of a single melt system origin for the norite and granophyre of the SIC is also presented by the occurrence of the quartz gabbro transition zone between the bimodal units (Ames et al., 2002; Therriault et al., 2002; Zieg and Marsh, 2005). It is clear that transition zones are inherent in single melt systems including the SIC, as observed along the UCU-granophyre contact; upper regions of the clast-rich granophyre are interpreted to be part of the “transitional” contact with the UCU, whereby both units appear blended. (Fig. 2.12).

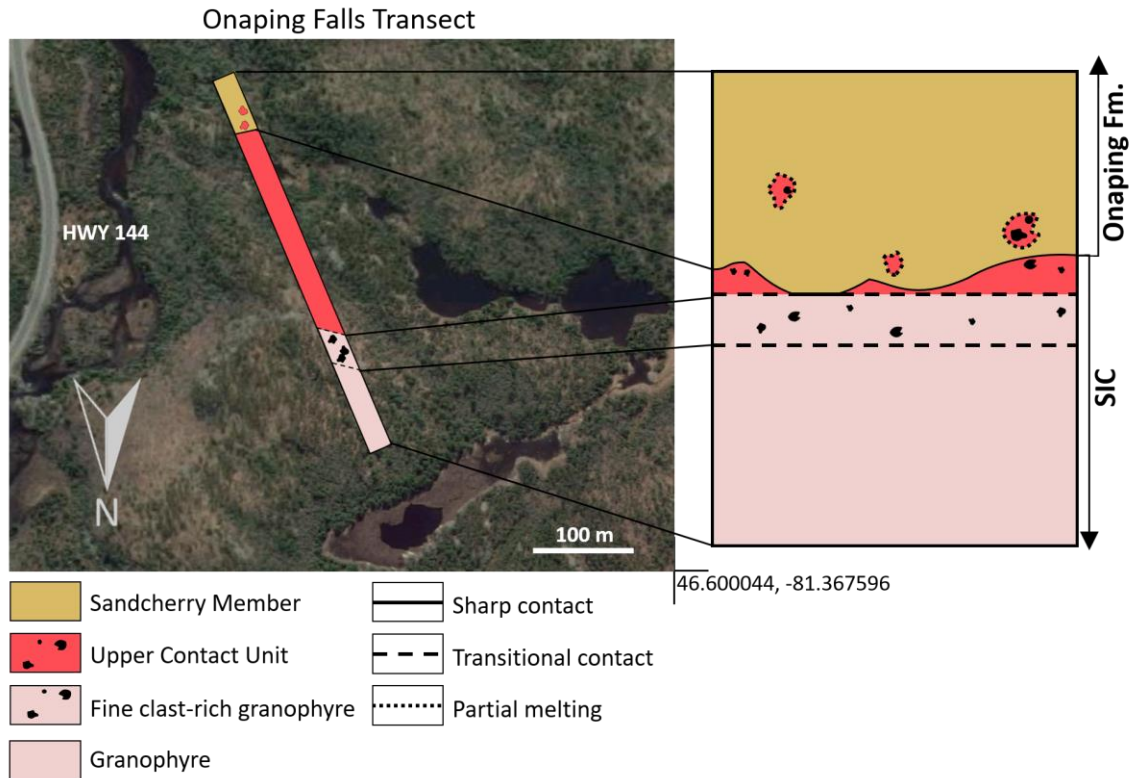


Figure 2.12. A simplified stratigraphic column (not to scale) representing a transect performed west of Highway 144, from the granophyre, fine-grained quartz-rich granophyre, UCU (as discontinuous sheets), and the Onaping Formation. Note the transitional contact relationships of a single-melt system (the SIC) between the granophyre (clast-rich) and UCU (clast-rich). A sharp contact is indicated between the UCU and Sandcherry Member. Clasts of UCU are seen hosted within the Sandcherry Member, emplaced via MFCI activity.

Evidence of a single-melt system between the UCU and the remaining SIC is also evident in the major element and REE geochemical data (Figs. 11 A, C, D). Major element compositions and relative REE ratios between the UCU and remaining SIC draw parallels regarding the impact melt sheet being the origin for the UCU (Fig. 2.11). The close compositional relationship between the UCU and offset dykes brings into question which unit represents the initial composition of the SIC (Brockmeyer and Deutsch, 1989; Anders et al., 2015). The similar major element compositions and REE ratios between the

UCU and offset dykes produces implications on the conventional interpretation that the offset dykes represent the initial composition of the SIC (Fig. 2.11). The negative europium anomaly observed in the UCU is identical to that of the average SIC in the North Range, unlike the average offset dykes in the North Range (Figs. 2.11 B – D), implying a stronger geochemical relationship between the SIC and the UCU. The major element geochemistry reveals that the average UCU is more mafic in composition than the average SIC, and most comparable to the norite and offset dykes (Fig. 2.11 A). Due to the “early-stage” nature of the norite (Therriault et al., 2002) and the compositional similarity between the norite and UCU, as well as the relatively primitive REE composition of the UCU melt, it is logical to conclude that it is the UCU, not the offset dykes, that represents the initial composition of the SIC prior to differentiation (Fig. 2.11).

While this study focused on the occurrence of the UCU, including the melt bodies and Onaping Intrusion in the North Range of the SIC, the findings presented here are consistent with a recent study on the Garson Member by Coulter and Osinski (2015). It was suggested that the Garson is a highly deformed remnant of the upper chilled phase (the UCU) of the SIC (Coulter and Osinski, 2015), which is further supported by a description made by Muir and Peredery (1984) that the Garson is the “Basal Member (Onaping Intrusion) of the South Range”, and by field and petrographic observations in this study (Figs. 2.6; 2.7). By unifying the Garson Member, melt bodies, and Onaping Intrusion as the UCU, the unit occurs in the North, South, and East ranges of the SIC, consistently along the granophyre-Onaping Formation contact (Fig. 2.1).

2.4.3 The Effects of MFCI Activity on the UCU

As previously mentioned, the UCU occurs as discontinuous sheets occupying 50% of the contact zone between the granophyre-Onaping Formation contact. Apparently isolated or distinct pods mapped as Onaping Intrusion have also been mapped higher up in the Sandcherry Member of the Onaping Formation (Muir and Peredery, 1984; Avermann and Brockmeyer, 1992; Gibbins, 1994; Ames, 1999). Although the emplacement of UCU pods in the Sandcherry Member has been previously noted, the mechanisms of emplacement have not been discussed.

The “lens-shaped or irregularly shaped” melt bodies, described by Muir and Peredery (1984) are mineralogically and geochemically identical to that of the so-called Onaping Intrusion, and hosts clasts of identical composition and abundance as the Onaping Intrusion. Such melt bodies have been reported to occur throughout the stratigraphy of the Onaping Formation and proximal to the granophyre contact. According to Muir and Peredery (1984) the melt bodies exhibit either sharp or abruptly sharp contacts with neighbouring lithologies such as the Onaping Formation and the granophyre. Based on detailed field, microscopic, and geochemical analysis, we conclude that previously mapped pods of quartz diorite occurring within the Sandcherry Member (Gibbins et al., 2004; Ames et al., 2005) are, in fact, the UCU.

Outcrops of UCU, melt bodies, and quartz diorite pods observed in this study did not appear distinct or sharp, but rather gradational over a short range of <1 m with the Sandcherry Member. In some cases, thin sections of samples taken along such contacts reveal the UCU matrix fining towards the Sandcherry Member to the extent where the matrices of the two lithologies nearly appear indistinct from the other. Such a contact

where the UCU matrix grades to very fine towards the Sandcherry Member, suggests a heat gradient between the UCU pod and Sandcherry Member. Another predominant feature of the UCU pods is the majority (~85%) contain a clast content of >60%. The gradational contacts are interpreted to be analogous to areas of partial melting around the pods of UCU within the Onaping Formation (Fig. 2.12). High clast content in such pods of UCU indicates that these UCU pods are derived, specifically, from the clast-rich upper reaches of the UCU.

The previously mentioned features exhibited by the “pods” of UCU, “melt bodies”, and “quartz diorite” within the Sandcherry Member serve as thorough evidence that such “pods” are actually clasts of the UCU that have been fragmented and emplaced into the still evolving Onaping Formation via MFCI activity. This hypothesis is further supported by a study by Petrus et al. (2016) who investigated uranium-lead zircon ages of the Onaping Formation and found a considerable abundance of zircons aged at 1.85 Ga, the youngest zircon age detected in the Onaping Formation. We interpret these to be derived from the UCU material that was explosively ejected by MFCI activity and incorporated within the Onaping Formation. This is consistent with suggestions made by Anders et al. (2015), that the discordancy of the Onaping Intrusion could be the result of still liquid Onaping Intrusion injecting into the overlying Onaping Formation by explosive MFCI forces.

The MFCI explosions are a critical component in the formation of the Sudbury impact structure as it is observed today, as the process resulted in the random emplacement of the UCU pods and, thus, likely dilutes any potential trends that would otherwise be observed in the conformable UCU.

2.5 Summary and Concluding Remarks

Traditionally, there has been little recognition of a chilled upper phase of the SIC.

However, a study of the upper contact of the SIC by Anders et al. (2015) determined the existence of a chilled phase or “roof rocks” for the SIC in a geographically limited region of the North Range. By extending the study of Anders et al. (2015) to the entire North Range of the SIC, field and microscopic observations reveal that all rocks previously mapped as “Onaping Intrusion” can be explained as clast-rich impact melt rock representing the roof rocks of the SIC. Thus, as roof rocks of the SIC, the “Onaping Intrusion” should thereafter be termed the “Upper Contact Unit” (UCU) of the SIC.

The data in this study is representative of samples of Onaping Intrusion, “melt bodies”, granophyre, and the Sandcherry Member collected across the North Range of the Sudbury Basin. The following conclusions are derived from the results presented in this study:

- 1) Field work, microscopy, and geochemical data demonstrate a clast-rich upper chilled phase or roof rocks of the SIC, namely, the UCU, is extensive across the entire North Range. The UCU hosts sulfide blebs that appear immiscible with the silicate melt matrix; this is consistent with the occurrence of such immiscibility between sulfides and the silicate melt of the proto-SIC, indicating that the UCU is part of the single-melt system of the SIC.
- 2) The presence of PDFs in quartz in clasts suspended in the igneous matrix of the Onaping Intrusion, previously mapped “melt bodies” and “quartz diorite”

indicates that these units formed at the time of impact and are by definition, impact melt rocks, which comprise the UCU.

- 3) Major and rare-earth element data reveals that the UCU is genetically related to, and derives from the SIC, evidenced by the inherent europium anomaly in both the UCU, SIC, and offset dykes. The primitive geochemical composition of the UCU relative to the SIC is a robust indication that the UCU represents the initial composition of the SIC prior to differentiation, rather than the offset dykes, as was conventionally thought.
- 4) Inconsistencies were discovered in this study via ground truthing using Geological Survey of Canada maps (Ames et al. 2005; Gibbins et al., 2004). Considering the effects of MFCI on the emplacement of the UCU presented here, detailed re-mapping along and proximal to the granophyre-Onaping Formation contact is warranted, and must be investigated through a new lens accordingly.
- 5) Combining the results of this study with those in Anders et al (2015), and Coulter and Osinski (2015), as well as considering stratigraphic consistency, we propose unifying the Garson Member, melt bodies, and Onaping Intrusion, to comprise the “Upper Contact Unit” of the SIC. This study supports the recommendation the rocks of the UCU are not a member of the complex series of breccias of the Onaping Formation, but rather a component of the SIC impact melt sheet (Fig. 2.12).

2.6 References

- Ames, D.E., 1999, Geology and regional hydrothermal alteration of the crater-fill, Onaping Formation: Association with Zn-Pb-Cu mineralization, Sudbury structure, Canada. PhD. Thesis #406, Dept. of Earth Sciences, Carleton University, Ottawa, Ontario, Canada.
- Ames, D.E., Davidson, A., Buckle, J., Card, K.D., 2005. Sudbury bedrock compilation; Geology. Geological Survey of Canada Open File 4570.
- Ames, D.E., Davidson, A., and Wodicka, N., 2008, Geology of the Giant Sudbury Polymetallic Mining Camp, Ontario, Canada: *Economic Geology*, v. 103, p. 1057–1077.
- Ames, D.E., Golightly, J.P., Lightfoot, P.C., and Gibson, H.L., 2002, Vitric compositions in the Onaping Formation and their relationship to the Sudbury Igneous Complex, Sudbury structure: *Economic Geology*, v. 97, p. 1541–1562.
- Ames, D.E., Watkinson, D.H., and Parrish, R.R., 1998, Dating of a regional hydrothermal system induced by the 1850 Ma Sudbury impact event: *Geology*, v. 26, p. 447–450.
- Anders, D., 2016, The Sudbury Impact Structure – New insights into the origin and emplacement of the Basal Onaping Intrusion and the Parkin, Trill, and Foy Offset Dykes of the North Range. PhD. Thesis #4223, Dept. of Earth Sciences, University of Western Ontario, Ontario, Canada, 237 p.
- Anders, D., Osinski, G.R., Grieve, R.A.F., and Brillinger, D.T.M., 2015, The Basal Onaping Intrusion in the North Range: Roof rocks of the Sudbury Igneous Complex:

- Meteoritics & Planetary Science, v. 50, p. 1577–1594.
- Avermann, M., and Brockmeyer, P., 1992, The Onaping Formation of the Sudbury Structure (Canada): an example of allochthonous impact breccias: *Tectonophysics*, v. 216, p. 227–234.
- Barlow, A.E., 1904, Report on the Origin, Geological Relations and Composition of the Nickel and Copper Deposits in the Sudbury Mining District, Ontario, Canada: *Geological Survey of Canada Annual Report*, Canada, p. 873.
- Barlow, A.E., 1906, On the origin and relations of the nickel and copper deposits of Sudbury, Ontario, Canada: *Economic Geology*, v. 1, p. 454–466.
- Barnes, S.J., Cruden, A.R., Arndt, N., and Saumur, B.M., 2016, The mineral system approach applied to magmatic Ni–Cu–PGE sulphide deposits: *Ore Geology Reviews*, v. 76, p. 296–316.
- Beales, F.W., and Lozej, G.P., 1975, Sudbury Basin Sediments and the Meteoritic Impact Theory of Origin for the Sudbury Structure: *Canadian Journal of Earth Sciences*, v. 12, p. 629–635.
- Bell R. 1893. On the Sudbury Mining District. *Geological Survey of Canada Annual Report* 5, p. 1–95.
- Brillinger, D.T.M., 2011, Possible evolution of the Onaping Intrusion as an impact melt rock at the Joe Lake Area, Sudbury, Ontario: University of Western Ontario, 44 p.
- Brockmeyer P. and Deutsch A. 1989. The origin of the breccias in the lower Onaping

- Formation, Sudbury structure, Canada: Evidence from petrographic observations and Sr-Nd isotope data. Proceedings, 20th Lunar and Planetary Science Conference. p. 113.
- Brocoum, S.J., and Dalziel, I.W.D., 1974, The Sudbury Basin, the Southern Province, the Grenville Front, and the Penokean Orogeny: Bulletin of the Geological Society of America, v. 85, p. 1571–1580.
- Burrows A. G. and Rickaby H. C. 1930. Sudbury Basin area. Ontario Department of Mines Annual Report 38, 55 p.
- Card, K.D., 1978, Geology of the Sudbury-Manitoulin Area: Districts of Sudbury and Manitoulin: Ontario Ministry of Natural Resources, v. 166.
- Coleman A. P. 1905. The Sudbury nickel region. Ontario Department of Mines Annual Report 14, p. 1–188.
- Coulter, A.B., 2016, Recent discoveries in the Ni-Cu-PGE bearing Trill and Parkin offset dykes, Sudbury impact structure, Canada: MSc. Thesis #3473, University of Western Ontario, Ontario, Canada, 137 p.
- Coulter, A.B., and Osinski, G.R., 2015, The nature and origin of the Garson Member of the Onaping Formation, Sudbury impact structure, Canada: Geological Society of America, v. Special Paper, p. 165–176.
- Craig, J., and Kullerud, G., 1969, Phase relations in the Cu-Fe-Ni-S system and their application to magmatic ore deposits: Economic Geology Monograph, p. 344–358.

- Deutsch A., Brockmeyer P., and Buhl D. 1990. Sudbury again: New and old isotope data. Proceedings, 21st Lunar and Planetary Science Conference. p. 282–283.
- Deutsch, A., Grieve, R.A.F., Avermann, M., Bischoff, L., Brockmeyer, P., Buhl, D., Lakomy, R., Müller-Mohr, V., Ostermann, M., and Stöffler, D., 1995, The Sudbury Structure (Ontario, Canada): a tectonically deformed multi-ring impact basin: *Geologische Rundschau*, v. 84, p. 697–709.
- Dietz, R.S., 1964, Sudbury Structure as an Astrobleme: *The Journal of Geology*, v. 72, p. 412–434.
- Ebel, D.S., and Naldrett, A.J., 1996, Fractional crystallization of sulfide ore liquids at high temperature: *Economic Geology*, v. 91, p. 607–621.
- Francis, C.A., Fleet, M.E., Misra, K., and Craig, J.R., 1976, Orientation of exsolved pentlandite in natural and synthetic nickeliferous pyrrhotite: *American Mineralogist*, v. 61, p. 913–920.
- French, B.M., 1967, Sudbury structure, ontario: Some petrographic evidence for an origin by meteorite impact. In French, B.M., Short, N.M., eds., *Shock metamorphism of natural materials*. Mono Book Corporation, Balitmore, p. 383–412.
- Gibbins, S., 1994, *Geology, geochemistry, stratigraphy and mechanisms of emplacement of the Onaping Formation, Dowling area, Sudbury Structure, Ontario, Canada*: Laurentian University.

- Gibbins, S., Ames, D.E., and Gibson, H.L., 2004, Geology of the Onaping Formation: Dowling, Morgan, Levack, and Balfour Townships, Sudbury, Ontario. Geological Survey of Canada Open File 4569.
- Gibbins, W., and McNutt, R., 1975, Rubidium-Strontium mineral ages and polymetamorphism at Sudbury, Ontario: *Canadian Journal of Earth Sciences*, v. 12, p. 1990–2003.
- Giblin, P.E., 1984, History of exploration and development, of geological studies and development of geological concepts. In Pye, E.G., Naldrett A.J., and Giblin P.E., eds., *The geology and ore deposits of the Sudbury Structure: Ontario Geological Survey Special Volume 1*, p. 3–23.
- Grieve, R.A.F., Ames, D.E., Morgan, J. V., and Artemevia, N., 2010, The evolution of the Onaping Formation at the Sudbury impact structure: *Meteoritics & Planetary Science*, v. 45, p. 759–782.
- Grieve, R.A.F., Stöffler, D., and Deutsch, A., 1991, The Sudbury Structure - controversial or misunderstood? *Journal of Geophysical Research-Planets*, v. 96, p. 22753–22764.
- Krogh, T.E., Davis, D.W., and Corfu, F., 1984, Precise U-Pb zircon and baddeleyite ages for the Sudbury area: *The geology and ore deposits of the Sudbury structure*, v. 1, p. 431–446.
- Lafrance, B., Legault, D., and Ames, D.E., 2008, The formation of the Sudbury breccia in the North Range of the Sudbury impact structure: *Precambrian Research*, v. 165, p.

107–119.

Lightfoot, P.C., 2017, Nickel Sulfide Ores and Impact Melts: Origin of the Sudbury Igneous Complex: Elsevier.

Lightfoot, P.C., Morrison, G.G., Bite, A., and Farrell, P., 1997, Geochemical Relationships in the Sudbury Igneous Complex: Origin of the Main Mass and Offset Dikes: *Economic Geology*, v. 92, p. 289–307.

McNamara, G.S., Leshner, C.M., and Kamber, B.S., 2017, New feldspar lead isotope and trace element evidence from the Sudbury igneous complex indicate a complex origin of associated Ni-Cu-PGE mineralization involving underlying country rocks: *Economic Geology*, v. 112, p. 569–590.

Morrison, G.G., 1984, Morphological features of the Sudbury structure in relation to an impact origin. In Pye, E.G., Naldrett, A.J., and Giblin, P.E., eds., *The Geology and Ore Deposits of the Sudbury Structure: Ontario Geological Survey, Special Volume 1*, p. 513–520.

Muir T. L. 1981. *Geology of the Capreol Area, District of Sudbury; Ontario. Geological Survey of Canada Open File 5344.*

Muir T. L. 1983. *Geology of the Morgan Lake - Nelson Lake area, District of Sudbury; Ontario. Geological Survey of Canada Open File 5426.*

Muir, T.L., and Peredery, W. V., 1984, The Onaping Formation. In Pye, E.G., Naldrett, A.J., and Giblin, P.E., eds., *The geology and ore deposits of the Sudbury Structure:*

- Ontario Geological Survey Special Volume 1, p. 235–251.
- Naldrett A.J., (1989) Magmatic sulfide deposits. New York: Clarendon Press, Oxford University Press, 186 pp.
- Naldrett, A.J., and Hewins, R.H., 1984, The main mass of the Sudbury Igneous Complex. In Pye, E.G., Naldrett A.J., and Giblin P.E., eds., The geology and ore deposits of the Sudbury Structure: Ontario Geological Survey Special Volume 1, p. 235-251.
- Naldrett, A.J., and Hewins, R.H., Dressler, B.O., and Rao, B.V., 1984, The contact sublayer of the Sudbury Igneous Complex. In Pye, E.G., Naldrett A.J., and Giblin P.E., eds., The geology and ore deposits of the Sudbury Structure: Ontario Geological Survey Special Volume 1, p. 253-270.
- Naldrett, A.J., and Kullerud, G., 1967, A study of the Strathcona mine and its bearing on the origin of the nickel-copper ores of the Sudbury district, Ontario: *Journal of Petrology*, v. 8, p. 453–531.
- O’Sullivan, E.M., Goodhue, R., Ames, D.E., and Kamber, B.S., 2016, Chemostratigraphy of the Sudbury impact basin fill: Volatile metal loss and post-impact evolution of a submarine impact basin: *Geochimica et Cosmochimica Acta*, v. 183, p. 198–233.
- Onorato, P.I.K., Uhlmann, D.R., and Simonds, C.H., 1978, The thermal history of the Manicouagan impact melt sheet, Quebec: *Journal of Geophysical Research*, v. 83, p. 2789–2798.
- Osinski, G.R., Grieve, R.A.F., Bleacher, J.E., Neish, C.D., Pilles, E.A., and Tornabene,

- L.L., 2018, Igneous rocks formed by hypervelocity impact: *Journal of Volcanology and Geothermal Research*, v. 353, p. 25–54.
- Pattison, E.F., 2009, Sudbury Igneous Complex. In Rousell, D., and Brown, G., eds., *A Field Guide to the Geology of Sudbury, Ontario*: Ontario Geological Survey, p. 56–74.
- Péntek, A., Molnár, F., Tuba, G., Watkinson, D.H., and Jones, P.C., 2013, The significance of partial melting processes in hydrothermal low sulfide Cu-Ni-PGE mineralization within the footwall of the Sudbury Igneous Complex, Ontario, Canada: *Economic Geology*, v. 108, p. 59–78.
- Péntek, A., Molnár, F., Watkinson, D.H., and Jones, P.C., 2008, Footwall-type Cu-Ni-PGE mineralization in the Broken Hammer area, Wisner township, north range, Sudbury structure: *Economic Geology*, v. 103, p. 1005–1028.
- Peredery W. V. 1972a. Chemistry of fluidal glasses and melt bodies in the Onaping Formation. In Guy-Bray, J.V., eds., *New developments in Sudbury geology*: Geological Association of Canada Special Paper v. 10, p. 49–59.
- Peredery W. V. 1972b. The origin of rocks at the base of the Onaping Formation, Sudbury, Ontario. PhD. Thesis, University of Toronto, Toronto, Ontario, Canada.
- Petrus, J.A., Kenny, G.G., Ayer, J.A., Lightfoot, P.C., and Kamber, B.S., 2016, Uranium–lead zircon systematics in the Sudbury impact crater-fill: implications for target lithologies and crater evolution: *Journal of the Geological Society*, v. 173, p. 59–75.

- Pilles, E., 2016, Emplacement of the Foy, Hess and Pele Offset Dykes at the Sudbury impact structure, Canada: PhD. Thesis #4158, Dept. of Earth Sciences, University of Western Ontario, Ontario, Canada.
- Pilles, E.A., Osinski, G.R., Grieve, R.A.F., Coulter, A.B., Smith, D., and Bailey, J., 2018, The Pele Offset Dykes, Sudbury impact structure, Canada: Canadian Journal of Earth Sciences, v. 55, p. 230–240.
- Pilles, E.A., Osinski, G.R., Grieve, R.A.F., Smith, D.A., and Bailey, J.M., 2017, Chemical variations and genetic relationships between the Hess and Foy offset dikes at the Sudbury impact structure: Meteoritics and Planetary Science, v. 52, p. 2647–2671.
- Prevec, S.A., and Cawthorn, R.G., 2002, Thermal evolution and interaction between impact melt sheet and footwall: A genetic model for the contact sublayer of the Sudbury Igneous Complex, Canada: Journal of Geophysical Research, v. 107, p. 1–14.
- Spray, J.G., and Scott, R.G., 2000, The South Range Breccia Belt of the Sudbury Impact Structure: A possible terrace collapse feature: Meteoritics and Planetary Science, v. 35, p. 505–520.
- Stevenson J. S. 1961. Recognition of the quartzite breccia in the White Water Series,

- Sudbury Basin, Ontario. Transactions of the Royal Society of Canada v. 60, p. 57–66.
- Stevenson J. S. 1963. The upper contact phase of the Sudbury micropegmatite. Canadian Mineralogist v. 7, p. 413–419.
- Stevenson J. S. 1972. The Onaping Ash-Flow Sheet, Sudbury, Ontario. In Guy-Bray, J.V., eds., New developments in Sudbury geology: Geological Association of Canada Special Paper v. 10, p. 41–48.
- Stöffler, D., Avermann, M. E., Bischoff, L., Brockmeyer, P., Deutsch, A., Dressler, B. O., Lakomy, R., and Müller-Mohr, V., 1989, Sudbury, Canada: Remnant of the only multi-ring (?) impact basin on Earth. Meteoritics v. 24, 328 p.
- Stöffler, D., and Grieve, R.A.F., 2007, Impactites: Metamorphic Rocks: A Classification and Glossary of Terms, Recommendations of the International Union of Geological Sciences, p. 82–92, 111-125-242.
- Sun, S. -s., and McDonough, W.F., 1989, Chemical and isotopic systematics of oceanic basalts: implications for mantle composition and processes: Geological Society, London, Special Publications, v. 42, p. 313–345.
- Therriault, A.M., Fowler, A.D., and Grieve, R.A.F., 2002, The Sudbury Igneous Complex - an impact melt sheet?: Economic Geology, v. 97, p. 1521–1540.
- Thomson J. E. 1957. Geology of the Sudbury Basin. Ontario Department of Mines Annual Report 65, p. 1–56.
- Zieg, M.J., and Marsh, B.D., 2005, The Sudbury Igneous Complex: Viscous emulsion

differentiation of a superheated impact melt sheet: Geological Society of America
Bulletin, v. 117, p. 1427.

Chapter 3

3 Conclusions and Suggestions for Future Work

3.1 Conclusions

The goal of this study was to extrapolate from the working hypothesis made by Anders et al. (2015) on the origin of rocks currently mapped as the Onaping Intrusion and more recently interpreted as the clast-rich upper chilled phase of the SIC, recently termed the UCU. Prior to Anders et al. (2015), recognition of an upper chilled phase of the SIC was lacking; subsequently, this study was aimed to conduct a targeted investigation of such a suite of rocks. The importance of better understanding the SIC is implied in the extensive exploitation of SIC-associated ore deposits. Specifically, the upper chilled phase of the SIC holds clues regarding the nature of the superheated impact melt sheet prior to differentiation and fractionation of ores.

The North Range was selected as the location for this investigation due to the lower degree of alteration and metamorphism of the rocks compared to the East and South ranges of the Sudbury Basin. Field work included sample collection and ground truthing of existing maps, followed by petrographic analysis, bulk rock geochemistry, and field emission electron microprobe techniques (EDS, BSE).

The following conclusions were produced in this study:

- 1) A clast-rich upper chilled phase or roof rocks of the SIC, namely, the UCU, is extensive across the entire North Range. Sulfide blebs found suspended throughout

the UCU represent sulfide-silicate immiscibility within the superheated proto-SIC, and supports that the UCU is part of the single-melt system of the SIC.

- 2) The previously mapped Onaping Intrusion, melt bodies, and quartz diorite units are determined to be components of the UCU, based on field, petrographic, and geochemical analyses. Furthermore, PDFs in quartz in clasts suspended in the igneous matrix of such units indicates that these units formed at the time of impact, and by definition, are impact melt rocks comprising the UCU.
- 3) ICP-MS and XRF bulk rock geochemistry indicates that the UCU represents the initial composition of the SIC, rather than the offset dykes, as was conventionally thought.
- 4) Ground truthing revealed mapping inconsistencies which warrants the need for re-mapping along the granophyre-Onaping Formation contact. Re-mapping is also warranted due to the effects of MFCIs on erratic emplacement of UCU in the Onaping Formation.
- 5) Based on Anders et al. (2015), Coulter and Osinski (2015), and this study, is it logical to conclude that the Garson Member, melt bodies (Muir and Peredery, 1984), and so-called Onaping Intrusion (Gibbins et al., 2004; Ames et al., 1998; Ames et al., 2005) are of the same lithology and, thus, comprise the UCU. As such, the rocks of the UCU are to be considered a unit of the SIC rather than a unit in the complex series of breccias of the Onaping Formation.

3.2 Suggestions for Future Work

The robust evidence presented in this study has demonstrated that the UCU of the SIC is extensive across the North Range and represents the initial composition of the SIC; the UCU is genetically related to the SIC in a single-melt system rather than occurring as a basal igneous unit of the Onaping Formation; and the UCU of the SIC is comprised of the Garson Member, melt bodies, and so-called Onaping Intrusion, thus is continuous throughout the North, South, and East ranges of the Sudbury Basin. With these conclusions established, it is recommended that the following is considered upon future work on the UCU:

- MFCI activity subjected to the upper the UCU of the SIC resulted in the erratic dismemberment and emplacement of UCU pods in the Onaping Formation, as observed in the field. The majority of such UCU pods contain an ~85% clast content, which was attributed to the clast-rich upper reaches experiencing a greater degree of MFCI explosions relative to the clast-poor lower reaches. This must be considered when sampling of the erratic pods is being conducted, particularly because the undisturbed conformable units of the UCU present greater consistencies and regularities in terms of the matrix and clast characteristics. Drill-core sampling of the conformable UCU is recommended in order to obtain a record of the unit and the associated contact relationships with surrounding lithologies.
- Considering the above point and the inconsistencies noted via ground truthing, detailed re-mapping of the UCU and associated lithologies is determined to be a high priority prior to further work on the UCU.

- The roof rock nature of the UCU of the SIC implies that the unit acted as an insulator to the hotter, underlying impact melt sheet. Therefore, it is suggested that future work involves investigating any correlations between the presence or absence and/or thickness of the UCU with the thickness of the underlying SIC units.
- Future isotopic analysis of the sulfide blebs observed in the UCU could support or refute the relation to SIC ores discerned in this study, particularly, as the pre-fractionation occurrence of immiscible sulfides hosted in proto-SIC silicate melt. Additionally, a focus on a comparison of the metal content in the UCU and SIC should be considered to delineate a potential relationship (if any) between the sulfide blebs observed in the UCU and the sulfide ores of the SIC.

3.3 References

- Ames, D.E., Watkinson, D.H., and Parrish, R.R., 1998, Dating of a regional hydrothermal system induced by the 1850 Ma Sudbury impact event: *Geology*, v. 26, p. 447–450.
- Ames, D.E., Davidson, A., Buckle, J.L., and Card, K.D., 2005, Sudbury Bedrock Compilation: Geological Survey of Canada Open File 4570.
- Anders, D., Osinski, G.R., Grieve, R.A.F., and Brillinger, D.T.M., 2015, The Basal Onaping Intrusion in the North Range: Roof rocks of the Sudbury Igneous Complex: *Meteoritics & Planetary Science*, v. 50, p. 1577–1594.
- Coulter, A.B., and Osinski, G.R., 2015, The nature and origin of the Garson Member of the Onaping Formation, Sudbury impact structure, Canada: *Geological Society of America*, v. Special Paper, p. 165–176.
- Gibbins, S., Ames, D.E., and Gibson, H.L., 2004, Geology of the Onaping Formation: Dowling, Morgan, Levack, and Balfour Townships, Sudbury, Ontario. Geological Survey of Canada Open File 4569.
- Muir, T.L., and Peredery, W. V, 1984, The Onaping Formation. In Pye, E.G., Naldrett, A.J., and Giblin, P.E., eds., *The geology and ore deposits of the Sudbury Structure: Ontario Geological Survey Special Volume 1*, p. 235–251.

4 Appendices

Appendix A. Geochemical data used for this study.

Sample ID	Lithology	Source	SiO ₂ %	Al ₂ O ₃ %	Fe ₂ O ₃ %	CaO%	MgO%	Na ₂ O%	K ₂ O%	Cr ₂ O ₃ %	TiO ₂ %	MnO%	Ce ppm	Dy ppm	Eu ppm	Gd ppm	Ho ppm	La ppm	Lu ppm	Nd ppm	Pr ppm	Sm ppm	Tb ppm	Yb ppm
70011	Granophyre	Anders et al., 2015	69.30	12.50	5.90	2.17	0.88	3.10	3.85	ND	0.80	0.07	100	5	0.88	5.6	0.94	52	0.38	43	12	7.2	0.78	2.5
70011	Granophyre	Anders et al., 2015	69.90	12.70	6.30	1.37	1.05	3.50	3.40	ND	0.68	0.07	140	7	1.3	7.8	1.4	78	0.59	59	16	10	1.2	4
70011	Granophyre	Anders et al., 2015	68.90	13.10	6.10	2.15	0.65	3.50	3.66	ND	0.69	0.08	87	5.7	1.4	5.9	1.1	45	0.5	40	10	7.1	0.92	3.3
70011	Granophyre	Anders et al., 2015	69.40	12.80	5.40	2.36	0.39	3.30	3.99	ND	0.66	0.07	110	6.1	1.3	6.9	1.2	56	0.5	50	13	8.6	1	3.5
70011	Granophyre	Anders et al., 2015	67.90	13.20	6.40	2.48	0.54	3.80	3.41	ND	0.80	0.08	110	5.8	1.5	6.5	1.2	54	0.51	50	13	8.6	0.96	3.2
52847	Granophyre	Anders et al., 2015	67.74	12.73	6.71	2.46	0.85	3.31	3.62	ND	0.95	0.08	110	5.9	2	7	1.2	58	0.54	49	13	9	1.1	3.3
70011	Granophyre	Anders et al., 2015	68.56	13.07	5.19	2.51	1.25	4.59	2.47	ND	0.96	0.06	98	5.7	1.8	7	1.2	45	0.48	48	12	8.9	1.1	3
70011	Granophyre	Anders et al., 2015	68.47	12.65	6.22	2.49	0.90	3.61	3.21	ND	0.95	0.08	94	5	1.6	6	1.1	50	0.46	41	11	7.4	0.94	3
70011	Granophyre	Anders et al., 2015	66.63	13.39	7.29	2.71	0.96	3.50	3.38	ND	0.65	0.08	150	7.8	2.3	9.5	1.6	83	0.66	66	18	12	1.6	4.3
70011	Granophyre	Anders et al., 2015	70.43	12.59	5.39	1.64	0.85	3.30	4.04	ND	0.70	0.06	110	5.2	1.6	6.7	1.1	54	0.48	44	12	8.1	0.97	3.1
70011	Granophyre	Anders et al., 2015	67.77	13.11	6.51	1.16	1.72	3.30	3.87	ND	0.92	0.05	120	5.4	1.3	6.9	1.2	56	0.53	48	13	9	0.95	3.4
70011	Granophyre	Anders et al., 2015	68.49	12.86	5.88	2.52	0.91	3.19	4.00	ND	0.81	0.07	120	5.4	1.3	6.9	1.3	62	0.54	49	14	9.4	0.97	3.3
70011	Granophyre	Anders et al., 2015	69.90	12.70	6.30	1.13	0.85	3.50	3.92	ND	0.67	0.07	140	6.3	1.2	7.8	1.3	67	0.53	58	16	10	1.1	3.7
70011	Granophyre	Anders et al., 2015	70.00	12.30	5.50	1.80	0.97	3.00	3.99	ND	0.80	0.06	100	4.7	0.69	5.9	0.96	49	0.38	43	11	7.4	0.8	2.6
70011	Granophyre	Anders et al., 2015	69.90	12.40	5.90	1.81	0.88	3.00	3.99	ND	0.81	0.06	100	4.7	0.74	5.9	0.95	51	0.37	42	11	7.3	0.81	2.7
70011	Granophyre	Anders et al., 2015	68.60	12.40	5.80	1.76	1.33	3.10	4.21	ND	0.83	0.04	110	4.2	0.76	5.5	0.87	51	0.38	44	11	6.9	0.8	2.3
70011	Granophyre	Anders et al., 2015	69.40	12.50	6.10	2.18	0.75	3.40	3.70	ND	0.85	0.07	110	4.9	0.91	6	1	51	0.39	45	11	7.6	0.84	2.6
70011	Granophyre	Anders et al., 2015	70.70	12.60	5.30	2.20	0.94	3.50	3.61	ND	0.79	0.06	140	6.1	1.2	7.7	1.2	71	0.54	59	16	9.5	1.1	3.4
70011	Granophyre	Anders et al., 2015	70.50	12.50	5.50	2.11	0.52	3.50	3.98	ND	0.66	0.08	110	5.9	1	6.9	1.2	55	0.5	47	12	7.9	0.96	3.4
52848	Granophyre	Anders et al., 2015	68.80	12.90	5.50	3.15	0.65	3.30	3.90	ND	0.80	0.08	110	6	1.1	7.6	1.2	58	0.49	47	12	8.7	0.99	3.2
52848	Granophyre	Anders et al., 2015	69.80	12.70	6.00	1.68	0.51	3.40	4.29	ND	0.68	0.09	130	5.9	1.2	7.1	1.2	63	0.51	52	14	8.9	0.98	3.5
52848	Granophyre	Anders et al., 2015	69.50	12.80	6.20	2.09	0.59	3.50	3.93	ND	0.72	0.08	120	6.1	1.2	7.5	1.2	61	0.51	53	14	9	1	3.4
52848	Granophyre	Anders et al., 2015	69.20	12.90	6.30	2.10	0.41	3.80	3.69	ND	0.77	0.08	130	6.1	1.2	7.6	1.2	63	0.5	53	14	9.2	1	3.4
52848	Granophyre	Anders et al., 2015	57.90	14.70	10.00	2.41	0.95	5.80	3.46	ND	1.20	0.18	140	6.8	1.8	8.9	1.3	72	0.57	64	16	11	1.2	3.8
SUD-LED-1132	Granophyre	This study	70.13	12.19	5.23	0.82	0.93	2.22	4.22	< D.L.	0.53	0.13	ND	ND	ND	ND	ND	ND	ND	ND	ND	ND	ND	ND

SUD-LED-1222	Granophyre	This study	70.64	12.27	5.58	1.21	0.68	2.58	4.44	<D.L.	0.76	0.09	ND	ND	ND	ND	ND	ND	ND	ND	ND	ND	ND	ND
SUD-LED-1233	Granophyre	This study	89.02	3.77	2.72	0.11	0.46	0.98	0.48	<D.L.	0.07	0.05	ND	ND	ND	ND	ND	ND	ND	ND	ND	ND	ND	ND
SUD-LED-3072	Granophyre	This study	66.4	13.4	6.07	2.68	1.7	3.44	3.21	<0.01	0.52	0.14	62.8	2.94	1.18	3.76	0.56	34.2	0.22	26	7.62	4.64	0.52	1.54
SUD-LED-3084	Granophyre	This study	73.4	11.45	4.64	0.77	0.63	2.52	4.85	<0.01	0.54	0.07	55.3	2.73	0.95	3.32	0.56	28.9	0.25	22.4	6.83	4.12	0.5	1.54
SUD-LED-3099	Granophyre	This study	67	12.4	7.55	1.71	1.22	3.46	3.93	<0.01	0.93	0.11	92.3	4.66	1.29	5.78	0.96	49.7	0.39	39.2	11.5	7.25	0.84	2.73
SUD-LED-3110	Granophyre	This study	67.7	11.7	7.89	1.49	1.11	2.53	3.56	<0.01	0.75	0.16	96	4.26	1.37	5.61	0.86	52.4	0.36	38.5	11.45	6.74	0.79	2.46
SUD-LED-3112	Granophyre	This study	69.3	12.45	6.36	1.4	1.26	3.01	3.83	<0.01	0.6	0.13	77	2.99	1.12	4.05	0.56	42.9	0.22	30	9.07	4.99	0.54	1.51
SUD-LED-3117	Granophyre	This study	66.1	13.25	9.08	1.23	1.97	3.68	2.32	<0.01	0.78	0.21	25	2.8	0.85	3.04	0.59	13	0.25	13.4	3.36	3.13	0.51	1.73
SUD-LED-1195	Granophyre	This study	72.1	11.55	5.42	1.31	0.62	2.65	4.41	<0.01	0.65	0.11	61.8	3.29	1.05	3.98	0.69	29.7	0.31	26.7	6.94	5.27	0.61	1.96
52847	Norite	Anders et al., 2015	59.50	16.00	7.90	6.01	3.84	2.90	1.81	ND	0.65	0.13	71	3.5	1	4.1	0.7	36	0.28	30	8.4	5	0.61	1.9
52847	Norite	Anders et al., 2015	60.60	18.00	4.00	4.26	3.96	5.40	1.47	ND	0.27	0.05	24	0.8	0.84	1.3	0.15	12	0.06	11	2.9	1.7	0.16	0.35
52848	Norite	Anders et al., 2015	45.00	13.70	17.00	10.26	5.46	2.50	0.54	ND	4.16	0.18	47	3.2	1.4	5	0.59	22	0.19	28	6.5	5.4	0.63	1.3
52848	Norite	Anders et al., 2015	54.80	6.00	16.70	4.87	13.01	0.40	1.24	ND	0.77	0.18	43	2.6	0.36	2.8	0.54	22	0.29	19	5.1	3.3	0.44	1.9
70011	Norite	Anders et al., 2015	58.40	15.90	7.50	7.93	3.82	3.60	1.21	ND	0.54	0.12	61	3.8	1.5	4.2	0.75	28	0.29	28	7	5.5	0.62	2
70011	Norite	Anders et al., 2015	59.00	15.80	7.60	6.75	3.69	3.10	1.97	ND	0.58	0.12	61	3.6	1.3	3.8	0.74	30	0.29	26	7	4.9	0.61	1.9
70011	Norite	Anders et al., 2015	58.50	16.40	7.70	6.11	4.35	3.20	1.23	ND	0.67	0.12	60	3.4	1.2	3.8	0.64	30	0.27	27	6.8	4.7	0.54	1.8
70011	Norite	Anders et al., 2015	58.30	16.00	7.80	6.33	4.80	2.90	1.58	ND	0.50	0.12	56	3.3	1.2	3.8	0.64	28	0.26	24	6.1	4.3	0.57	1.8
70011	Norite	Anders et al., 2015	57.50	17.40	7.30	6.85	4.90	3.00	1.33	ND	0.48	0.10	51	2.8	1.3	3	0.58	24	0.25	20	5.3	3.9	0.48	1.6
70011	Norite	Anders et al., 2015	59.40	16.90	6.90	6.09	4.15	3.10	1.92	ND	0.44	0.09	61	3.2	1.3	3.6	0.67	30	0.29	24	6.4	4.5	0.54	2
70011	Norite	Anders et al., 2015	58.10	16.60	6.70	5.54	3.69	6.70	0.37	ND	0.67	0.12	62	3.8	1.6	4.6	0.78	30	0.31	27	6.7	5.3	0.64	2
52847	Norite	Anders et al., 2015	60.88	15.47	7.29	5.66	3.24	3.09	2.07	ND	0.63	0.11	63	3.2	1.3	3.7	0.66	33	0.29	27	7.3	4.7	0.59	1.8
52847	Norite	Anders et al., 2015	60.12	15.75	7.58	5.84	3.46	2.99	1.87	ND	0.58	0.12	66	3.3	1.4	4	0.69	34	0.3	29	7.5	5.1	0.64	1.8
70011	Norite	Anders et al., 2015	54.94	15.25	8.18	5.80	3.89	4.79	0.78	ND	0.59	0.11	58	2.9	1.3	3.6	0.61	30	0.26	25	6.7	4.1	0.54	1.6
70011	Norite	Anders et al., 2015	59.34	16.28	7.19	5.35	3.82	4.10	1.38	ND	0.65	0.12	61	3	1.4	3.6	0.66	32	0.3	25	7	4.2	0.57	1.9
70011	Norite	Anders et al., 2015	59.22	15.63	7.62	7.10	3.67	3.31	1.71	ND	0.59	0.12	69	3.7	1.3	4.4	0.77	35	0.31	30	7.9	5.7	0.62	2.1
70011	Norite	Anders et al., 2015	59.32	15.75	6.78	6.54	3.82	5.58	0.55	ND	0.59	0.12	59	3.4	1.4	4.3	0.76	27	0.3	25	6.8	5	0.54	2
70011	Norite	Anders et al., 2015	59.54	15.66	7.33	6.78	3.71	3.11	1.88	ND	0.56	0.11	60	3.3	1.1	3.9	0.72	30	0.29	24	6.5	4.9	0.55	1.9
70011	Norite	Anders et al., 2015	58.30	16.40	7.20	5.37	4.39	3.50	1.91	ND	0.63	0.11	53	2.7	0.66	3.4	0.55	27	0.23	23	5.8	4.2	0.46	1.7
52847	Norite	Anders et al., 2015	59.90	17.10	6.30	6.35	3.58	3.70	1.58	ND	0.54	0.10	57	2.8	1	3.3	0.56	29	0.24	24	6.2	4	0.46	1.7
52848	Norite	Anders et al., 2015	51.10	14.80	13.30	8.62	4.14	2.90	1.04	ND	2.66	0.15	66	4.1	1.7	5.9	0.78	31	0.24	36	8.1	6.6	0.73	1.8
52848	Norite	Anders et al., 2015	52.40	16.30	12.00	8.89	4.29	2.80	1.13	ND	1.74	0.13	32	2	0.77	2.6	0.38	15	0.13	16	3.9	3	0.36	0.99
SUD-ABC-077	Offset Dyke	Coulter, 2016	61.3	14.45	7.37	3.1	3.43	3.51	2.66	0.02	0.71	0.09	80	3.88	1.37	5.07	0.74	40	0.28	32.3	8.97	5.82	0.73	1.81

SUD-EAP-280	Offset Dyke	Pilles 2016; Pilles et al., 2016, 2017	60.6	14.85	7.59	5.01	3.7	3.28	2.26	0.02	0.75	0.11	82.3	3.39	1.44	4.67	0.68	42.2	0.26	35.1	9.44	6.07	0.66	1.76
SUD-EAP-509	Offset Dyke	Pilles 2016; Pilles et al., 2016, 2017	49.3	17.9	10.9	7.35	4.46	4.21	1.68	<0.01	1	0.11	107	5.42	2.34	7.68	1.07	42.2	0.37	58.6	15.05	10.85	1	2.5
SUD-EAP-518	Offset Dyke	Pilles 2016; Pilles et al., 2016, 2017	47.4	13.45	14.95	9.83	6.39	1.98	0.64	0.02	1.53	0.21	27.4	5.57	1.42	4.81	1.16	13.2	0.48	15.3	3.71	3.87	0.84	3.22
SUD-EAP-521	Offset Dyke	Pilles 2016; Pilles et al., 2016, 2017	52.4	13.65	9.79	9.71	8.09	2.12	0.7	0.08	0.57	0.15	31	3.66	0.82	3.5	0.77	16.1	0.3	14.7	3.86	3.57	0.61	2.16
SUD-EAP-531	Offset Dyke	Pilles 2016; Pilles et al., 2016, 2017	52.9	13.25	15.25	9.46	5.28	2.03	0.75	0.01	1.12	0.21	32.7	5.43	1.15	4.64	1.13	16.3	0.52	17.3	4.21	4.4	0.81	3.17
SUD-SI-004	Offset Dyke	Pilles 2016; Pilles et al., 2016, 2017	50.2	13.05	13.7	7.49	7.33	3.35	0.41	0.01	1.1	0.25	20.1	4.09	0.81	3.43	0.88	9.6	0.42	11	2.62	2.9	0.63	2.61
SUD-SI-007	Offset Dyke	Pilles 2016; Pilles et al., 2016, 2017	49.7	14.75	12.35	10.6	5.7	2.12	0.71	0.02	1.07	0.2	22.3	4.54	1.05	3.78	0.92	10.1	0.38	12.6	2.86	3.18	0.67	2.81
SUD-SI-010	Offset Dyke	Pilles 2016; Pilles et al., 2016, 2017	51.4	12.65	14.45	8.66	5.52	2.15	1.27	0.01	1.13	0.24	25.6	5.18	1.15	4.49	1.19	12.1	0.52	14.2	3.24	3.67	0.81	3.24
SUD-SI-011	Offset Dyke	Pilles 2016; Pilles et al., 2016, 2017	52.6	13.2	15	8.73	5.24	2.54	0.86	<0.01	1.25	0.26	35	5.52	1.23	4.71	1.15	16.5	0.54	17.9	4.28	4.2	0.86	3.44
SUD-SI-013	Offset Dyke	Pilles 2016; Pilles et al., 2016, 2017	61.8	12.35	8.95	4.19	1.46	3.37	2.49	<0.01	1.54	0.14	109	5.84	2.17	7.89	1.22	51.8	0.47	49.5	12.85	9.56	1.08	2.8
SUD-SI-182	Offset Dyke	Pilles 2016; Pilles et al., 2016, 2017	59.3	15.45	7.5	4.71	3.92	3.15	2.29	0.02	0.72	0.1	81.7	3.31	1.48	5.04	0.69	40	0.26	34.6	9.51	6.06	0.64	1.67
SUD-SI-184	Offset Dyke	Pilles 2016; Pilles et al., 2016, 2017	59.3	16	8.39	4.57	4.22	3.13	2.61	0.03	0.73	0.1	79.9	3.27	1.44	4.54	0.67	39.7	0.25	34.2	9.12	5.79	0.62	1.57
SUD-SI-185	Offset Dyke	Pilles 2016; Pilles et al., 2016, 2017	61.1	15.45	8.16	4.78	3.96	3.34	2.19	0.02	0.74	0.1	87.4	3.5	1.5	4.82	0.68	43.8	0.26	37.5	9.72	6.33	0.69	1.76
SUD-SI-187	Offset Dyke	Pilles 2016; Pilles et al., 2016, 2017	58.8	14.9	7.93	5.8	4.36	2.78	2.69	0.02	0.72	0.12	70.5	3.27	1.52	4.52	0.7	34.8	0.27	30.5	8.17	5.36	0.65	1.75
SUD-SI-196	Offset Dyke	Pilles 2016; Pilles et al., 2016, 2017	63.4	14.55	6.93	4.86	3.49	3.03	2.33	0.02	0.65	0.09	77	3.37	1.24	4.6	0.68	38.8	0.28	32.3	8.69	6.04	0.66	1.73
SUD-SI-200	Offset Dyke	Pilles 2016; Pilles et al., 2016, 2017	61.9	15.1	7.67	4.78	3.79	3.22	2.45	0.02	0.72	0.1	77	3.55	1.43	5.03	0.77	38.7	0.27	33.1	9.02	6.17	0.67	1.71
SUD-SI-201	Offset Dyke	Pilles 2016; Pilles et al., 2016, 2017	56.4	15.65	9.78	7.15	4.85	2.89	1.81	0.03	0.88	0.14	58.5	3.96	1.36	4.96	0.83	29	0.33	27.1	7	5.22	0.72	2.22
SUD-SI-205	Offset Dyke	Pilles 2016; Pilles et al., 2016, 2017	60.4	14.4	7.81	5.72	3.98	3.07	1.75	0.02	0.73	0.11	65.2	3.51	1.37	4.08	0.68	31.8	0.3	28.7	7.62	5.1	0.66	1.92
SUD-SI-206	Offset Dyke	Pilles 2016; Pilles et al., 2016, 2017	62.5	14.95	7.52	5.97	4.02	3.21	1.74	0.02	0.71	0.12	74.5	3.72	1.38	4.84	0.79	36.6	0.31	31.2	8.6	5.77	0.64	2.01
SUD-SI-212	Offset Dyke	Pilles 2016; Pilles et al., 2016, 2017	56.9	15.55	9.37	6.91	4.84	2.59	2.21	0.03	0.83	0.14	59.9	4	1.45	4.87	0.86	29.6	0.35	27.4	7	5.08	0.73	2.17
SUD-SI-223	Offset Dyke	Pilles 2016; Pilles et al., 2016, 2017	61.2	14.95	7.86	4.14	3.77	2.98	2.84	0.02	0.7	0.09	76.1	3.66	1.48	4.74	0.7	43.8	0.28	34.9	9.49	6.25	0.7	1.9
SUD-SI-225	Offset Dyke	Pilles 2016; Pilles et al., 2016, 2017	62.9	14.8	7.66	5.16	3.7	3.21	2.32	0.02	0.69	0.11	71.4	3.27	1.36	5.03	0.74	36.7	0.3	30.8	8.54	5.72	0.67	1.94
SUD-SI-228	Offset Dyke	Pilles 2016; Pilles et al., 2016, 2017	61.3	15.15	8.09	5.78	4.11	3.17	2.07	0.02	0.76	0.12	69	3.59	1.36	4.98	0.76	35	0.28	30.4	8.18	5.53	0.68	1.75
SUD-SI-256	Offset Dyke	Pilles 2016; Pilles et al., 2016, 2017	59.1	15.45	8.64	6.36	4.57	3.04	1.42	0.03	0.74	0.12	66.8	3.5	1.43	4.58	0.77	33	0.25	29	7.85	5.26	0.66	1.9
SUD-SI-272N	Offset Dyke	Pilles 2016; Pilles et al., 2016, 2017	62.1	14.35	6.99	5.25	3.6	3.55	0.5	0.02	0.66	0.1	77.7	3.73	1.47	5.11	0.72	38.5	0.25	31.5	8.68	5.42	0.7	1.66
SUD-SI-272S	Offset Dyke	Pilles 2016; Pilles et al., 2016, 2017	51.2	15.4	9.18	9.45	7.18	1.84	1.67	0.02	0.51	0.17	11.2	2.05	0.66	2.16	0.46	5.4	0.18	6.3	1.46	1.68	0.36	1.06
SUD-DA-021	Offset Dyke	Anders, 2016	71.1	14.35	1.62	0.81	0.72	3.51	5.75	<0.01	0.1	0.02	74.6	0.65	1.48	1.74	0.1	40.3	0.03	25.1	2.68	3.39	0.17	0.19
SUD-DA-022	Offset Dyke	Anders, 2016	49.5	13.8	14.3	8.68	6.22	1.76	0.82	0.02	1.02	0.21	20.9	4.19	1.12	3.94	0.96	9.6	0.44	12	3.05	3.33	0.71	2.69
SUD-DA-023	Offset Dyke	Anders, 2016	50	13.5	14.25	7.74	5.82	1.26	2.72	0.03	0.95	0.18	24.5	3.73	1.08	3.82	0.83	11.2	0.36	12.9	14.2	3.07	0.66	2.29

70011	Quartz Gabbro	Anders et al., 2015	56.85	15.28	10.12	7.08	3.43	2.78	2.07	ND	0.99	0.12	56	3.3	1.3	3.9	0.66	28	0.28	25	6.6	4.6	0.6	1.8
52848	Quartz Gabbro	Anders et al., 2015	67.30	13.24	6.42	3.34	1.11	5.52	1.12	ND	1.04	0.06	100	4.7	2.4	6	1	55	0.43	41	11	7.4	0.78	2.7
70011	Quartz Gabbro	Anders et al., 2015	53.90	13.20	14.20	7.14	3.57	3.10	1.64	ND	1.85	0.16	77	4.6	1.5	6.1	0.91	35	0.33	38	8.9	7.2	0.79	2.1
70011	Quartz Gabbro	Anders et al., 2015	53.80	13.70	14.10	7.74	3.68	2.70	1.63	ND	1.85	0.15	59	3.6	1.3	4.7	0.71	28	0.3	27	6.6	5.1	0.62	1.9
52848	Quartz Gabbro	Anders et al., 2015	52.90	13.20	13.20	7.79	3.78	2.90	1.27	ND	2.98	0.18	78	4.8	1.7	6.8	0.94	36	0.32	41	9.6	7.6	0.87	2.1
52848	Quartz Gabbro	Anders et al., 2015	54.80	14.40	11.60	7.09	3.70	3.10	1.70	ND	2.15	0.15	73	4	1.5	5.3	0.76	35	0.27	37	9	6.4	0.73	2
52848	Quartz Gabbro	Anders et al., 2015	61.64	13.49	7.89	4.89	2.36	4.80	1.39	ND	1.81	0.10	110	5.8	1.1	7.8	1.2	54	0.47	52	13	10	0.97	3
52848	Quartz Gabbro	Anders et al., 2015	62.34	13.39	7.59	4.91	2.33	5.00	1.29	ND	1.81	0.11	100	5.4	1.5	7.1	1.2	48	0.42	49	12	9.2	0.95	2.7
52848	Quartz Gabbro	Anders et al., 2015	68.37	13.11	4.40	4.25	1.34	5.01	1.44	ND	0.95	0.05	77	3.5	1.9	4.4	0.74	40	0.3	30	8.1	5.7	0.6	2
52848	Quartz Gabbro	Anders et al., 2015	51.30	13.43	14.03	6.81	3.63	3.21	1.42	ND	3.43	0.21	110	6.2	2.1	8.8	1.3	52	0.44	54	13	10	1.1	2.8
52848	Quartz Gabbro	Anders et al., 2015	52.00	13.60	13.50	6.60	3.55	3.20	1.54	ND	3.28	0.21	92	5.1	2.1	6.9	1.1	42	0.37	44	11	8.8	0.94	2.6
BVR-1	Sublayer	Naldrett et al., 1984	62.93	14.90	6.90	4.59	3.71	2.96	2.28	ND	0.93	0.11	ND	ND	ND	ND	ND	ND	ND	ND	ND	ND	ND	ND
BVR-2	Sublayer	Naldrett et al., 1984	52.87	15.51	11.11	8.66	6.18	3.15	1.16	ND	1.20	0.16	ND	ND	ND	ND	ND	ND	ND	ND	ND	ND	ND	ND
BVR-3	Sublayer	Naldrett et al., 1984	52.92	13.71	12.61	8.76	6.79	2.35	1.16	ND	1.32	0.18	ND	ND	ND	ND	ND	ND	ND	ND	ND	ND	ND	ND
BVR-4	Sublayer	Naldrett et al., 1984	62.00	14.73	9.14	4.58	3.69	2.73	2.25	ND	0.75	0.13	ND	ND	ND	ND	ND	ND	ND	ND	ND	ND	ND	ND
BVR-5	Sublayer	Naldrett et al., 1984	52.48	14.55	8.41	2.73	3.95	3.00	3.20	ND	0.92	0.13	ND	ND	ND	ND	ND	ND	ND	ND	ND	ND	ND	ND
BVR-6	Sublayer	Naldrett et al., 1984	52.48	14.50	12.67	8.41	6.04	3.17	1.56	ND	1.30	0.19	ND	ND	ND	ND	ND	ND	ND	ND	ND	ND	ND	ND
BVR-7	Sublayer	Naldrett et al., 1984	61.44	15.26	7.60	5.25	3.81	3.17	2.56	ND	0.50	0.11	ND	ND	ND	ND	ND	ND	ND	ND	ND	ND	ND	ND
BVR-8	Sublayer	Naldrett et al., 1984	60.39	12.68	8.94	4.94	8.37	1.83	1.90	ND	0.78	0.17	ND	ND	ND	ND	ND	ND	ND	ND	ND	ND	ND	ND
BVR-9	Sublayer	Naldrett et al., 1984	60.39	14.59	7.06	5.15	3.91	2.41	2.39	ND	0.97	0.11	ND	ND	ND	ND	ND	ND	ND	ND	ND	ND	ND	ND
BVR-10	Sublayer	Naldrett et al., 1984	61.76	15.25	8.16	3.15	4.07	3.42	3.20	ND	0.81	0.18	ND	ND	ND	ND	ND	ND	ND	ND	ND	ND	ND	ND
BVR-11	Sublayer	Naldrett et al., 1984	51.66	14.67	12.84	9.52	6.21	2.81	0.81	ND	1.31	0.17	ND	ND	ND	ND	ND	ND	ND	ND	ND	ND	ND	ND
BVR-20	Sublayer	Naldrett et al., 1984	59.49	15.39	8.73	5.93	4.07	3.23	1.98	ND	1.08	0.14	ND	ND	ND	ND	ND	ND	ND	ND	ND	ND	ND	ND
SUD-LED-1219	UCU	This study	66.6	13.3	5.41	3.67	2.69	3.87	1.86	0.01	0.45	0.14	41.3	2.27	0.83	2.86	0.47	20.5	0.19	19.9	4.98	3.81	0.41	1.36
SUD-LED-1220	UCU	This study	67.3	12.9	5.34	2.22	2.7	3.49	3.31	0.01	0.45	0.13	50.1	2.26	0.79	3.03	0.44	25.8	0.18	22	5.77	3.94	0.42	1.18
SUD-LED-1235	UCU	This study	69.3	14.3	4.17	1.77	1.81	4.1	2.93	0.01	0.36	0.06	36.2	1.2	0.75	1.64	0.22	20.4	0.09	14.5	3.93	2.33	0.23	0.61
SUD-LED-1239	UCU	This study	68.87	13.26	4.30	1.45	1.67	3.72	3.72	< D.L.	0.46	0.09	ND	ND	ND	ND	ND	ND	ND	ND	ND	ND	ND	ND
SUD-LED-1311	UCU	This study	64.9	13.55	6.45	2.2	3.09	4.97	2.3	0.02	0.48	0.13	40.8	2.49	0.79	2.94	0.51	20.3	0.19	19.9	4.78	3.59	0.42	1.17
SUD-LED-1100	UCU	This study	61.6	13.3	8.7	5.06	3.77	3.1	2.16	0.02	0.58	0.17	56.7	3.11	1.06	3.9	0.66	29	0.24	25.7	6.58	4.77	0.54	1.64
SUD-LED-1168	UCU	This study	68.8	12.15	5.17	1.31	3	4.68	1.11	0.01	0.46	0.13	45.5	2.39	0.8	2.94	0.52	22.4	0.22	20.5	5.24	3.72	0.42	1.4
SUD-LED-1201	UCU	This study	61.8	13.55	8.48	5.22	3.99	2.85	2.4	0.02	0.59	0.16	61.2	3.19	1.12	3.85	0.65	31.3	0.23	27.6	7.11	5.41	0.56	1.7

OI-50-1	UCU	Anders et al., 2015	63.5	12.55	7.86	3.79	4.77	4.59	0.95	0.02	0.51	0.08	52.7	3.31	0.91	4.13	0.68	24.4	0.31	23.7	6.2	4.46	0.58	1.86
OI-50-2	UCU	Anders et al., 2015	63.2	11.95	8.03	3.76	4.4	4.55	1.03	0.02	0.49	0.08	51.3	3.14	0.9	3.99	0.63	24.1	0.27	23.1	6.13	4.03	0.56	1.76
OI-100-1	UCU	Anders et al., 2015	65.5	12.4	6.36	3.78	4.26	4.66	1.15	0.01	0.53	0.12	58.9	3.2	1	4.12	0.63	28.2	0.25	26.5	6.88	4.94	0.62	1.65
OI-100-2	UCU	Anders et al., 2015	62.7	12.25	6.67	3.76	4.48	4.74	0.84	0.01	0.53	0.11	59.2	3.21	0.91	4.14	0.66	27.9	0.27	26.9	7.05	4.63	0.59	1.64
OI 150-1	UCU	Anders et al., 2015	66.3	12.45	5.08	3.04	3.38	4.35	1.6	0.01	0.46	0.07	38.7	2.44	1.16	3.24	0.53	18.5	0.23	19.1	4.73	3.47	0.45	1.46
50-3 Onaping	UCU	Anders et al., 2015	65.27	12.19	5.93	3.82	4.43	4.68	1.21	0.16	0.54	0.08	ND	ND	ND	ND	ND	ND	ND	ND	ND	ND	ND	ND
100-3 Onaping	UCU	Anders et al., 2015	63.63	12.51	7.14	3.57	4.97	4.83	0.83	0.03	0.54	0.11	ND	ND	ND	ND	ND	ND	ND	ND	ND	ND	ND	ND
200-3 Onaping	UCU	Anders et al., 2015	67.49	12.87	4.92	2.23	3.83	4.82	1.75	0.03	0.51	0.07	ND	ND	ND	ND	ND	ND	ND	ND	ND	ND	ND	ND
241-3 Onaping	UCU	Anders et al., 2015	65.95	12.98	5.75	2.14	4.09	3.25	3.08	0.06	0.48	0.06	ND	ND	ND	ND	ND	ND	ND	ND	ND	ND	ND	ND
SBD-001	UCU	Anders et al., 2015	62.8	11.4	8.82	3.63	4.91	4.09	1.99	0.02	0.49	0.15	ND	ND	ND	ND	ND	ND	ND	ND	ND	ND	ND	ND
SBD-002	UCU	Anders et al., 2015	62.2	11.5	8.63	3.59	5.07	3.96	2.26	0.01	0.49	0.16	ND	ND	ND	ND	ND	ND	ND	ND	ND	ND	ND	ND
SBD-003	UCU	Anders et al., 2015	66.6	12.8	2.75	5.15	3.39	7.67	0.12	0.03	0.49	0.09	ND	ND	ND	ND	ND	ND	ND	ND	ND	ND	ND	ND
SBD-005	UCU	Anders et al., 2015	69.5	12	5.26	1.96	2.87	3.35	2.22	0.02	0.42	0.08	ND	ND	ND	ND	ND	ND	ND	ND	ND	ND	ND	ND
SBD-011	UCU	Anders et al., 2015	65.6	12.9	3.6	2.36	4.56	6.53	0.29	0.02	0.55	0.08	ND	ND	ND	ND	ND	ND	ND	ND	ND	ND	ND	ND
SBD-012	UCU	Anders et al., 2015	70.1	12.5	2.15	2.72	3.55	6.96	0.61	0.02	0.45	0.07	ND	ND	ND	ND	ND	ND	ND	ND	ND	ND	ND	ND
SBD-016	UCU	Anders et al., 2015	71	12.9	3.24	0.94	1.55	4.54	3.96	0.01	0.23	0.04	ND	ND	ND	ND	ND	ND	ND	ND	ND	ND	ND	ND
SDB-020	UCU	Anders et al., 2015	68.8	12.9	2.71	0.97	2.06	6.92	0.43	0.01	0.28	0.04	ND	ND	ND	ND	ND	ND	ND	ND	ND	ND	ND	ND
SBD-024	UCU	Anders et al., 2015	69.9	13.4	3.54	0.74	1.63	4.07	4.66	0.01	0.27	0.05	ND	ND	ND	ND	ND	ND	ND	ND	ND	ND	ND	ND
SBD-031	UCU	Anders et al., 2015	64.3	11.5	6.41	3.37	5.93	5.01	0.11	0.02	0.52	0.13	ND	ND	ND	ND	ND	ND	ND	ND	ND	ND	ND	ND
SBD-034	UCU	Anders et al., 2015	67.7	12.4	5.64	1.76	2.86	4.73	2.89	0.02	0.46	0.08	ND	ND	ND	ND	ND	ND	ND	ND	ND	ND	ND	ND
SBD-037	UCU	Anders et al., 2015	60.6	11.7	8.17	4.83	5.16	5.11	1	0.01	0.52	0.19	ND	ND	ND	ND	ND	ND	ND	ND	ND	ND	ND	ND
SBD-039	UCU	Anders et al., 2015	62	11.6	8.64	4.16	4.84	3.83	2.05	0.01	0.5	0.19	ND	ND	ND	ND	ND	ND	ND	ND	ND	ND	ND	ND
SBD-054	UCU	Anders et al., 2015	69.5	10.8	4.74	2.39	4.61	4.92	0.68	0.02	0.49	0.1	ND	ND	ND	ND	ND	ND	ND	ND	ND	ND	ND	ND
SBD-055	UCU	Anders et al., 2015	69.8	10.7	4.85	1.86	3.99	4.84	0.62	0.02	0.38	0.09	ND	ND	ND	ND	ND	ND	ND	ND	ND	ND	ND	ND
SBD-058	UCU	Anders et al., 2015	67.7	12.7	4.61	1.98	3.49	5.15	1.59	0.02	0.51	0.06	ND	ND	ND	ND	ND	ND	ND	ND	ND	ND	ND	ND
SBD-50	UCU	Anders et al., 2015	69.02	12.29	5.49	1.98	3.31	3.79	1.8	0.02	0.49	0.11	ND	ND	ND	ND	ND	ND	ND	ND	ND	ND	ND	ND
SUD-LED-1100	UCU	This study	61.6	13.3	8.7	5.06	3.77	3.1	2.16	0.02	0.58	0.17	56.7	3.11	1.06	3.9	0.66	29	0.24	25.7	6.58	4.77	0.54	1.64
SUD-LED-1168	UCU	This study	68.8	12.15	5.17	1.31	3	4.68	1.11	0.01	0.46	0.13	45.5	2.39	0.8	2.94	0.52	22.4	0.22	20.5	5.24	3.72	0.42	1.4
SUD-LED-1195	UCU	This study	72.1	11.55	5.42	1.31	0.62	2.65	4.41	<0.01	0.65	0.11	61.8	3.29	1.05	3.98	0.69	29.7	0.31	26.7	6.94	5.27	0.61	1.96

SUD-LED-3060A	UCU	This study	61.9	13.9	8.71	1.59	4.54	3.99	1.35	0.02	0.66	0.15	50.4	2.76	0.61	3.36	0.59	25.8	0.22	21.5	6.38	4.1	0.51	1.55
SUD-LED-3060B	UCU	This study	61.2	14.15	8.48	1.56	4.73	3.85	1.35	0.02	0.64	0.14	57.7	3.07	0.77	3.96	0.62	30.5	0.25	25.4	7.29	4.64	0.56	1.77
SUD-LED-3137	UCU	This study	67.5	13.55	6.73	0.57	1.99	4.91	1.7	<0.01	0.38	0.11	61.2	2.09	1.08	2.69	0.42	37.1	0.19	22.2	6.93	3.47	0.38	1.34
SUD-LED-3148	UCU	This study	69	12.05	7.12	0.75	3.34	3.74	1.15	0.02	0.51	0.12	40.5	2.11	0.63	2.61	0.46	21.1	0.19	16.3	4.78	2.98	0.39	1.34
SUD-LED-1219	UCU	This study	66.6	13.3	5.41	3.67	2.69	3.87	1.86	0.01	0.45	0.14	41.3	2.27	0.83	2.86	0.47	20.5	0.19	19.9	4.98	3.81	0.41	1.36
SUD-LED-1220	UCU	This study	67.3	12.9	5.34	2.22	2.7	3.49	3.31	0.01	0.45	0.13	50.1	2.26	0.79	3.03	0.44	25.8	0.18	22	5.77	3.94	0.42	1.18
SUD-LED-1235	UCU	This study	69.3	14.3	4.17	1.77	1.81	4.1	2.93	0.01	0.36	0.06	36.2	1.2	0.75	1.64	0.22	20.4	0.09	14.5	3.93	2.33	0.23	0.61
SUD-LED-1239	UCU	This study	68.87	13.26	4.30	1.45	1.67	3.72	3.72	< D.L.	0.46	0.09	ND	ND	ND	ND	ND	ND	ND	ND	ND	ND	ND	ND
SUD-LED-1311	UCU	This study	64.9	13.55	6.45	2.2	3.09	4.97	2.3	0.02	0.48	0.13	40.8	2.49	0.79	2.94	0.51	20.3	0.19	19.9	4.78	3.59	0.42	1.17
SUD-LED-1201	UCU	This study	61.8	13.55	8.48	5.22	3.99	2.85	2.4	0.02	0.59	0.16	61.2	3.19	1.12	3.85	0.65	31.3	0.23	27.6	7.11	5.41	0.56	1.7
SUD-LED-3107	UCU	This study	66.6	12.95	5.79	1.93	2.45	5.73	0.24	<0.01	0.76	0.09	88.7	4.19	1.15	5.4	0.81	47.7	0.32	36.3	10.9	6.84	0.74	2.15
SUD-LED-3091	UCU	This study	69.9	12.35	6.54	1	1.45	2.8	4.02	<0.01	0.65	0.14	76.7	3.35	0.99	4.46	0.67	40.8	0.26	31.3	9.24	5.58	0.64	1.87
SUD-LED-3083	UCU	This study	71.9	11.65	4.49	0.99	2.58	4.15	1.85	0.01	0.42	0.11	30.9	1.88	0.57	2.25	0.37	16.6	0.17	13	3.87	2.62	0.34	1.14
SUD-LED-3092	UCU	This study	66.8	13	4.4	1.59	1.68	3.22	4.54	<0.01	0.32	0.09	57.6	1.48	0.95	2.26	0.27	34.5	0.1	20.8	6.48	3.15	0.28	0.72
SUD-LED-3120	UCU	This study	71.3	11.35	4.48	1.26	2.42	4.86	0.94	0.01	0.41	0.14	34.8	2.02	0.68	2.21	0.39	19.2	0.2	13.9	4.19	2.56	0.34	1.22
SUD-LED-1085	UCU	This study	79.7	10.25	2.64	0.26	1.33	5.26	0.38	0.01	0.23	0.03	33.9	1.74	0.61	1.99	0.34	18.4	0.13	13.8	4.11	2.44	0.3	0.94
SUD-LED-1090	UCU/Melt bodies	This study	69.4	11.1	6.19	1.63	3.54	3.92	1.84	0.01	0.45	0.21	30.6	2.17	0.68	2.67	0.44	14.7	0.18	15.4	4.18	3.16	0.39	1.34
SUD-LED-1096	UCU/Melt bodies	This study	68.8	11.4	6.47	2.79	3.51	4.03	2.59	0.02	0.46	0.16	32.2	2.63	0.48	3.13	0.51	14	0.22	17	4.56	3.56	0.46	1.47
SUD-LED-1098	UCU/Melt bodies	This study	68.7	10.6	6.64	2.52	3.63	3.76	2.18	0.01	0.42	0.21	31.7	2.53	0.61	2.94	0.5	15.2	0.2	16.1	4.22	3.39	0.44	1.44
SUD-LED-3069	UCU/Melt bodies	This study	67	11.65	6.66	0.54	3.58	3.91	1.15	0.02	0.48	0.18	22	1.9	0.5	2.14	0.35	10.5	0.17	12.4	3.26	2.38	0.34	1.19
SUD-LED-3074	UCU/Melt bodies	This study	65.7	11.75	9.95	0.46	4.18	3.57	0.25	0.02	0.47	0.3	11.2	1.83	0.5	1.68	0.39	6.3	0.18	6.3	1.57	1.58	0.3	1.22

ND = No data

DL = Detection limit

Curriculum Vitae

Name Lindsay E. Debono

Post-secondary Education and Degrees University of Western Ontario
London, Ontario, Canada
2016-2018 MSc. Geology, Candidate

The University of Western Ontario
London, Ontario, Canada
2010-2016 BSc. Geology, Minor in Health Science, Dean's List

Honours and Awards 2017-2018
Society of Economic Geologists Canada Foundation Fellowship
Oil, Gas and Salt Resources Library Award of Merit

2013-2015
Robert and Ruth Lumsden Undergraduate Award in Earth Science
Robert W. Hodder Travel Bursary

Related Work Experience 2016-2018
Graduate Research/Teaching Assistant
University of Western Ontario, London, Canada

2017-2018, 2016-2017
President, Secretary
Society of Economic Geologists, London Student Chapter

2013-2015
Undergraduate Research/Geological Field Assistant
University of Western Ontario, London, Canada

Publications

Debono, L.E., Osinski, G.R., 2018. Spatial and geochemical relationships between footwall granophyre and sulfide Ni-Cu-PGE veins, Sudbury impact structure, Canada. Abstract #2369. Poster, 49th LPSC, Woodlands, TX.

Debono, L.E., Osinski, G.R., Grieve, R.A.F., 2018. The Upper Contact (roof rocks) of the Sudbury Igneous Complex, Sudbury impact structure, Canada. Abstract #2389. Presentation, 49th LPSC, Woodlands, TX.

Debono, L.E., Osinski, G.R., 2018. Spatial and geochemical relationships between footwall granophyre and sulfide Ni-Cu-PGE veins, Sudbury impact structure, Canada. Poster, 2018 PDAC, Toronto, ON.